CHARACTERIZATION OF THE DIVERSE SUBSTRATE SPECIFICITIES AND BIOLOGICAL ROLES OF POLYAMINE BIOSYNTHETIC ENZYMES IN MICROORGANISMS

APPROVED BY SUPERVISORY COMMITTEE

Meg. Phillips, Ph.D.

Nick Grishin, Ph.D.

Elizabeth Goldsmith, Ph.D.

Kim Orth, Ph.D.

Vanessa Sperandio, Ph.D.

DEDICATION

I would like to thank my family for their continuous love, support and encouragement that they have provided throughout my life.

CHARACTERIZATION OF THE DIVERSE SUBSTRATE SPECIFICITIES AND BIOLOGICAL ROLES OF POLYAMINE BIOSYNTHETIC ENZYMES IN MICROORGANISMS

by

JEONGMI LEE

DISSERTATION

Presented to the Faculty of the Graduate School of Biomedical Sciences

The University of Texas Southwestern Medical Center at Dallas

In Partial Fulfillment of the Requirements

For the Degree of

DOCTOR OF PHILOSOPHY

The University of Texas Southwestern Medical Center at Dallas

Dallas, Texas

June, 2008

CHARACTERIZATION OF THE DIVERSE SUBSTRATE SPECIFICITIES AND BIOLOGICAL ROLES OF POLYAMINE BIOSYNTHETIC ENZYMES IN MICROORGANISMS

JEONGMI LEE, Ph.D.

The University of Texas Southwestern Medical Center at Dallas, 2008

MENTOR: MARGARET A. PHILLIPS, Ph.D.

The β/α-barrel fold-type basic amino acid decarboxylases include eukaryotic ornithine decarboxylases (ODC), and bacterial and plant enzymes with activity on L-arginine and *meso*-diaminopimelate. These enzymes catalyze essential steps in polyamine and lysine biosynthesis. Phylogenetic analysis suggests that diverse bacterial species also contain ODC-like enzymes from this fold-type. However, in comparison to the eukaryotic ODCs, amino acid differences were identified in the sequence of the 3_{10}-helix that forms a key specificity element in the active site, suggesting they might function on novel substrates. Putative decarboxylases from a phylogenetically diverse range of bacteria were characterized to determine their substrate preference. Enzymes from

species within *Methanosarcina*, *Pseudomonas*, *Bartonella*, *Nitrosomonas*, *Thermotoga* and *Aquifex* showed a strong preference for L-ornithine, while the enzyme from *Vibrio vulnificus* (*Vv*L/ODC) had dual specificity functioning well on both L-ornithine and L-lysine. The X-ray structure of *Vv*L/ODC was solved in the presence of the reaction products putrescine and cadaverine to 1.7 and 2.15 Å, respectively. The overall structure is similar to eukaryotic ODC, however reorientation of the 3_{10}-helix enlarges the substrate binding-pocket, thereby allowing L-lysine to be accommodated. The structure of the putrescine-bound enzyme suggests that a bridging water molecule between the shorter L-ornithine and key active site residues provides the structural basis for *Vv*L/ODC to also function on this substrate. Our data demonstrate that there is greater structural and functional diversity in bacterial polyamine biosynthetic decarboxylases than previously suspected. The β/α-barrel fold decarboxylases also include a group of bacterial putative carboxynorspermidine decarboxylases (CANSDCs), which were hypothesized to be involved in norspermidine biosynthesis. Putative norspermidine biosynthetic enzymes including *V.vulnificus* CANSDC were characterized to determine their substrate specificities. The polyamine biosynthetic pathway in *V.cholerae* was confirmed by *in vivo* reconstitution of norspermidine biosynthetic genes in *E.coli*. Knockout of polyamine biosynthetic genes in *V.cholerae* revealed that normal levels of norspermidine are not essential for cell viability and that norspermidine is important for biofilm formation as a signaling molecule in more than one regulatory pathways for this process. Our preliminary data from real time RT-PCR suggest that norspermidine may also be related to quorum sensing and virulence gene expressions in *V.cholerae*.

TABLE OF CONTENTS

PRIOR PUBLICATIONS

1. J Lee, AJ Michael, D Martynowski, EJ Goldsmith and MA Phillips, 2007, Phylogenetic diversity and the structural basis of substrate specificity in the β/α-barrel fold basic amino acid decarboxylases, Journal of Biological Chemistry, **282** (37), 27115-27225

2. J Lee, D Kang, KH Lee, M Ichiba, J Zhang, K Tomokuni, ES Hwang, M Ha, SG Kim, SB Han, JW Choi, E Lee, JY Jang, PT Strickland, A Hirvonen and SH Cho, 2002, Influence of *GSTM1* genotype on association between aromatic DNA adducts and urinary PAH metabolites in incineration workers, Mutation Research – Genetic Toxicology and Environmental Mutagenesis, **514**, 213-221

3. KH Lee, J Lee, M Ha, JW Choi, SH Cho, ES Hwang, PT Strickland, A Hirvonen and D Kang, 2002, Influence of polymorphism of *GSTM1* gene on association between glycophorin A mutant frequency and urinary PAH metabolites in incineration workers, Journal of Toxicology and Environmental Health – Part A, **65**, 355-363

LIST OF FIGURES

LIST OF SCHEMES AND TABLES

LIST OF ABBREVIATION

Å	angstrom
AAT	aspartate aminotransferase
ADC	arginine decarboxylase
AdoMet	*S*-adenosylmethionine
AdoMetDC	*S*-adenosylmethionine decarboxylase
AI	autoinducer
AIH	agmatine iminohydrolase
Ap	ampicillin
AR	alanine racemase
ASA	L-aspartic β-semialdehyde
AT	aminotransferase
ATCC	American Tissue and Culture Collection
CANS	carboxynorspermidine
CANSDC	carboxynorspermidine decarboxylase
CANSDH	carboxynorspermidine dehydrogenase
Cb	carbenicillin
cm	centimeter
Cm	chloramphenicol
CT	cholera toxin
*cv*ADC	*Plasmodium bursaria* chlorella virus-1 arginine decarboxylase
DABA	L-2,4-diaminobutyrate
DABA AT/DC	fusion protein of diaminobutyrate aminotransferase and diaminobutyrate decarboxylase
DABA DC	diaminobutyrate decarboxylase
DAPDC	diaminopimelate decarboxylase
DFMO	α-difluoromethylornithine
DNA	deoxyribonucleic acid
DTT	dithiothreitol
g	gram
H-bond	hydrogen bond
HPLC	high performance liquid chromatography
hr	hour
kDa	kilodalton
kg	kilogram
Kn	kanamycin
L	liter
L/ODC	dual function lysine and ornithine decarboxylase
L-Arg	L-arginine

LB	Luria Bertani media
L-Lys	L-lysine
L-Orn	L-ornithine
M	molar
min	minute
ml	milliliter
mM	millimolar
MTA	5'-methylthioadenosine
NCPAH	*N*-carbamoylputrescine aminohydrolase
NIH	National Institute of Health
nm	nanometer
nM	nanomolar
OD_{595}	optical density at 595 nm
OD_{600}	optical density at 600 nm
ODC	ornithine decarboxylase
ORF	open reading frame
PCR	polymerase chain reaction
PDB	Protein Data Bank
PLP	pyridoxal 5′-phosphate
Pmol	picomoles
PMSF	phenylmethylsulfonyl fluoride
QS	quorum sensing
r.m.s.d.	root mean square deviation
rbs	ribosome binding site
RNA	ribonucleic acid
rpm	revolutions per minute
RT	real-time
s	second
SDS-PAGE	sodium dodecyl sulfate polyacrylamide gel electrophoresis
Sm	streptomycin
SpdSyn	spermidine synthase
SpmSyn	spermine synthase
TCA	trichloroacetic acid
TCP	toxin-coregulated pilus
UV	ultraviolet
*Vc*CANSDC	*Vibrio cholerae* carboxynorspermidine decarboxylase
*Vc*CANSDH	*Vibrio cholerae* carboxynorspermidine dehydrogenase
*Vc*DABA AT/DC	*Vibrio cholerae* diaminobutyrate aminotransferase and decarboxylase
Vis	visible

vps	*vibrio* polysaccharide
*Vv*CANSDC	*Vibrio vulnificus* carboxynorspermidine decarboxylase
*Vv*L/ODC	*Vibrio vulnificus* lysine/ornithine decarboxylase
µg	microgram
µl	microliter
µM	Micromolar

CHAPTER 1

Introduction

A. FUNCTIONAL DIVERSITY OF β/α-BARREL FOLD BASIC AMINO ACID DECARBOXYLASES

1. Diverse Enzymatic Reactions Catalyzed by the β/α-Barrel Fold Decarboxylases

Pyridoxal Phosphate Enzymes with Different Structural Folds

Pyridoxal-5′-phosphate (PLP), an active form of vitamin B_6, is used as a cofactor in enzymes catalyzing a wide range of reactions, such as transamination, racemization, decarboxylation and elimination (Eliot and Kirsch, 2004). These catalytically versatile PLP-dependent enzymes play roles in diverse biochemical pathways, largely involved in amino acid metabolism. In addition to their mechanistic diversity, they are structurally diverse: all characterized structures of PLP-dependent enzymes fall into five distinct structural groups I-V (Grishin et al., 1995). Although the reaction type is generally believed to have evolved within the same structural fold in PLP enzymes (Schneider et al., 2000), a number of enzymes using the same chemical reaction are found in different structural folds, suggesting that evolution of those reaction types occurred later within the same structural fold. For example, enzymes that catalyze the decarboxylation of basic amino acids evolved within two distinct structural classes: those with structural homology to aspartate aminotransferase (group III/AAT-fold decarboxylases), and those that are homologs of alanine racemase (group IV/β/α-barrel fold decarboxylases) (Grishin et al., 1995; Sandmeier et al., 1994).

Substrate Specificity of β/α-Barrel Fold Basic Amino Acid Decarboxylases

Decarboxylases belonging to the group III/AAT fold-type are largely prokaryotic, whereas the group IV/β/α-barrel fold enzymes are extensively represented in both eukaryotes and prokaryotes. β/α-barrel fold enzymes include the eukaryotic ornithine decarboxylases (ODC), plant and eubacterial arginine decarboxylases (ADC), prokaryotic diaminopimelate decarboxylases (DAPDC), which have substrate specificity for L-ornithine, L-arginine and *meso*-diaminopimelate, respectively (Figure 1.1). Based on one report, a bacterial decarboxylase from *Selenomonas ruminantium* with dual specificity for L-lysine and L-ornithine (L/ODC) (Takatsuka et al., 2000) is one member of the family and there are also a group of bacterial sequences from the family that have been annotated as carboxynorspermidine decarboxylases (CANSDCs) (Yamamoto et al., 1994) (Figure 1.1), though direct enzymatic proof of this is lacking. Finally, an enzyme from this family was identified in *Paramecium bursaria* chlorella virus (*cv*ADC). Whereas β/α-barrel fold enzymes with different substrate specificities share low sequence identity with one another (<20%), *cv*ADC groups in phylogenetic analysis with the eukaryotic ODCs, and it shares high sequence identity (~40%) with the eukaryotic ODCs, and it has specificity for L-arginine (Shah et al., 2007; Shah et al., 2004).

Classical studies based on *Escherichia coli* had suggested that the L-ornithine specific decarboxylase activity in bacteria was limited to the AAT-fold enzymes, and that the dual specificity enzyme from *S. ruminantium* represented an isolated example of a β/α-barrel fold decarboxylase in bacteria with activity on L-ornithine. However a number of novel bacterial sequences with homology to the β/α-barrel fold decarboxylases were

recently identified in sequenced bacterial genomes (Kidron et al., 2007) and their real substrate specificities have not been determined.

Biochemistry and Roles of the β/α-Barrel Fold Basic Amino Acid Decarboxylases

The basic amino acid decarboxylases catalyze essential steps in two important metabolic pathways, polyamine (ODC, ADC and CANSDC) and lysine biosynthesis (DAPDC) (Figure 1.1). Polyamines, represented by putrescine, spermidine and spermine, are naturally occurring polycationic compounds with two or more primary amines. Polyamines are present in all living organisms and essential for cell growth. In mammals they play important roles in cell cycle (Oredsson, 2003), cancer (Pegg, 2006; Seiler et al., 1998) and embryonic development (Heby, 1995). In addition to their roles in growth, they function in biofilm formation (Karatan et al., 2005; Patel et al., 2006) and motility (Sturgill and Rather, 2004) in bacteria.

Enzymes involved in the polyamine biosynthetic pathway have been identified as potential targets for drugs (Casero and Marton, 2007). ODC catalyses the decarboxylation of L-ornithine to putrescine, which is the first committed step in polyamine biosynthesis in the metazoans, fungi and many protozoans (Figure 1.2). ODC is a well-known drug target for therapeutic intervention in the polyamine pathway, and DL-α-difluoromethylornithine (DFMO), an irreversible inhibitor of ODC, is a clinically proven treatment for African sleeping sickness caused by *Trypanosoma brucei* (Bacchi et al., 1980; Fries and Fairlamb, 2003). While polyamine biosynthesis through catalysis by ODC is predominantly found in animals and fungi, plants utilize an alternative pathway by employing ADC as a key enzyme in addition to ODC (Figure 1.2). ADC catalyzes

decarboxylation of L-arginine to agmatine, which is further converted to putrescine. ADC in plants is regarded as a general stress enzyme (Galston and Sawhney, 1990). *Selenomonas ruminantium* was regarded as the only prokaryotic organism that has a β/α-barrel fold decarboxylase with dual substrate specificity on L-ornithine and L-lysine (Takatsuka et al., 2000). Diamines, putrescine and cadaverine, which are decarboxylated products of L-ornithine and L-lysine, respectively (Figure 1.1), have been found to be essential components for cell wall synthesis in some bacteria including *S.ruminatium* (Takatsuka and Kamio, 2004). Based on the report on the *Vibrio alginolyticus* CANSDC (Yamamoto et al., 1994), CANSDC produces norspermidine (Figure 1.1), which is one of the major polyamines in *Vibrio* species (Yamamoto et al., 1986b), from carboxynorspermidine (Figure 1.1). Norspermidine was proposed to be an intercellular signaling molecule involed in biofilm formation in *V.cholerae* (Karatan et al., 2005).

In bacteria, L-lysine is produced from L-aspartate via the lysine biosynthetic pathway, which is absent in humans because humans take up L-lysine from diet. In the lysine pathway, *meso*-diaminopimelate is converted to L-lysine through the decarboxylation reaction of DAPDC (Figure 1.1). L-lysine is often an essential component of the bacterial cell wall, which makes the lysine biosynthetic pathway a good target for antibacterial drugs (Born and Blanchard, 1999).

2. Structures of the β/α-Barrel Fold Decarboxylases

Overall Structure of β/α-Barrel Fold Decarboxylases

X-ray structures of several β/α-barrel fold decarboxylases including eukaryotic ODCs (Almrud et al., 2000; Grishin et al., 1999; Jackson et al., 2003; Kern et al., 1999),

bacterial DAPDCs (Gokulan et al., 2003; Ray et al., 2002), and *cv*ADC (Shah et al., 2007) have been solved. The enzymes are obligate homodimers and the monomers are composed of a β/α-barrel N-terminal domain and a β-sheet C-terminal domain (Figure 1.4). Two identical active sites are formed at the dimer interface between the N-terminal domain from one subunit and the C-terminal domain from the other. The PLP binding site is formed at the loops of β/α-barrel and C-terminal β-strands inside the active site. In the solved structures, substrate analogs are often found forming a Schiff base with PLP whereas Lys69, which is absolutely conserved in all β/α-barrel fold decarboxylase sequences, often forms a Schiff base with PLP in the absence of substrate analogs. Substrate analogs make key contacts with residues from both monomers. In *T. brucei* ODC the δ-amino group of the co-crystallized ligand (e.g. putrescine, DFMO and D-ornithine) interacts with Asp361 from one monomer and with Asp332 from the other. The Asp332 residue projects from a short 3_{10}-helix at the back of the substrate-binding pocket.

Structural Insights into Different Substrate Specificities of β/α-Barrel Fold Decarboxylases

Structures of the β/α-barrel fold enzymes with different substrate specificities have been compared to study the structural basis of substrate specificity. Eukaryotic ODCs and *cv*ADC share about 40% sequence identity and are globally very similar with rmsd of less than 1.5 Å. Bacterial DAPDCs share less than 20% sequence identity with eukaryotic ODCs but they are still superimposable to the eukaryotic ODCs and *cv*ADC

(rmsd > 2 Å). Overlays of the product bound structures of ODCs, bacterial DAPDCs and *cv*ADC identified the 3_{10}-helix at the active site as a key determinant of substrate specificity (Shah et al., 2007). The 3_{10}-helix takes a different position in each structure depending on its substrate while the overall structures are similar. The 3_{10}-helix of *cv*ADC moved further from PLP, enlarging the active site pocket to accommodate the larger substrate L-arginine compared to the ODCs that act on the smaller substrate L-ornithine. The helix of bacterial DAPDCs assumes the most different position among the enzymes (see Figure 3.2B). The distance between C4′ of PLP and the helix (C_α of Asp-332, Glu-296 and Glu-348 of *T.brucei* ODC, *cv*ADC and *Methanococcus jannaschii* DAPDC, respectively) is 9.7 Å for *T.brucei* ODC, 12.1 Å for *cv*ADC and 15.3 Å for *M.jannaschii* DAPDC. While the flexible position of the 3_{10}-helix enables the enzyme to accommodate different size substrates, changes in amino acid composition of the 3_{10}-helix allow specific interactions to occur with the full range of substrates. Asp332, absolutely conserved in eukaryotic ODCs, is replaced by E296 in *cv*ADC (Figure 1.3), allowing the helix to move further to accommodate L-arginine while keeping interaction with the bound agmatine. Tyr337 substitutes for Asp332 in *M.jannaschii* DAPDC and it interacts with the bound product L-lysine. Therefore both the amino acid composition of the helix and its position were proposed to be major determinants for substrate specificity in the β/α-barrel fold decarboxylases (Shah et al., 2007).

B. BIOSYNTHESIS AND FUNCTION OF POLYAMINES IN *VIBRIO* SPECIES

1. Polyamine Biosynthetic Pathways

Eukaryotic Polyamine Biosynthesis Pathway

Polyamine biosynthetic pathways in mammalian cells have been well characterized (Figure 1.2) (Morgan, 1999). L-arginine is converted to L-ornithine by the action of arginase, and then L-ornithine is converted to putrescine by ODC. *S*-adenosylmethionine decarboxylase (AdoMetDC) catalyzes the conversion of *S*-adenosylmethionine (AdoMet) into decarboxylated *S*-adenosylmethionine (dcAdoMet). Spermidine synthase, which has aminopropyltransferase activity, incorporates the aminopropyl group of dcAdoMet into putrescine, forming spermidine. Similar to spermidine synthase, spermine synthase adds an additional propylamine moiety to spermidine to form spermine. 5'-methylthioadenosine (MTA) is produced as a byproduct from the aminopropyltransferase reactions of spermidine synthase and spermine synthase.

In plants, putrescine can be produced either directly from L-ornithine by the action of ODC or indirectly from L-arginine by the actions of ADC, agmatine iminohydrolase (AIH) and N-carbamoylputrescine amidohydrolase (NCPAH) (Figure 1.2) (Slocum et al., 1984). Agmatine, which is a decarboxylated product of L-arginine by ADC, is converted to N-carbamolyputrescine via AIH, which is further transformed to putrescine via NCPAH.

Prokaryotic Polyamine Biosynthesis Pathway

Putrescine and spermidine, which are the most common polyamines in eukaryotes, are also found as the major polyamines in most prokaryotic cells. Prokaryotes were reported to biosynthesize putrescine and spermidine in a similar fashion to plants (Figure 1.2) (Tabor and Tabor, 1985). Putrescine can be produced either directly from L-

ornithine by ODC activity or indirectly from L-arginine. After agmatine is produced from L-arginine via ADC, bacteria utilize an enzyme called agmatinase to remove urea from agmatine, producing putrescine whereas two enzymes AIH and NCPAH are used in plants for putrescine production from agmatine.

In addition to these common polyamines above however, a wide variety of unusual polyamines such as homospermidine, norspermidine, 1, 3-diaminopropane and 2-hydroxyputrescine are produced particularly in prokaryotes. This suggests there should be more diverse polyamine biosynthesis pathways in prokaryotes than represented in the Figure 1.2. Although polyamine compositions have been comprehensively studied in a number of bacteria in an attempt to utilize polyamines as chemotaxonomic markers for classification of prokaryotes (Hamana and Matsuzaki, 1992), studies on the unusual polyamines from a biological point of view have been neglected and their biosynthesis and physiological roles remain largely unknown.

Norspermidine is found as one of the major polyamines in a number of prokaryotes and eukaryotes: thermophilic bacteria (Hamana et al., 2001), archaea (Hamana and Itoh, 2001), and aquatic organisms such as algae (Hamana et al., 2004). Together with spermidine, it is the most abundant polyamine in *Vibrio* species (Yamamoto et al., 1991). There is no established pathway for norspermidine biosynthesis, although Yamamoto et al. (Yamamoto et al., 1986a) proposed a novel pathway for norspermidine synthesis in *Vibrio alginolyticus* and *V. parahaemolyticus* without direct evidence at the genetic and molecular level (Figure 1.5; see below).

Biochemistry of Putative Norspermidine Biosynthetic Enzymes and Proposed Norspermidine Pathway in Vibrio Species

Many bacteria including *E.coli* utilize dcAdoMet as a propylamine group donor to make spermidine via aminopropyltransferase activity of spermidine synthase. However, several bacteria including *Vibrio* species (Tait, 1976; Yamamoto et al., 1986a) and seedlings of *Lathyrus sativus* (grass pea) (Srivenugopal and Adiga, 1980) were reported to lack the aminopropyltransferase activity, which suggested an alternative mode of polyamine biosynthesis bypassing AdoMetDC and spermidine synthase. Yamamoto et al. showed that L-aspartic β-semialdehyde (ASA), derived from L-aspartate, was incorporated into norspermidine and that 1,3-diaminopropane (DAP) was used to form carboxynorspermidine, which was decarboxylated to norspermidine in *V.alginolyticus* and *V.parahaemolyticus* (Yamamoto et al., 1986a). In subsequent studies, they partially characterized three enzymes from *V.alginolyticus*: diaminobutyrate decarboxylase (DABA DC), carboxynorspermidine (CANS) synthase and carboxynorspermidine decarboxylase (CANSDC) (Nakao et al., 1989; Nakao et al., 1991; Yamamoto et al., 1994) (Figure 1.5). DABA DC produces 1, 3-diaminopropane (DAP), of which the precursor is unknown, through decarboxylation of L-2, 4-diaminobutyrate (DABA). DAP was found to condense with L-aspartic β-semialdehyde (ASA) through Schiff base formation and the Schiff base intermediate was subsequently reduced to carboxynorspermidine by CANS synthase in a nicotinamide adenine dinucleotide phosphate (NADPH)-dependent manner (Nakao et al., 1991). Nakao et al. claimed that CANS synthase accepted putrescine as a less preferred substrate compared to DAP, to form carboxyspermidine (Nakao et al., 1991). CANS synthase is now annotated as

carboxynorspermidine dehydrogenase (CANSDH) in the sequenced genome of *Vibrio* species. Carboxynorspermidine was decarboxylated to norspermidine by CANSDC, which was also active on carboxyspermidine with similar catalytic efficiency to carboxynorspermidine (Yamamoto et al., 1994).

2. Biological Aspects of Norspermidine in *Vibrio cholerae*

Vibrio cholerae as a Model Organism to Study Biosynthesis and Biology of Norspermidine

Species of the genus *Vibrio* belong to the γ-subdivision of the Proteobacteira. They contain norspermidine as one of the most abundant polyamines (Yamamoto et al., 1986b) and some *Vibrio* species such as *V.cholerae, V.parahaemolyticus* and *V.vulnificus* are important human pathogens. *V.cholerae* is a Gram-negative human pathogen that causes an acute disease called cholera. Cholera is transmissible through the ingestion of contaminated water or food and is characterized in profuse watery diarrhea, which can lead to death when not properly treated. Two serogroups of *V.cholerae* can cause outbreaks: O1 that has been responsible for seven cholera pandemics since 1817 and O139 that caused the eighth pandemic most recently in 1992 (Faruque et al., 1998). *V.cholerae* O1 is further divided into two biotypes: classical, that caused the first six pandemics and El Tor that was responsible for the seventh and is currently a predominant biotype. The massive diarrhea of cholera is induced by the activity of an enterotoxin called cholera toxin (CT) that activates the adenylate cylase in the intestinal epithelial cells, resulting in hypersecretion of water and chloride ions (Kaper et al., 1995). Toxin-

coregulated pilus (TCP) is the other major virulence factor that is required for adherence to the epithelial cells to for colonization of the small intestine (Kaper et al., 1995).

Known Biological Roles of Norspermidine in V.cholerae

Although polyamines are essential for normal cell growth, their biological roles in detail are largely unknown. There are only a few studies on the *in vivo* effect of norspermidine, which are described briefly below. Iron is an essential element in almost all microorganisms required for many metabolic processes. In microbial habitats iron exits mostly as Fe^{+3}, which is extremely insoluble. Also iron is exclusively stored in various proteins such as ferritin and strictly regulated in mammalian hosts, which leaves very little free iron available for transport in microbes. Many microbes including important human pathogens have developed small organic molecules called siderophores that are secreted and chelate Fe^{+3} with high affinity under iron-limiting environment (Miethke and Marahiel, 2007). Once Fe^{+3} is captured by siderophores, the iron-siderophore complex is transported inside as the whole complex or as single ion. *V.cholerae* is known to produce only one siderophore, vibriobactin, which is a catechol (benzenediol) (Griffiths et al., 1984) though it can also utilize siderophores that are synthesized by other species of bacteria. In vibriobactin norspermidine is found as a backbone molecule and dihydroxybenzoate (DHB) moieties are attached to norspermidine either directly or through cyclized threonine bridges (Figure 1.6).

Recently norspermidine has been found as an extracellular signaling molecule for biofilm formation in *V.cholerae* (Karatan et al., 2005). Biofilm, a niche created by microbes, is a multicellular aggregate that is associated with abiotic surfaces. Biofilm

formation is initiated from a monolayer consisting of exopolysaccharide termed VPS (*Vibrio* polysaccharide), which is synthesized by a number of proteins encoded by the *vps* genes and it is regulated by a few environmental signals including nutrients and quorum sensing (Stanley and Lazazzera, 2004). *V.cholerae* is a natural inhabitant of the aquatic environments as a free-living organism or in biofilm. Its adhesion to surfaces by biofilm formation seems crucial for survival in the environment (Islam et al., 1993). When it enters the human intestine as a pathogen, intestinal colonization through adherence to epithelial cells by TCP (toxin coregulated pilus) is a prerequisite for the survival of *V.cholerae*. Karatan et al. have shown that norspermidine activates biofilm formation in a NspS- and MbaA-dependent manner (Karatan et al., 2005). NspS, norspermidine sensor protein, is a periplasmic protein homologous to PotD, a spermidine-binding protein of *E.coli*. MbaA is a putative integral membrane protein containing GGDEF and EAL domains and is a repressor of biofilm formation. Karatan et al. proposed that MbaA decreases the level of 3′, 5′-cyclic diguanylic acid (c-di-GMP) that activates biofilm formation and represses virulence and motility genes, and norspermidine-NspS disrupts the function of MbaA, therefore increasing biofilm formation (Karatan et al., 2005).

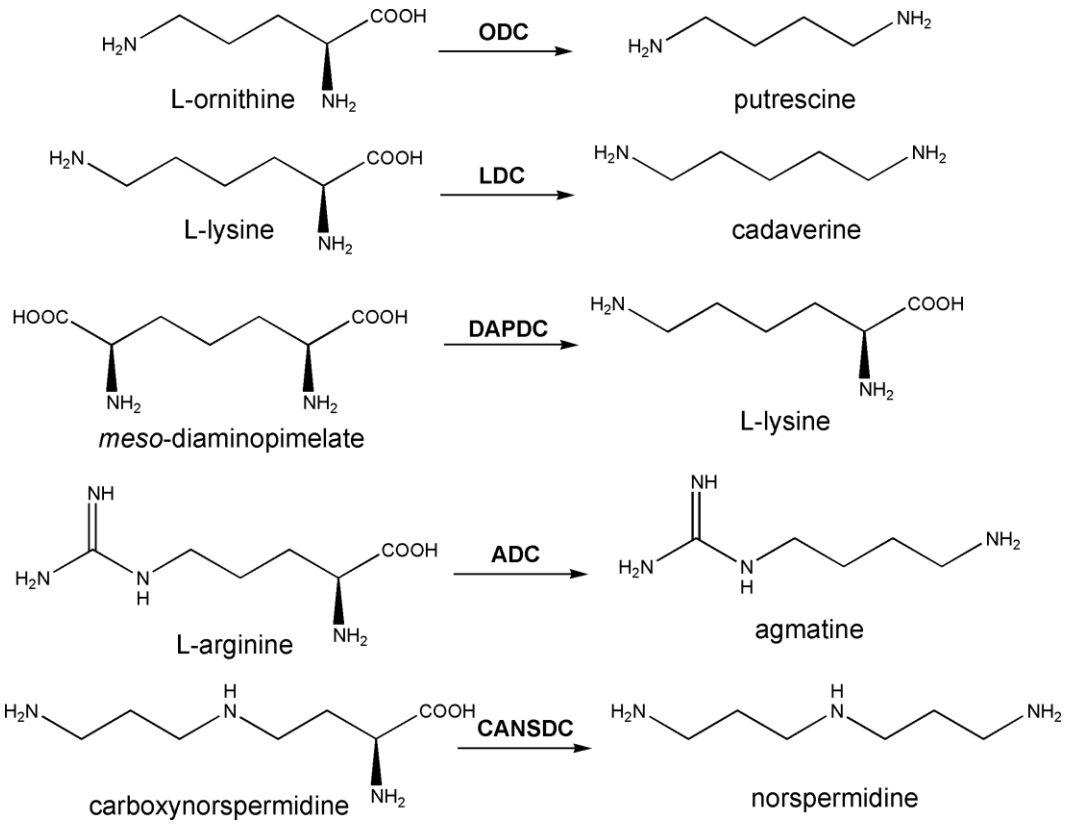

Figure 1.1 Enzymatic reactions catalyzed by the β/α-barrel fold decarboxylases

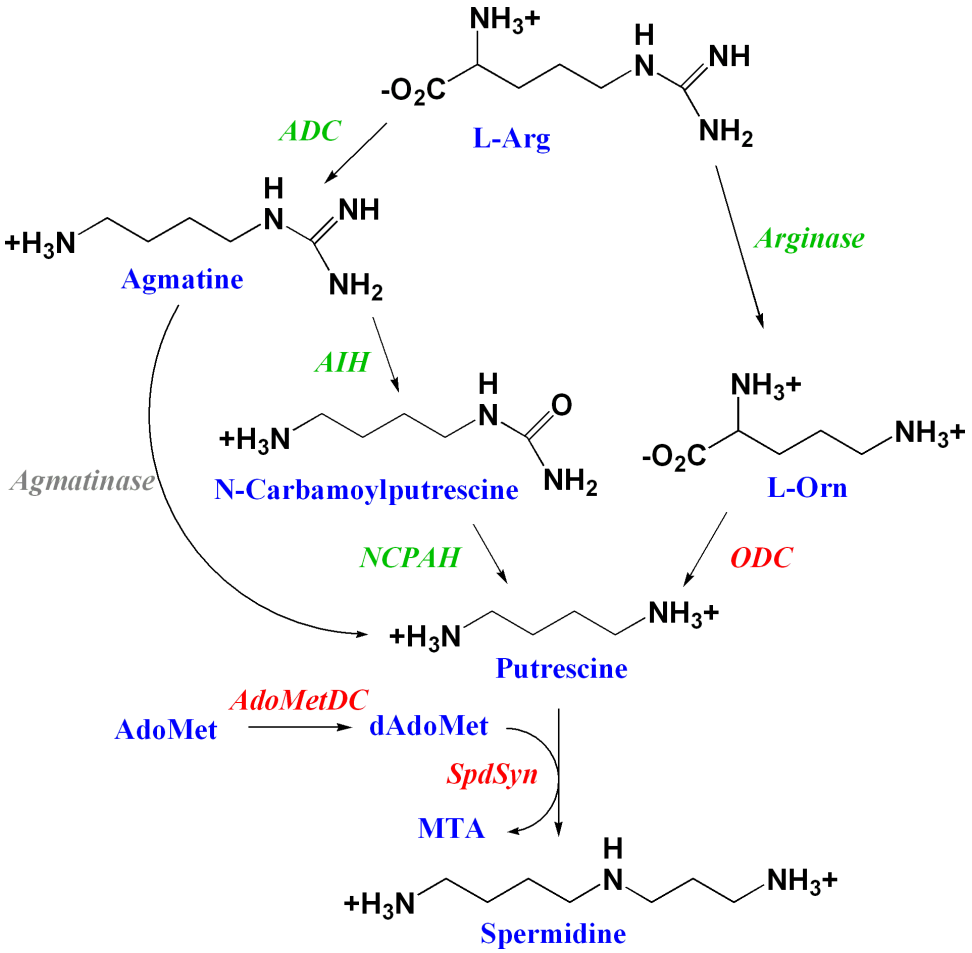

Figure 1.2 Polyamine biosynthetic pathways in mammals, plants and bacteria. Enzymes found in only plants are in green; common enzymes found in mammals, plants and bacteria are in red; bacteria can utilize L-arginine to produce putrescine via ADC and agmatinase, which is found only in bacteria. *ADC*, arginine decarboxylase; *AIH*, agmatine iminohydrolase; *NCPAH*, *N*-carbamolyputrescine amidohydrolase; *ODC*, ornithine decarboxylase; *AdoMetDC*, *S*-adenosylmethionine decarboxylase; *SpdSyn*, spermidine synthase; *AdoMet*, *S*-adenosylmethionine; *dcAdoMet*, decarboxylated *S*-adenosylmethionine; *MTA*, 5'-methylthioadenosine.

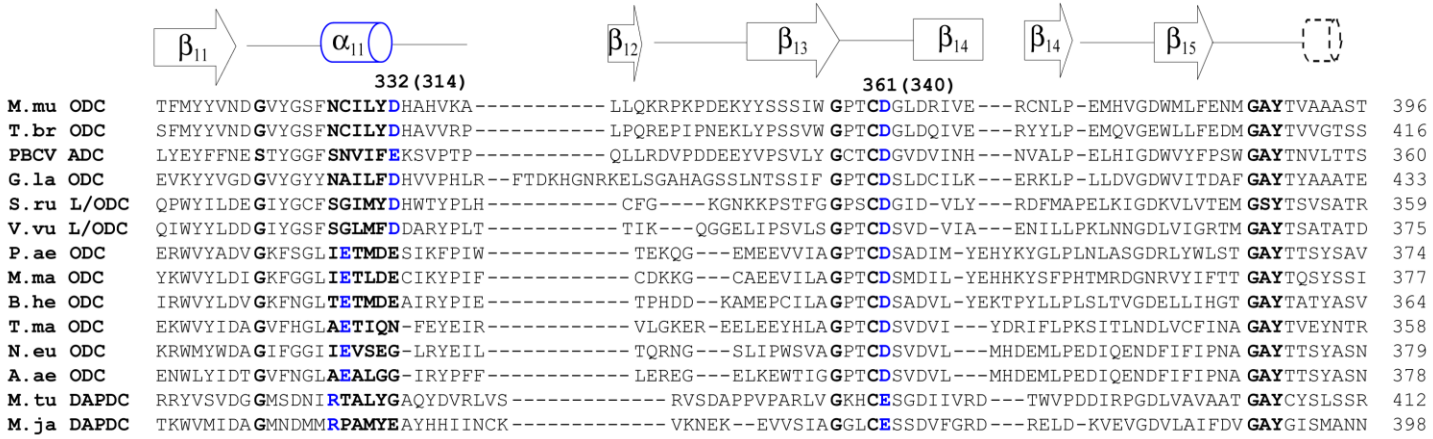

Figure 1.3 Sequence alignment of ODC and DAPDC in the active site region. The sequences of the eukaryotic ODCs (mouse ODC, TbODC), viral *cv*ADC (PBCV-1 ADC) and DAPDCs (*Methanococcus* DAPDC, *Mycobacterium* DAPDC) of known structures are aligned with those of the dual specificity L/ODCs and prokaryotic ODCs that were characterized in this study. The secondary structure elements are displayed as cartoons above the sequence and are based on the eukaryotic ODC structures. The 3_{10}-helix (specificity element) is displayed in blue. Residues labeled in blue form the unique consensus sequence that is predictive of the substrate specificity. Consensus sequences are based on structural data and sequence based structural alignment except for the bacterial ODCs, where the consensus is derived from sequence alignment data only. Numbering above the sequences is for

mouse ODC, or for *Vv*L/ODC in parenthesis. For NCBI accession numbers see Figure 1, and for the full sequence alignment see Supplemental Figure 1. Species names are abbreviated using one letter for the genus followed by two for the species, e.g. *Mus musculus*, is M.mu ODC. See (Lee et al., 2007) for the full species names.

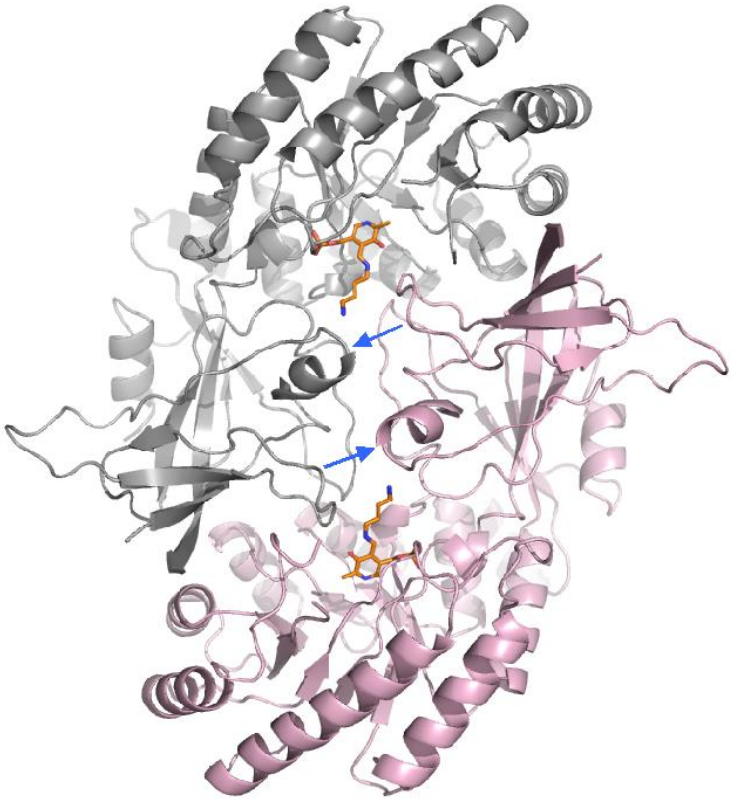

Figure 1.4 X-ray structure of *T.brucei* ODC. Two monomers are displayed in different colors. The bound PLP-putrescine is displayed in orange stick. Two 3_{10}-helices are indiated by arrows. This figure was created by PyMol (DeLano, 2003).

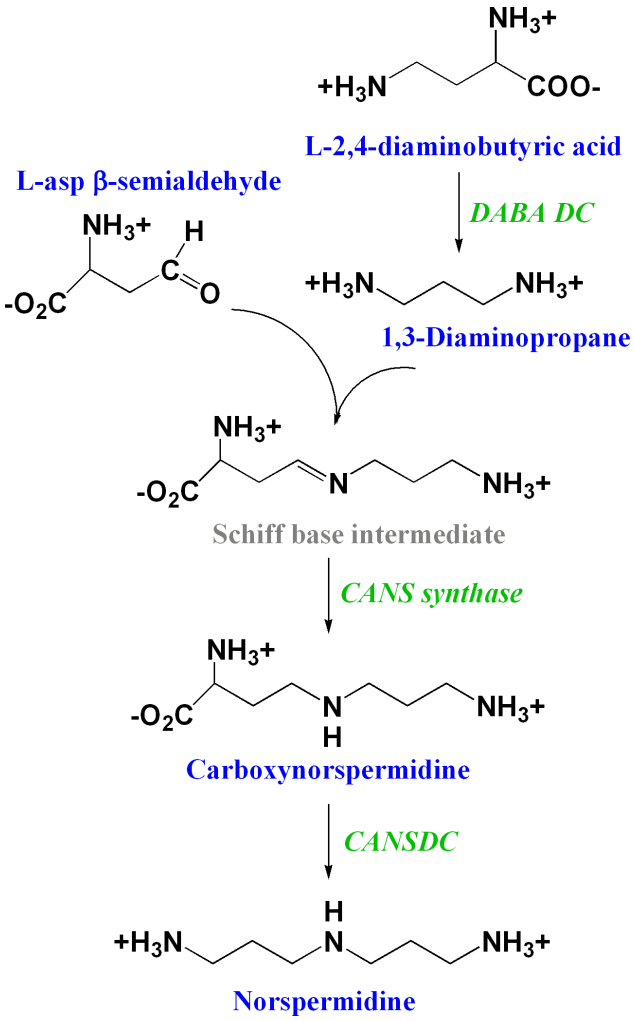

Figure 1.5 Previously proposed norspermidine biosynthesis pathway in *Vibrio* species. *DABA DC*, 2, 4-diaminobutyrate decarboxylase; *CANS synthase*, carboxynorspermidine synthase; *CANSDC*, carboxynorspermidine decarboxylase.

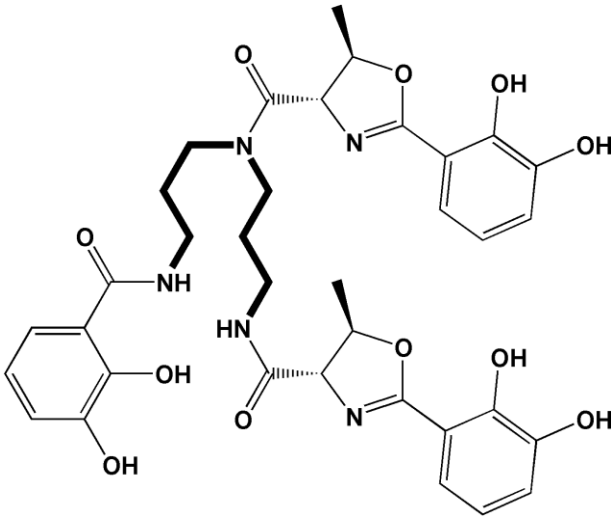

Figure 1.6 Structure of vibriobactin (adapted from Griffiths et al. (Griffiths et al., 1984)). Norspermidine backbone is shown in bold.

CHAPTER 2

BIOCHEMICAL CHARACTERIZATION OF β/α-BARREL FOLD BASIC AMINO ACID DECARBOXYLASES FROM DIVERSE MICROORGANISMS

A. Introduction

Basic amino acid decarboxylation occurs in important metabolic pathways such as polyamine and lysine biosynthesis. The reaction is catalyzed by PLP-dependent decarboxylases of two different structural folds (Grishin et al., 1995; Sandmeier et al., 1994): structural homologs of aspartate aminotransferase (AAT-fold/group III decarboxylases) and homologs of alanine racemase (β/α-barrel fold/group IV decarboxylases). β/α-barrel fold enzymes are represented in both eukaryotes and prokaryotes whereas AAT-fold enzymes are almost exclusively found in prokaryotes. Eukaryotic ODCs, plant and eubacterial ADCs, prokaryotic DAPDCs, dual substrate specificity enzyme L/ODC from *S.ruminantium* and prokaryotic putative CANSDCs belong to the β/α-barrel fold-type enzymes, indicating the functional diversity of β/α-barrel fold decarboxylases.

Structures of several β/α-barrel fold decarboxylases including eukaryotic ODCs (Almrud et al., 2000; Grishin et al., 1999; Jackson et al., 2003; Kern et al., 1999), prokaryotic DAPDCs (Gokulan et al., 2003; Ray et al., 2002) and chlorella virus ADC (Shah et al., 2007) have been solved . The structural data together with sequence alignment analysis provided insights into understanding how these homologous enzymes have different substrate preferences within the same structural fold (Figure 1.3). Two

amino acid compositions at 332 and 361 positions and the position of the 3_{10}-helix were identified as key determinants for the different substrate specificities of β/α-barrel fold decarboxylases (Shah et al., 2007). The amino acid residue at the 361 position is conserved as Asp in all eukaryotic ODCs and the chlorella virus, whereas it is replaced by Glu in the prokaryotic DAPDCs. Eukaryotic ODCs contain an Asp residue at the 332 position. Asp332 is invariant amongst the eukaryotic ODCs while it is substituted for Tyr and Glu in *Methanococcus jannaschii* DAPDC and *cv*ADC, respectively (Figure 1.3).

Recently a number of novel bacterial sequences with homology to the β/α-barrel fold decarboxylases were identified in sequenced bacterial genomes (Kidron et al., 2006). In our current study, phylogenetic and experimental analysis suggested that the β/α-barrel fold decarboxylases segregate into 4 distinct groups containing ADCs, DAPDCs, ODCs, and putative CANSDCs (Figure 2.1). The ODCs can be further classified into three subclades: the eukaryotic ODCs, bacterial sequences containing the *S. ruminantium* dual specificity L/ODC and a third group of uncharacterized bacterial ODC-like sequences. Interestingly, most of the putative ODCs have Asp to Glu change at their 332 position while the other active site residues including Asp361 were conserved (Figure 1.3). This observation led us to address the question of whether this amino acid change in these enzymes could also be indicative of substrate specificity change as observed in *cv*ADC. Herein we have experimentally determined the substrate preferences of these putative ODCs from a diverse group of bacteria for the first time. Despite the presence of key amino acid changes in the 3_{10}-helix specificity element relative to the eukaryotic ODCs, these enzymes utilize L-ornithine as their primary substrate. In addition, the study

provides experimental confirmation for a distinct clade of dual function enzymes with specificity for both L-ornithine and L-lysine, similar to that reported for the enzyme from *S. ruminantium*.

B. Experimental Procedures

1. Materials

L-ornithine, L-lysine, L-arginine, *meso*-diaminopimelic acid, pyridoxal 5'-phosphate (PLP), and all other reagents were purchased from Sigma (St. Louis, MO) unless noted otherwise. L-[1-^{14}C]ornithine hydrochloride (52.0 mCi/mmol), L-[U-^{14}C]lysine monohydrochloride (304 mCi/mmol) and L-[U-^{14}C]arginine monohydrochloride (308 mCi/mmol) were purchased from Amersham Biosciences (Piscataway, NJ). D/L-DFMO was obtained from Marion Merrell Dow Inc. (Cincinnati, OH). Infinity^{TM} carbon dioxide detection reagent was from Thermo Electron (Lousville, CO).

Genomic DNA from *Methanosarcina mazei* (ATCC BAA-159D), *Nitrosomonas europaea* (ATCC 19718), *Bartonella henselae* (ATCC 49882) and *Thermotoga maritima* (ATCC 43589) were purchased from ATCC (Manassas, VA). Genomic DNA from *Giardia lamblia*, *Pseudomonas aeruginosa* (ATCC 47085D), *V. vulnificus* CMCP6 and *Aquifex aeolicus* were kindly provided by Drs. Ching C. Wang (University of California San Francisco, San Francisco, CA), Hong Zhang (University of Texas Southwestern Medical Center, Dallas, TX), Joon Haeng Rhee (Chonnam University, Gwangju, Korea) and Michael Thomm (Universität Regensburg, Regensburg, Germany), respectively.

2. Phylogenetic Analysis

Mouse ODC, *E. coli* ADC, *S. ruminantium* L/ODC and *V. alginolyticus* CANSDC were each used to search the non-redundant protein database at the National Center for Biotechnology Information GenBank using BLAST. Sequences were chosen to optimally represent diverse bacterial phyla and to reduce the number of members from the same phylum for the phylogenetic analysis. Sequences were aligned using ClustalX (version 1.8) (Thompson et al., 1997) and edited for display with GeneDoc (version 2.6.002) (Nichloas, 1997). Sequences from the N- and C-termini were removed to facilitate the alignment. Phylogenetic analysis of the aligned sequences was implemented in PAUP* (Swofford, 2000). A neighbor-joining tree with nodes assessed by 1000 bootstrap replicates was constructed and imported into TreeView (Page, 1996). Taxonomic descriptions were obtained from the NCBI (http://ncbi.nlm.nih.gov). Secondary structure predictions were performed on the sequences using the PSIPRED program (http://bioinf.cs.ucl.ac.uk/psipred/).

3. Cloning of the Putative Decarboxylase Genes

The genes for the selected ODC homologs were amplified by PCR from the genomic DNA using the primers described in Table 2.3 and cloned into one of the following His_6-tag expression vectors: pET-15b (Novagen), pET-22b (Novagen) or a modified pRSET B (Invitrogen). The pRSET construct was generated from pfDHODH/pRSET (Hurt et al., 2006) provided by Dr. John Clardy (Harvard Medical School, Boston, MA), and the *BamHI* restriction site in pfDHODH/pRSET was mutated

by QuickChange™ site-directed mutagenesis kit (Stratagene, La Jolla, CA) using the primers mtpRSET_F and mtpRSET_R to introduce a *NcoI* site.

Cloning of the putative ODCs was as follows: open reading frames (ORFs) from *G. lamblia*, *M. mazei*, *N. europaea* were cloned into the *NcoI* and *HindIII* sites of the modified pRSET B vector, ORFs from *V. vulnificus*, *T. maritima*, *A. aeolicus and P. aeruginosa* were cloned into the *NdeI* and *XhoI* sites of pET-15b, and the ORF from *B. henselae* was cloned into the *BamHI* and *NdeI* sites of pET-15b. In the case of the ORFs from *P. aeruginosa (Xho I) and B. henselae (BamHI)* each contained a site (in parenthesis) that was removed by QuickChange™ mutagenesis before the final cloning step could be accomplished. The DAPDC and ADC genes of *V. vulnificus* CMCP6 were also amplified by PCR from genomic DNA and cloned into the *NdeI* and *XhoI* sites of pET-15b vector.

4. Protein Expression and Purification of the Putative Decarboxylases

E.coli BL21(DE3) cells transformed with protein expression vectors were grown to exponential phase at 37°C in LB medium containing ampicillin (50 μg/ml). Expression of the recombinant proteins was induced by 200 μM of isopropyl-1-thio-β-D-galactopyranoside (IPTG) at 16°C overnight. All recombinant proteins except *T. maritima* and *A. aeolicus* enzymes were purified to homogeneity using Ni^{2+}-affinity and gel filtration chromatography as described (Osterman et al., 1994; Osterman et al., 1995). For protein purification of the thermophilic enzymes (*T. maritima* and *A. aeolicus*), the cleared cell lysates were first heat-treated at 80°C for 15 min and precipitated proteins were removed by centrifugation. The *T. maritima* enzyme was further purified by anion

exchange column chromatography (MonoQ 5/50 GL column; GE Healthcare), and the *A. aeolicus* enzyme by Ni^{2+}-affinity and gel filtration chromatography. Protein purity was analyzed by SDS-PAGE and the protein concentration was determined by absorbance measurements at 280 nm. All enzyme preparations were used in assays without cleavage of the His_6-tag.

5. Spectroscopy-based Enzymatic Assays

Enzyme catalyzed decarboxylation was measured in a coupled enzyme system at 37°C using the Infinity™ carbon dioxide detection reagent. The assay method has been described previously (Osterman et al., 1994; Osterman et al., 1995). Briefly, decarboxylation is coupled to phosphoenolpyruvate carboxylase and malate dehydrogenase, allowing the rate of CO_2 formation to be monitored by the oxidation of NADH (λ_{max}=340 nm), detected at 340 nm. All assays were performed in the presence of 50 μM PLP and 4 mM DTT. Substrate stocks used in this study were adjusted to pH 7.5 except *meso*-diaminopimelic acid, which was adjusted to pH 8.5 where it has greater solubility.

6. Radiolabel-based Enzymatic Assays

The coupled enzyme assay is unsuitable for analysis at high temperature, thus the activity of the *T. maritima* and *A. aeolicus* decarboxylases was determined using the standard $^{14}CO_2$ –release assay as described previously (Pegg and McGill, 1979; Shah et al., 2004). Assays were conducted using L-[1-^{14}C]ornithine, L-[U-^{14}C]lysine or L-[U-^{14}C]arginine at 63°C or 80°C in assay buffer (50 mM NaCl, 5 mM DTT and 250 μM

PLP, 20 mM HEPES pH 8.2 and pH 7.9 at 63°C and 80°C, respectively). Assay buffers for pH profile determination utilized pH appropriate buffers (MES, pH 6.0; HEPES, pH 7.0 and pH 8.1; Glycine·NaOH, pH 9.0 and 10.0; pHs were adjusted at the corresponding reaction temperature).

7. Enzymatic Inhibition by DL-DFMO

Enzymes with activity on L-ornithine were characterized to determine if DFMO inhibited their activity in a time-dependent manner. ODCs were incubated at 37°C with racemic D/L-DFMO in buffer (20 mM Tris·HCl pH 7.5, 1 mM DTT and 20 μM PLP). At different time intervals the enzyme/DFMO mixtures were diluted 100-fold into assay mix to determine the fraction of enzyme activity remaining. Assay mix contained the carbon dioxide detection reagent premixed with 10 mM L-ornithine, 2.5 mM DTT and 50 μM PLP. The data were analyzed by the method of Kitz and Wilson (Kitz and Wilson, 1962). The observed rate constant (k_{obs}) for the enzyme inactivation was determined at different inhibitor concentrations using Eq. 1 (Figure 2.3A). These values were then fitted to Eq. 2 to determine the inactivation rate (k_{inact}) and the apparent K_I for the reaction (Figure 2.3B).

$$\frac{v}{v_0} = \exp(-k_{obs} \cdot t) \quad \text{(Eq.1)}$$

$$k_{obs} = \frac{k_{inact}[I]}{K_i^{app} + [I]} \quad \text{(Eq.2)}$$

8. Statistical Methods

GraphPad Prism4 (GraphPad Software, Inc.) was used for graphing and analyzing data for kinetic parameters. Steady-state kinetic data were fitted to the Michaelis-Menten equation by non-linear regression to obtain k_{cat} and K_m. Data for DFMO inactivation were fitted similarly to Eq. 2.

C. Results

1. Phylogenetic Analysis of the β/α-Barrel Fold Decarboxylase Family

Protein sequences exhibiting similarity to the β/α-barrel fold decarboxylases were identified by PSI-BLAST analysis of the GeneBank protein database using selected query sequences of proteins with biochemically confirmed substrate specificity including, mouse ODC, *E. coli* ADC and *S. ruminantium* L/ODC. *V. alginolyticus* CANSDC was included as a representative of this putative specificity. Phylogenetic analysis was performed for a subset of the sequences identified in the BLAST searches, representative of different bacterial phyla and each type of decarboxylase (Figure 2.1). The sequence alignment used to build the Neighbor-Joining tree is shown in Figure 2.4. Prokaryotic sequences segregated into four distinct groups. These include clades of sequences with strong similarity to the well-characterized DAPDCs and ADCs, sequences that group with the putative CANSDC, and a group that is most closely related to the eukaryotic ODCs. The prokaryotic ODC-like sequences share high sequence identity to eukaryotic ODCs (28 - 33%) whereas the bacterial decarboxylase sequences from ADCs, DAPDCs and CANSDCs show relatively low sequence identity to eukaryotic ODCs (14 - 23%). Within the prokaryotic ODC-like sequences bootstrap analysis provided some support for

a separate clade that contains the dual function L/ODC from *S. ruminantium,* as well as several predicted decarboxylases from within the γ-Proteobacteria, Bacteroidetes/Chlorobi and Planctomycetes phyla. The L/ODC clade of sequences groups more closely with the eukaryotic ODCs than with the other bacterial ODC-like sequences. The ADCs do not form a distinct clade, probably due to the lack of an outgroup in the analysis but the outliers of the ADC group are functionally characterized ADCs (e.g. *E. coli* (Wu and Morris, 1973) and *N. tabacum* (Hiatt et al., 1986)). None of the β/α-barrel fold basic amino acid decarboxylases were found in the archaeal sub-kingdom Crenarcheota, and only the DAPDC family was widely distributed in both eubacteria and archaea. Archaeal and eubacterial sequences in the DAPDC clade are not clearly segregated. ADC sequences are found only in plants within the Eukaryota and while they are found in diverse phyla within the eubacteria, they are particularly ubiquitous within the Cyanobacteria (results not shown).

In contrast to the well-characterized ADC, DAPDC and eukaryotic ODCs, no biochemical analysis has been reported for the prokaryotic ODC-like enzymes. Comparison of the amino acid sequences of the ODC-like prokaryotic enzymes with the three dimensional structure of the eukaryotic ODCs (e.g. *T. brucei* ODC and the ODC-like *cv*ADC) was undertaken to provide insight into the function of these proteins (Figure 1.3). The amino acid residues found in the substrate-binding site (e.g. Asp361 and Asp332) of the eukaryotic ODCs are conserved in the clade of enzymes that groups with *S. ruminantium* L/ODC, consistent with the finding that this enzyme can catalyze the decarboxylation of L-ornithine (Takatsuka et al., 2000). In contrast the prokaryotic ODC-like enzymes that segregate outside of the L/ODC clade have evolved significant changes

in the predicted substrate-binding pocket. Specifically, Asp332 in the 3_{10}-helix specificity element is replaced either with a Glu similarly to *cv*ADC (e.g. *P. aeruginosa, Treponema denticola, M. mazei and B. henselae*), or in other cases an acidic residue at this position is missing altogether (*T. maritima, Streptomyces coelicolor, N. europaea, Nitrospira multiformis and A. aeolicus*). Sequence alignment in this region is of good quality and it is further supported by secondary structure predictions that suggest the bacterial sequences also contain a short helix in the position of the eukaryotic ODC "specificity element". The data predict that either the active site organization of these enzymes differs from the eukaryotic ODCs, or that these enzymes have evolved novel substrate specificity. The Glu at position 332 is suggestive of L-arginine as a possible substrate based on similarity to *cv*ADC, while the sequences that have substituted neutral amino acids at this position might be predicted to have even larger changes in function.

2. Functional Analysis of the Putative Prokaryotic of β/α-Barrel Fold Decarboxylases

To determine the substrate specificity and function of the putative prokaryotic ODCs we selected enzymes from eight microorganisms for biochemical analysis. One eukaryotic organism was selected (*G. lamblia*) because it represents a basal eukaryotic lineage, and the others were of prokaryotic origin selected to represent diverse phyla. These consist of *B. henselae*, a pathogenic α-proteobacterium, *P. aeruginosa*, a pathogenic γ-proteobacterium, *N. europaea*, a β-proteobacterium, *M. mazei*, representing the only archaeal genus containing a putative ODC-like gene, two thermophilic bacteria, *A. aeolicus* and *T. maritima* and finally *Vibrio vulnificus*, a pathogenic γ-proteobacterium , which contains a predicted dual specificity L/ODC. In addition, the ADC and DAPDC

from *V. vulnificus* were characterized to serve as controls for enzymes that should have *bona fide* activity on L-arginine and *meso*-diaminopimelate. The seven putative ODCs, and the putative *V. vulnificus* L/ODC (*Vv*L/ODC), ADC and DAPDC were cloned into bacterial expression vectors, and the proteins were expressed and purified as described in Experimental Procedures. Steady-state kinetic analysis was then undertaken using a range of basic amino acid substrates (e.g. L-ornithine, L-lysine, L-arginine and *meso*-diaminopimelate).

All seven of the prokaryotic putative ODCs, and the enzyme from *G. lamblia* are able to catalyze the decarboxylation of L-ornithine with similar kinetic parameters (Table 2.1; k_{cat} ranges from 4 – 12 s^{-1}; K_m ranges from 0.12 – 2.3 mM) to those reported for the well-characterized eukaryotic enzymes from mouse (Coleman et al., 1993) and *T. brucei* (Osterman et al., 1994). They also function on L-lysine, however the k_{cat}/K_m on L-lysine is 100 – 3000-fold lower than for L-ornithine. Activity on L-arginine could not be detected, thus demonstrating that these enzymes are *bona fide* ODCs. The ODC homologs from the two thermophiles (*T. maritima and A. aeolicus*) were characterized over a range of pH and temperatures (Table 2.1). Both enzymes displayed maximal activity at 80^{o}C. The k_{cat}/K_m for *T. maritima* ODC on L-ornithine as a substrate was comparable to that observed for the enzyme from other bacterial species, and like the other enzymes it also had a strong preference for L-ornithine over L-lysine. In contrast, the k_{cat}/K_m for the decarboxylation of L-ornithine by the *A. aeolicus* enzyme was about 100-fold lower than for the other ODCs even at the optimal temperature and pH which occurred over a broad range from pH 6 - 10. This difference is mostly reflected in the K_m (>100 mM at 80 ^{o}C), which is significantly elevated relative to the other enzymes in the

study. The *A. aeolicus* enzyme also had detectable activity on L-lysine, though it was significantly less active than for L-ornithine. Neither L-arginine nor *meso*-diaminopimelate are substrates.

*Vv*L/ODC efficiently catalyzes the decarboxylation of both L-ornithine and L-lysine confirming that it is a dual specificity enzyme (Figure 2.2, Table 2.1). In addition, the putative ADC and DAPDC from *V. vulnificus* catalyzed the decarboxylation of their expected substrates, L-arginine and diaminopimelate, respectively, further confirming the validity of the phylogenetically-determined decarboxylase clades. *V. vulnificus* DAPDC was active only towards *meso*-diaminopimelate (k_{cat} 5.9 ± 0.3 s^{-1} and K_m = 2.5 ± 0.4 mM), and showed similar catalytic efficiency to the enzyme from other species (Momany et al., 2002; Ray et al., 2002). The *V. vulnificus* ADC activity was measured in the presence and absence of 5 mM Mg^{+2} based on several reports that bacterial ADC activity is activated by Mg^{+2} (Wu and Morris, 1973). However the *V. vulnificus* ADC efficiently catalyzed the decarboxylation of L-arginine in the absence of Mg^{+2}, and the kinetic constants were the same in both conditions (k_{cat} = 20 ± 0.7 s^{-1} and K_m = 0.20 ± 0.04 mM).

3. Inhibition of the Bacterial ODCs with DFMO

Eukaryotic ODCs from human, mouse and *T. brucei* are known to be inactivated by DFMO, an enzyme-activated irreversible inhibitor (Coleman et al., 1993; Phillips et al., 1988; Qu et al., 2003). To determine if the enzymes characterized in the present study are also inhibited by DFMO, the *V. vulnificus* L/ODC and the ODCs from *M. mazei*, *P. aeruginosa* and *N. europaea* were incubated with various concentrations of DFMO over a range of time. DFMO inhibited all four enzymes with k_{inact}/K_i^{app} ranging from 32 – 180

$M^{-1}s^{-1}$ (Figure 2.3, Table 2.2). These values are comparable to those measured for mammalian and *T. brucei* ODC.

D. Discussion

Basic amino acid decarboxylases catalyze essential reactions involved in the formation of polyamines in both eukaryotes and prokaryotes, and in lysine biosynthesis in prokaryotes (Grishin et al., 1995; Sandmeier et al., 1994). Phylogenetic analysis of the β/α-barrel fold-type decarboxylases demonstrates that the sequences form four distinct groups that segregate by substrate preference. These include the prokaryotic and plant ADCs, the prokaryotic DAPDCs, the prokaryotic putative CANSDCs, and the ODCs (Figure 2.1). The ODC clade further subdivides into three groups containing the well characterized eukaryotic enzymes, the previously described dual function L/ODC from *S. ruminantium*, and bacterial homologs of formerly unknown function. We provide the first biochemical evidence that the prokaryotic ODC homologs have primary substrate specificity for L-ornithine despite substitution of key amino acids in their predicted active site structure. These data demonstrate that bacterial enzymes with activity on L-ornithine are widely distributed in both the AAT- and β/α-barrel families, and thus are not restricted to the AAT-fold as previously believed (Grishin et al., 1995; Sandmeier et al., 1994). In addition, we identify a second member (*Vv*L/ODC) of the dual function enzymes that is evolutionarily distant from *S. ruminantium*, suggesting that other sequences which group in this subclade will also catalyze decarboxylation of both L-ornithine and L-lysine.

The bacterial ODCs display robust catalytic activity against L-ornithine as a substrate with k_{cat}/K_m values equivalent to the eukaryotic enzymes from the family (Table 2.1). In addition, like the eukaryotic ODCs they are strongly specific for L-ornithine over L-lysine. One exception is the *A. aeolicus* enzyme, which has a high K_m for L-ornithine suggesting that it may prefer another substrate that remains unidentified. However, none of the tested basic amino acids other than L-ornithine served as substrates. Bacterial ODCs from the AAT-fold including the enzymes from *E. coli* are reported to be insensitive to inhibition by DFMO (Kallio and McCann, 1981). In contrast, we demonstrate here that the bacterial enzymes from the β/α-barrel fold, including *Vv*L/ODC are inhibited by DFMO with similar kinetics of inactivation to values reported for the eukaryotic enzymes (Table 2.2). Thus in contrast to the situation in *E. coli*, DFMO may be an effective agent for depleting polyamines in bacterial species that contain only β/α-barrel fold ODC. The one eukaryotic ODC characterized in this study, *G. lamblia*, was also inhibited by DFMO providing a rationale for the observation that parasite growth is sensitive to DFMO (Gillin et al., 1984).

It is clear from the current work that the β/α-barrel fold ODC is not exclusively eukaryotic and that it has evolved from the bacterial form. Among the β/α-barrel decarboxylases, DAPDC is the most phylogenetically widespread and is the only one found throughout the Euryarchaeota. It is also the only β/α-barrel fold decarboxylase found in the Chloroflexi, a eubacterial phylum recently postulated to be the most ancient bacterial lineage (Cavalier-Smith, 2006). Thus, a parsimonious explanation for the origin of the β/α-barrel decarboxylases is that they arose from DAPDC by gene duplication and

subsequent functional diversification to generate different substrate specificities. In support, the other activities in the family are less widely distributed. The β/α-barrel fold ADC seems to be excluded from the single-membraned Firmicutes and Actinobacteria phyla, while it is found in the double-membraned *E. coli*, a member of the γ-Proteobacteria (Buch and Boyle, 1985). It is also ubiquitous in the Cyanobacteria, which explains why only plants contain ADC amongst the eukaryotes (the chloroplast is derived from a cyanobacterial endosymbiont). ODC is the only β/α-barrel enzyme to be found extensively throughout the Eukaryota and, in the Metazoa and Fungi, it is the only route for polyamine biosynthesis.

Bacteria possess at least five routes for polyamine biosynthesis, including ADC and ODC, which are represented in both the AAT and β/α-barrel fold classes, and a pyruvoyl-dependent ADC found in Archaea (Graham et al., 2002). Convergent evolution has played an unusually important role in bacterial polyamine biosynthesis. A consequence of this is that a variety of AAT-/β/α-barrel fold, ODC/ADC enzyme combinations are found in sequenced bacterial genomes leading to the potential of redundant function. It is not clear how the various decarboxylase permutations in a given genome facilitate physiological adaptation, suggesting the possibility that the overlapping enzyme activities may be functionally compartmentalized for different cellular processes. Our data suggest that a systematic bioinformatic correlation of the polyamine biosynthetic gene configuration in individual bacterial strains, correlated with other genomic attributes, will provide a better understanding of the diversity of polyamine function.

In summary, our functional data on the prokaryotic DCs provides direct support for the activities of each class of basic amino acid decarboxylases from the β/α-barrel fold, with the exception of the putative CANSDCs. These data show that the phylogenetic analysis provides strong predictive indication of the substrate specificity of enzymes from each clade in this family, including the identification of prokaryotic ODCs and a subclade containing the dual function L/ODCs.

Organism	Reaction temp	Reaction pH	Substrate						Substrate preference (Orn/Lys)
			L-Ornithine			L-Lysine			
			k_{cat} (s^{-1})	K_m (mM)	k_{cat}/K_m($M^{-1}s^{-1}$)	k_{cat} (s^{-1})	K_m (mM)	k_{cat}/K_m($M^{-1}s^{-1}$)	
T. brucei ODC[a]			7.7	0.24	3.2×10^4	2.2	21	1.0×10^2	370
G.lamblia			8.6 ± 0.7	0.19 ± 0.04	4.5×10^4	0.93 ± 0.08	6.4 ± 1.3	1.5×10^2	310
M.mazei			6.4 ± 0.5	0.12 ± 0.03	5.3×10^4	0.24 ± 0.01	9.1 ± 0.9	2.6×10	2,000
P.aeruginosa	37°C	8.0	12 ± 0.4	0.18 ± 0.02	6.7×10^4	0.21 ± 0.01	8.5 ± 0.7	2.5×10	2,700
B. henselae			7.9 ± 0.2	0.19 ± 0.01	4.2×10^4	0.30 ± 0.01	9.0 ± 0.8	3.3×10	1,200
N. europaea			3.5 ± 0.4	2.3 ± 0.5	1.5×10^3	0.22 ± 0.01	18 ± 3.4	1.2×10	1,300
V. vulnificus			29 ± 0.4	1.7 ± 0.1	1.7×10^4	24 ± 0.50	5.8 ± 0.3	4.1×10^3	4.0
T. maritima	37°C	8.0	3.2 ± 0.2	0.92 ± 0.18	3.5×10^3	n.a.	n.a.		
	63°C	8.2	32 ± 1.3	1.2 ± 0.2	2.7×10^4	1.5 ± 0.1	9.3 ± 1.6	1.6×10^2	170
	80°C	7.9	95 ± 10	2.4 ± 0.8	4.0×10^4	n.d.	n.d.		
A. aeolicus	37°C	8.0	1.2 ± 0.1	6.7 ± 1.0	1.8×10^2	n.a.	n.a.		
	63°C	7.0	43 ± 1	60 ± 3	7.2×10^2	0.05 ± 0.003	15 ± 3	3.3×10^0	220
		6.0	84 ± 13	112 ± 28	7.5×10^2	n.d.	n.d.		
		7.0	98 ± 9	141 ± 19	7.0×10^2	n.d.	n.d.		
	80°C	8.1	75 ± 6	112 ± 14	6.7×10^2	n.d.	n.d.		
		9.0	61 ± 7	91 ± 18	6.8×10^2	n.d.	n.d.		
		10.0	77 ± 11	129 ± 29	6.0×10^2	n.d.	n.d.		

Table 2.1 Steady-state kinetic parameters and substrate specificity of the β/α-barrel fold basic amino acid decarboxylases. n.a., no measurable activity; n.d., not determined. Errors represent the standard error of the mean for n = 3. Substrate preference is

calculated based on the ratio of k_{cat}/K_m. [a]Data were taken from Ref. (29). For comparison, the k_{cat}/K_m for *S. ruminantium* L/ODC on L-ornithine and L-lysine are reported to be 8.9×10^3 and 1.1×10^4 $M^{-1}s^{-1}$, respectively at 30°C, pH 6.0 (3) and for *cv*ADC the k_{cat}/K_m for L-ornithine and L-arginine are reported to be 7.4 and 4.2×10^3 $M^{-1}s^{-1}$respectively, at 37°C, pH 8.0 (5,6).

Source organism of the enzyme	k_{inact} (min^{-1})	K_i^{app} (μM)	k_{inact}/ K_i^{app} ($M^{-1}s^{-1}$)
Mouse[a]	0.32	13	4.1×10^2
Human[b]	0.15	2.2	1.3×10^3
T.brucei[c]	3.6	160	3.8×10^3
P.aeruginosa	0.81	420	3.2×10
M.mazei	1.7	170	1.7×10^2
N.europaea	0.97	230	7.0×10
V.vulnificus	2.4	220	1.8×10^2

Table 2.2. Kinetic parameters for DFMO inhibition of ODC activity. [a,b,c]Data were taken from Refs.(Coleman et al., 1993), (Qu et al., 2003) and (Phillips et al., 1988), respectively.

Oligonucleotide	Oligonucleotide sequence (5' to 3') *
mtpRSET_F	GACGATGACGATAAGGCCATGGTTGAATCTTATAACCCGGAG
mtpRSET_R	CTCCGGGTTATAAGATTCAACCATGGCCTTATCGTCATCGTC
pRSET_GiaF	CCATGGCCGTGCTGACAAGAGCGTCCCTTGTCGAGTAC
pRSET_GiaR	AAGCTTCACTCCTCTATACAACAAACGACGCTAACATGGGG
pRSET_MethF	CAGGTTAAAAAGGCCATGGATATGAGAAAAGAGCCTTATG
pRSET_MethR	TAAAAGGGCAGATAAGCTTTAGATAACATAGGCTTTC
pRSET_NitF	CCAGGAGAAGCTCCCATGGAAAAATCATTCGCCGCA
pRSET_NitR	GTAATAGCATTTTCCGGAAGCTTAAATTACAACGACATCCGG
pET15_VibF	CATTACTTTGGAGGTTTCATATGGCACATTCACAATC
pET15_VibR	GATATTCGAGTGTGCTCGAGTTAGCCAATCATGCG
pET15_TherF	CCCGTTGAGGAGGAGCATATGATGGAATACTGG
pET15_TherR	GTAAAAATCGTTGAGGCTCGAGTGAGTTCTTCGATGAAAACC
pET15_AquiF	GTATTTATATTTATCCATATGACTAAGGTTGTAAATTACGGG
pET15_AquiR	CTTATTCATAAGATTGAATCTCGAGCTAAAAAGGAACAACCTC
pET15_BarF	CCCTGGGAGAATTGACATATGGCGACGCAACGTATTCGC
pET15_BarR	CTTTATACCATCTTATAAAGGATCCATTCAAATCACATAGGC
Q_BarF	CAATTAGGTTTGCAAGCTTATGGTGTTTCCTTTCATG
Q_BarR	CATGAAAGGAAACACCATAAGCTTGCAAACCTAATTG
pET15_PseuF	TGCCATTGGGAGTCCCACATATGTCCATCAAGGTCGAG
pET15_PseuR	TCTTCGTAGCAGACTCGAGTGCGCTAGAGGTAGAACGCC
Q_PseuF	CTGCCGGAAATCATCCTCGAACCGGGCCGTTCGCTG
Q_PseuR	CAGCGAACGGCCCGGTTCGAGGATGATTTCCGGCAG
VibDAP_F	CCATATTATAAGGGAAGTGACATATGGATTATTTC
VibDAP_R	GGAAATGCATAAAACTCGAGTTACTCCGGAAGAATGTG
VibADC_F	GATATACCATATGAGATTAGATGTGGAAC
VibADC_R	AATCATTCTCGAGGAAATCCTCTAAATAGG

*Engineered restriction sites are underlined.

Table 2.3 Oligonucleotides used for cloning ODC homologs

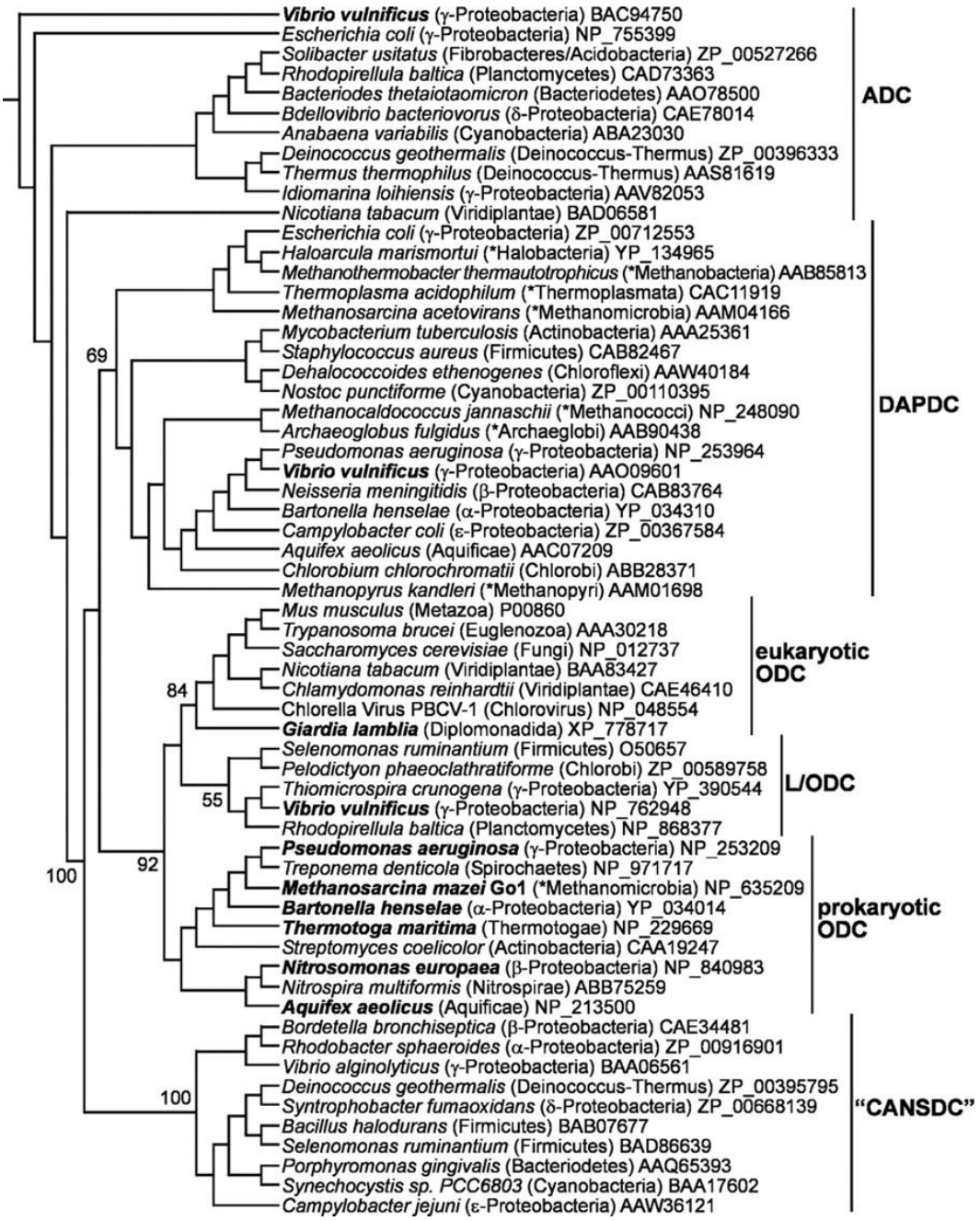

Figure 2.1 Neighbor joining tree of the β/α-barrel fold basic amino acid decarboxylases. The tree is based on the sequence alignment presented in Figure 2.4. The protein

accession number follows the phylum name in brackets. Phyla preceded by an asterisk are members of the Euryarchaeota. Numbers on the branches of the tree refer to the bootstrap support for nodes based on 1000 bootstrap replicates. The enzymes that were biochemically characterized in this study are displayed in bold. The enzyme from Chlorella virus PBCV-1 (*cv*ADC) groups on the tree with the eukaryotic ODCs, however it has been demonstrated to have specificity for L-arginine(5,6). "CANSDC" is depicted in quotation marks because direct enzymatic proof of this activity has not been reported.

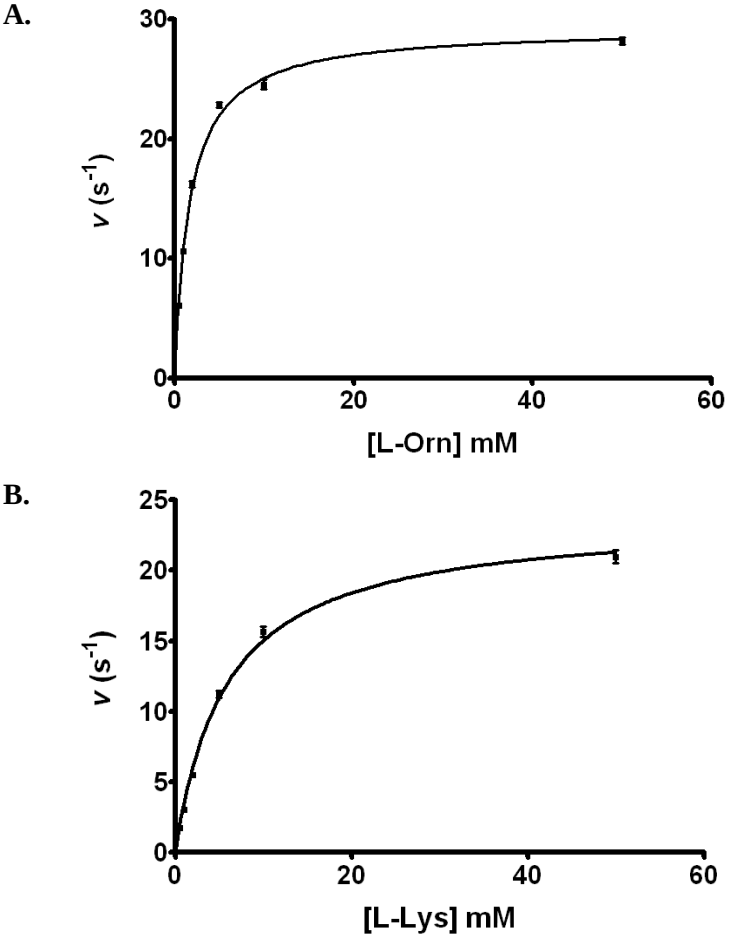

Figure 2.2 Steady-state kinetic analysis of the *Vibrio* enzyme for L-ornithine (A) and L-lysine (B). Decarboxylating activity was measured at 37°C by the spectroscopy-based coupled assay as described in the Experimental Procedures. The mean and S.E. were calculated from three experiments. GraphPad Prism4 was used to display and fit the data to the Michaelis-Menten equation by nonlinear regression. The kinetic parameters are as follows: k_{cat} = 29 ± 0.4 s^{-1} and K_m = 1.7 ± 0.1 mM for L-ornithine, k_{cat} = 24 ± 0.5 s^{-1} and K_m = 5.8 ± 0.3 mM for L-lysine.

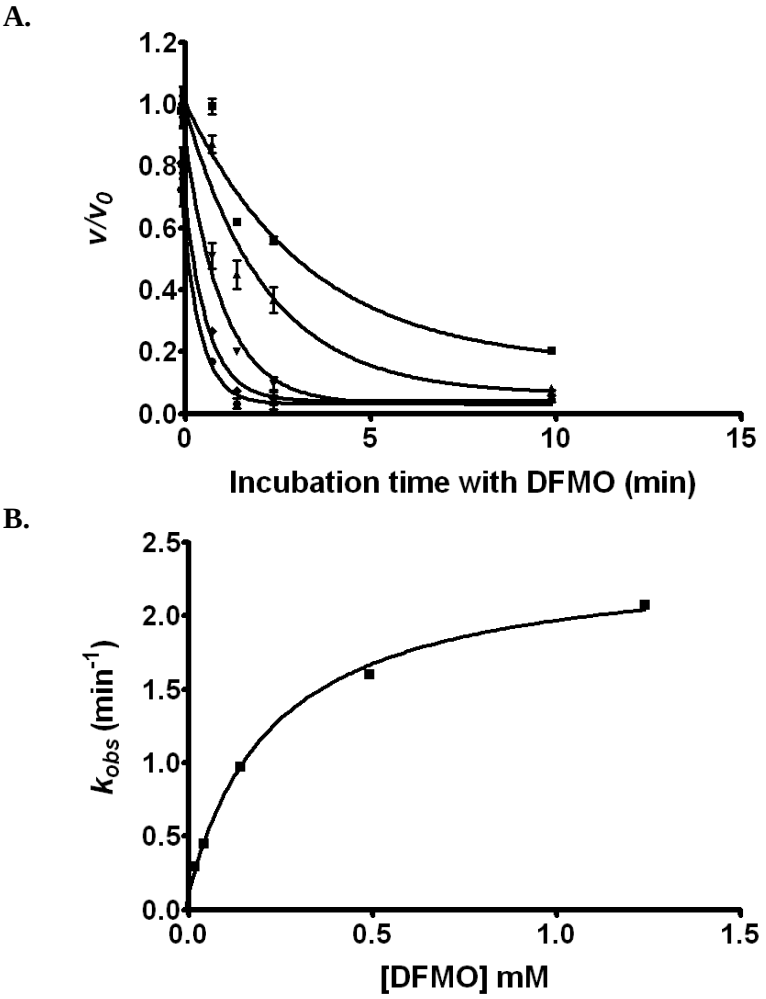

Figure 2.3 Inhibition of the ODC activities by DFMO. A. The *V. vulnificus* L/ODC was incubated with various concentrations of D/L-DFMO (■, 25μM; ▼, 50μM; ▲, 150μM; ◆, 500μM; ●, 1250μM) for different time periods at 37°C. Decarboxylation activity of the inactivated enzyme was tested toward 10 mM of L-ornithine using the spectroscopy-based coupled assay, and presented as fractional velocity to the enzyme activity without DFMO. Data were fitted to exponential decay, yielding k_{obs} at each DFMO concentration. The mean and S.E. were measured from two experiments. B. k_{obs}'s were fitted to the equation 2 by nonlinear regression using GraphPad Prism4. The resulting kinetic parameters were k_{inact} = 2.4 min^{-1} and K_i^{app} = 220 μM.

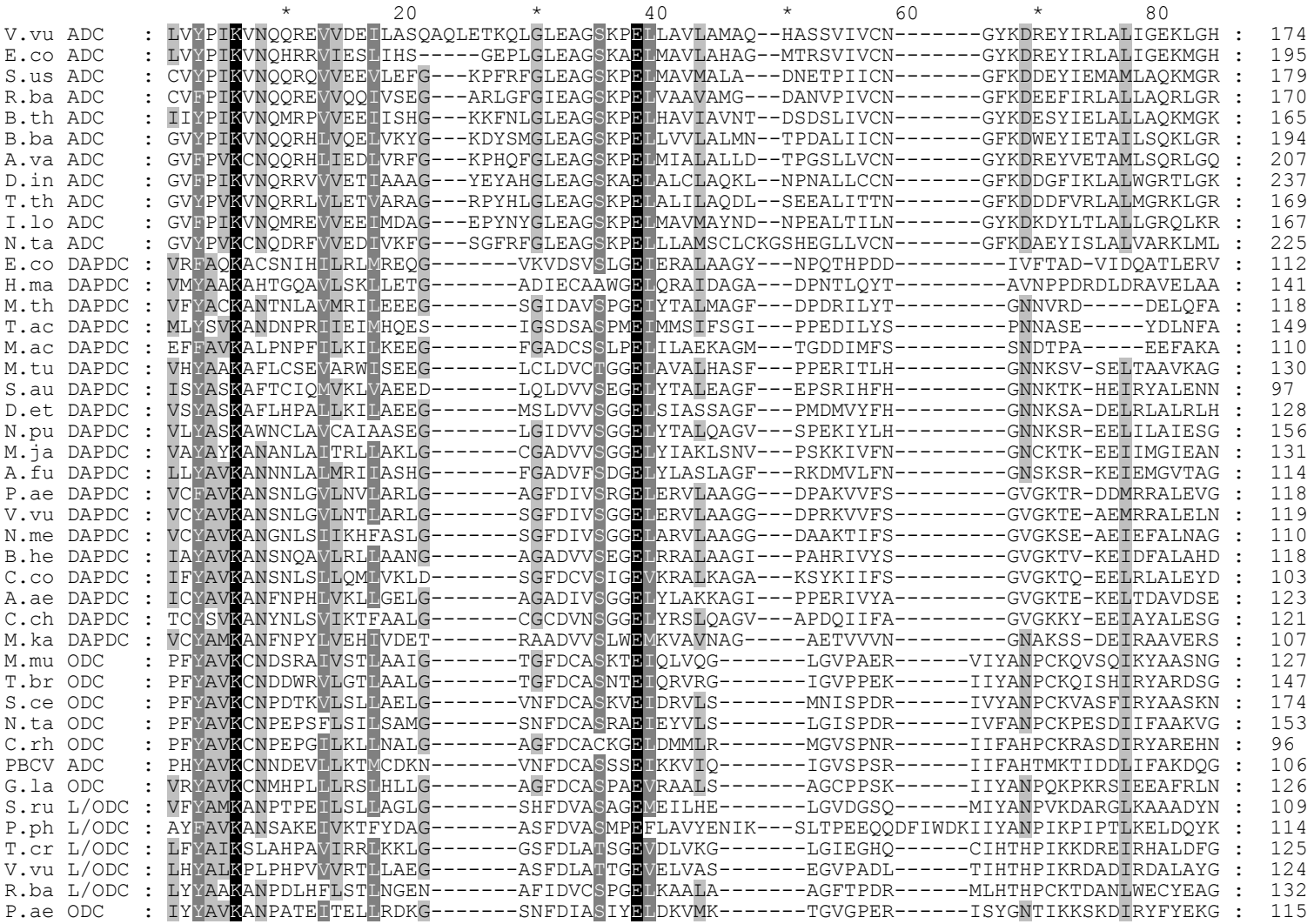
* 20 * 40 * 60 * 80
V.vu ADC : LVYPIKVNQQREVVDEILASQAQLETKQLGLEAGSKPELLAVLAMAQ--HASSVIVCN-------GYKDREYIRLALIGEKLGH : 174
E.co ADC : LVYPIKVNQHRRVIESLIHS-----GEPLGLEAGSKAELMAVLAHAG--MTRSVIVCN-------GYKDREYIRLALIGEKMGH : 195
S.us ADC : CVYPIKVNQQRQVVEEVLEFG---KPFRFGLEAGSKPELMAVMALA---DNETPIICN-------GFKDDEYIEMAMLAQKMGR : 179
R.ba ADC : CVFPIKVNQQREVVQQIVSEG---ARLGFGIEAGSKPELVAAVAMG---DANVPIVCN-------GFKDEEFIRLALLAQRLGR : 170
B.th ADC : IIYPIKVNQMRPVVEEIISHG---KKFNLGLEAGSKPELHAVIAVNT--DSDSLIVCN-------GYKDESYIELALLAQKMGK : 165
B.ba ADC : GVYPIKVNQQRHLVQELVKYG---KDYSMGLEAGSKPELLVVLALMN--TPDALIICN-------GFKDWEYIETAILSQKLGR : 194
A.va ADC : GVFPVKCNQQRHLIEDIVRFG---KPHQFGLEAGSKPELMIALALLD--TPGSLLVCN-------GYKDREYVETAMLSQRLGQ : 207
D.in ADC : GVFPIKVNQRRVVVETIAAAG---YEYAHGLEAGSKAELALCLAQKL--NPNALLCCN-------GFKDDGFIKLALWGRTLGK : 237
T.th ADC : GVYPVKVNQRRLVLETVARAG---RPYHLGLEAGSKPELALILAQDL--SEEALITTN-------GFKDDDFVRLALMGRKLGR : 169
I.lo ADC : GVFPIKVNQMREVVEEIMDAG---EPYNYGLEAGSKPELMAVMAYND--NPEALTILN-------GYKDKDYLTLALLGRQLKR : 167
N.ta ADC : GVYPVKCNQDRFVVEDIVKFG---SGFRFGLEAGSKPELLLAMSCLCKGSHEGLLVCN-------GFKDAEYISLALVARKLML : 225
E.co DAPDC : VRFAQKACSNIHILRLVREQG-------VKVDSVSLGEIERALAAGY---NPQTHPDD---------IVFTAD-VIDQATLERV : 112
H.ma DAPDC : VMYAAKAHTGQAVLSKLLETG-------ADIECAAWGELQRAIDAGA---DPNTLQYT---------AVNPPDRDLDRAVELAA : 141
M.th DAPDC : VFYACKANTNLAVMRILEEEG-------SGIDAVSPGEIYTALMAGF---DPDRILYT---------GNNVRD-----DELQFA : 118
T.ac DAPDC : MLYSVKANDNPRIIEIMHQES-------IGSDSASPMEIMMSIFSGI---PPEDILYS---------PNNASE-----YDLNFA : 149
M.ac DAPDC : EFFAVKALPNPFILKILKEEG-------FGADCSSLPELILAEKAGM---TGDDIMFS---------SNDTPA-----EEFAKA : 110
M.tu DAPDC : VHYAAKAFLCSEVARWLSEEG-------LCLDVCTGGELAVALHASF---PPERITLH---------GNNKSV-SELTAAVKAG : 130
S.au DAPDC : ISYASKAFTCIQMVKLVAEED-------LQLDVVSEGELYTALEAGF---EPSRIHFH---------GNNKTK-HEIRYALENN : 97
D.et DAPDC : VSYASKAFLHPALLKILAEEG-------MSLDVVSGGELSIASSAGF---PMDMVYFH---------GNNKSA-DELRLALRLH : 128
N.pu DAPDC : VLYASKAWNCLAVCAIAASEG-------LGIDVVSGGELYTALQAGV---SPEKIYLH---------GNNKSR-EELILAIESG : 156
M.ja DAPDC : VAYAYKANANLAITRLLAKLG-------CGADVVSGGELYIAKLSNV---PSKKIVFN---------GNCKTK-EEIIMGIEAN : 131
A.fu DAPDC : LLYAVKANNNLAIMRIIASHG-------FGADVFSDGELYLASLAGF---RKDMVLFN---------GNSKSR-KEIEMGVTAG : 114
P.ae DAPDC : VCFAVKANSNLGVLNVLARLG-------AGFDIVSRGELERVLAAGG---DPAKVVFS---------GVGKTR-DDMRRALEVG : 118
V.vu DAPDC : VCYAVKANSNLGVLNTLARLG-------SGFDIVSGGELERVLAAGG---DPRKVVFS---------GVGKTE-AEMRRALELN : 119
N.me DAPDC : VCYAVKANGNLSIIKHFASLG-------SGFDIVSGGELARVLAAGG---DAAKTIFS---------GVGKSE-AEIEFALNAG : 110
B.he DAPDC : IAYAVKANSNQAVLRLIAANG-------AGADVVSEGELRRALAAGI---PAHRIVYS---------GVGKTV-KEIDFALAHD : 118
C.co DAPDC : IFYAVKANSNLSLLQMLVKLD-------SGFDCVSIGEVKRALKAGA---KSYKIIFS---------GVGKTQ-EELRLALEYD : 103
A.ae DAPDC : ICYAVKANFNPHLVKLLGELG-------AGADIVSGGELYLAKKAGI---PPERIVYA---------GVGKTE-KELTDAVDSE : 123
C.ch DAPDC : TCYSVKANYNLSVIKTFAALG-------CGCDVNSGGELYRSLQAGV---APDQIIFA---------GVGKKY-EEIAYALESG : 121
M.ka DAPDC : VCYAMKANFNPYLVEHIVDET-------RAADVVSLWEMKVAVNAG-----AETVVVN---------GNAKSS-DEIRAAVERS : 107
M.mu ODC : PFYAVKCNDSRAIVSTLAAIG-------TGFDCASKTEIQLVQG-------VIYANPCKQVSQIKYAASNG : 127
T.br ODC : PFYAVKCNDDWRVLGTLAALG-------TGFDCASNTEIQRVRG-------IGVPPEK------IIYANPCKQISHIRYARDSG : 147
S.ce ODC : PFYAVKCNPDTKVLSLLAELG-------VNFDCASKVEIDRVLS-------MNISPDR------IVYANPCKVASFIRYAASKN : 174
N.ta ODC : PFYAVKCNPEPSFLSILSAMG-------SNFDCASRAEIEYVLS-------LGISPDR------IVFANPCKPESDIIFAAKVG : 153
C.rh ODC : PFYAVKCNPEPGILKLLNALG-------AGFDCACKGELDMMLR-------MGVSPNR------IIFAHPCKRASDIRYAREHN : 96
PBCV ADC : PHYAVKCNNDEVLLKTMCDKN-------VNFDCASSSEIKKVIQ-------IGVSPSR------IIFAHTMKTIDDLIFAKDQG : 106
G.la ODC : VRYAVKCNMHPLLLRSLHLLG-------AGFDCASPAEVRAALS-------AGCPPSK------IIYANPQKPKRSIEEAFRLN : 126
S.ru L/ODC : VFYAMKANPTPEILSLLAGLG-------SHFDVASAGEMEILHE-------LGVDGSQ------MIYANPVKDARGLKAAADYN : 109
P.ph L/ODC : AYFAVKANSAKEIVKTFYDAG-------ASFDVASMPEFLAVYENIK---SLTPEEQQDFIWDKIIYANPIKPIPTLKELDQYK : 114
T.cr L/ODC : LFYAIKSLAHPAVIRRIKKLG-------GSFDLATSGEVDLVKG-------LGIEGHQ------CIHTHPIKKDREIRHALDFG : 125
V.vu L/ODC : LHYALKPLPHPVVVRTLLAEG-------ASFDLATTGEVELVAS-------EGVPADL------TIHTHPIKRDADIRDALAYG : 124
R.ba L/ODC : LYYAAKANPDLHFLSTLNGEN-------AFIDVCSPGELKAALA-------AGFTPDR------MLHTHPCKTDANLWECYEAG : 132
P.ae ODC : IYYAVKANPATEITELLRDKG-------SNFDIASIYELDKVMK-------TGVGPER------ISYGNTIKKSKDIRYFYEKG : 115

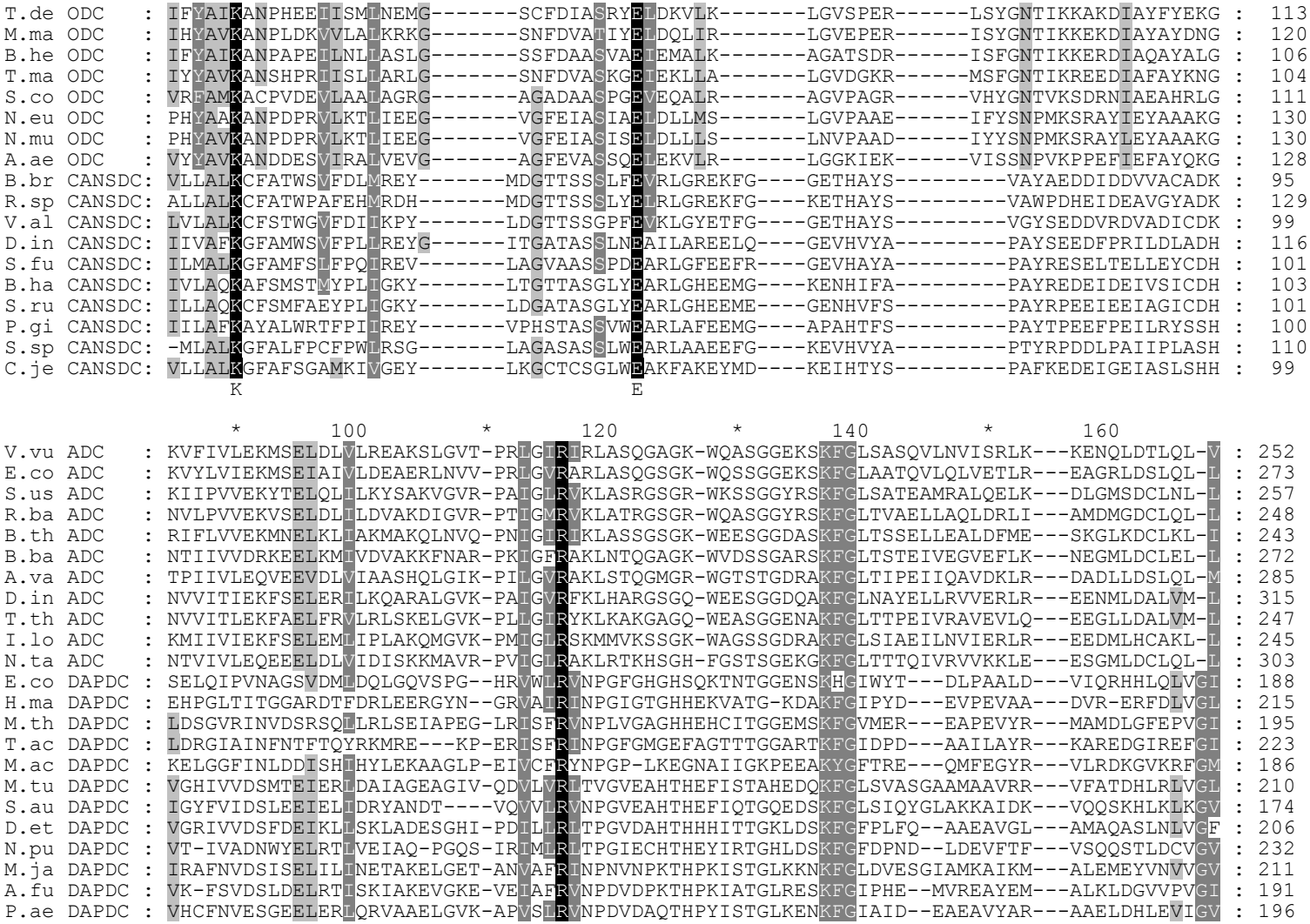
T.de ODC : IFYAIKANPHEEIISMTNEMG-------SCFDIASRYELDKVLK-------LGVSPER------LSYGNTIKKAKDIAYFYEKG : 113
M.ma ODC : IHYAVKANPLDKVVLAIKRKG-------SNFDVATIYELDQLIR-------LGVEPER------ISYGNTIKKEKDIAYAYDNG : 120
B.he ODC : IFYAIKANPAPEILNLLASLG-------SSFDAASVAEIEMALK-------AGATSDR------ISFGNTIKKERDIAQAYALG : 106
T.ma ODC : IYYAVKANSHPRIISLLARLG-------SNFDVASKGEIEKLLA-------LGVDGKR------MSFGNTIKREEDIAFAYKNG : 104
S.co ODC : VRFAMKACPVDEVLAALAGRG-------AGADAASPGEVEQALR-------AGVPAGR------VHYGNTVKSDRNIAEAHRLG : 111
N.eu ODC : PHYAAKANPDPRVLKTLIEEG-------VGFEIASIAELDLLMS-------LGVPAAE------IFYSNPMKSRAYIEYAAAKG : 130
N.mu ODC : PHYAVKANPDPRVLKTLIEEG-------VGFEIASISELDLLLS-------LNVPAAD------IYYSNPMKSRAYLEYAAAKG : 130
A.ae ODC : VYYAVKANDDESVIRALVEVG-------AGFEVASSQELEKVLR-------LGGKIEK------VISSNPVKPPEFIEFAYQKG : 128
B.br CANSDC: VLLALKCFATWSVFDLMREY-------MDGTTSSSLFEVRLGREKFG----GETHAYS----------VAYAEDDIDDVVACADK : 95
R.sp CANSDC: ALLALKCFATWPAFEHMRDH-------MDGTTSSSLYELRLGREKFG----KETHAYS----------VAWPDHEIDEAVGYADK : 129
V.al CANSDC: LVLALKCFSTWGVFDIIKPY-------LDGTTSSGPFEVKLGYETFG----GETHAYS----------VGYSEDDVRDVADICDK : 99
D.in CANSDC: IIVAFKGFAMWSVFPLLREYG------ITGATASSLNEAILAREELQ----GEVHVYA----------PAYSEEDFPRILDLADH : 116
S.fu CANSDC: ILMALKGFAMFSIFPQIREV-------LAGVAASSPDEARLGFEEFR----GEVHAYA----------PAYRESELTELLEYCDH : 101
B.ha CANSDC: IVLAQKAFSMSTMYPLIGKY-------LTGTTASGLYEARLGHEEMG----KENHIFA----------PAYREDEIDEIVSICDH : 103
S.ru CANSDC: ILLAQKCFSMFAEYPLIGKY-------LDGATASGLYEARLGHEEME----GENHVFS----------PAYRPEEIEEIAGICDH : 101
P.gi CANSDC: IILAFKAYALWRTFPIIREY-------VPHSTASSVWEARLAFEEMG----APAHTFS----------PAYTPEEFPEILRYSSH : 100
S.sp CANSDC: -MLALKGFALFPCFPWIRSG-------LAGASASSLWEARLAAEEFG----KEVHVYA----------PTYRPDDLPAIIPLASH : 110
C.je CANSDC: VLLALKGFAFSGAMKIVGEY-------LKGCTCSGLWEAKFAKEYMD----KEIHTYS----------PAFKEDEIGEIASLSHH : 99
K E
* 100 * 120 * 140 * 160
V.vu ADC : KVFIVLEKMSELDLVLREAKSLGVT-PRLGIRIRLASQGAGK-WQASGGEKSKFGLSASQVLNVISRLK---KENQLDTLQL-V : 252
E.co ADC : KVYLVIEKMSEIAIVLDEAERLNVV-PRLGVRARLASQGSGK-WQSSGGEKSKFGLAATQVLQLVETLR---EAGRLDSLQL-L : 273
S.us ADC : KIIPVVEKYTELQLILKYSAKVGVR-PAIGLRVKLASRGSGR-WKSSGGYRSKFGLSATEAMRALQELK---DLGMSDCLNL-L : 257
R.ba ADC : NVLPVVEKVSELDLILDVAKDIGVR-PTIGMRVKLATRGSGR-WQASGGYRSKFGLTVAELLAQLDRLI---AMDMGDCLQL-L : 248
B.th ADC : RIFLVVEKMNELKLIAKMAKQLNVQ-PNIGIRIKLASSGSGK-WEESGGDASKFGLTSSELLEALDFME---SKGLKDCLKL-I : 243
B.ba ADC : NTIIVVDRKEELKMIVDVAKKFNAR-PKIGFRAKLNTQGAGK-WVDSSGARSKFGLTSTEIVEGVEFLK---NEGMLDCLEL-L : 272
A.va ADC : TPIIVLEQVEEVDLVIAASHQLGIK-PILGVRAKLSTQGMGR-WGTSTGDRAKFGLTIPEIIQAVDKLR---DADLLDSLQL-M : 285
D.in ADC : NVVITIEKFSELERILKQARALGVK-PAIGVRFKLHARGSGQ-WEESGGDQAKFGLNAYELLRVVERLR---EENMLDALVM-L : 315
T.th ADC : NVVITLEKFAELFRVLRLSKELGVK-PLLGIRYKLKAKGAGQ-WEASGGENAKFGLTTPEIVRAVEVLQ---EEGLLDALVM-L : 247
I.lo ADC : KMIIVIEKFSELEMLIPLAKQMGVK-PMIGLRSKMMVKSSGK-WAGSSGDRAKFGLSIAEILNVIERLR---EEDMLHCAKL-L : 245
N.ta ADC : NTVIVLEQEEELDLVIDISKKMAVR-PVIGLRAKLRTKHSGH-FGSTSGEKGKFGLTTTQIVRVVKKLE---ESGMLDCLQL-L : 303
E.co DAPDC : SELQIPVNAGSVDMLDQLGQVSPG--HRVWLRVNPGFGHGHSQKTNTGGENSKHGIWYT---DLPAALD---VIQRHHLQLVGI : 188
H.ma DAPDC : EHPGLTITGGARDTFDRLEERGYN--GRVALRINPGIGTGHHEKVATG-KDAKFGIPYD---EVPEVAA---DVR-ERFDLVGL : 215
M.th DAPDC : LDSGVRINVDSRSQLLRLSEIAPEG-LRISFRVNPLVGAGHHEHCITGGEMSKFGVMER---EAPEVYR---MAMDLGFEPVGI : 195
T.ac DAPDC : LDRGIAINFNTFTQYRKMRE---KP-ERISFRINPGFGMGEFAGTTTGGARTKFGIDPD---AAILAYR---KAREDGIREFGI : 223
M.ac DAPDC : KELGGFINLDDISHIHYLEKAAGLP-EIVCFRYNPGP-LKEGNAIIGKPEEAKYGFTRE---QMFEGYR---VLRDKGVKRFGM : 186
M.tu DAPDC : VGHIVVDSMTEIERLDAIAGEAGIV-QDVLVRLTVGVEAHTHEFISTAHEDQKFGLSVASGAAMAAVRR---VFATDHLRLVGL : 210
S.au DAPDC : IGYFVIDSLEEIELLDRYANDT----VQVVLRVNPGVEAHTHEFIQTGQEDSKFGLSIQYGLAKKAIDK---VQQSKHLKLKGV : 174
D.et DAPDC : VGRIVVDSFDEIKLLSKLADESGHI-PDILLRLTPGVDAHTHHHITTGKLDSKFGFPLFQ--AAEAVGL---AMAQASLNLVGF : 206
N.pu DAPDC : VT-IVADNWYELRTIVEIAQ-PGQS-IRIMLRLTPGIECHTHEYIRTGHLDSKFGFDPND--LDEVFTF---VSQQSTLDCVGV : 232
M.ja DAPDC : IRAFNVDSISELILLNETAKELGET-ANVAFRINPNVNPKTHPKISTGLKKNKFGLDVESGIAMKAIKM---ALEMEYVNVVGV : 211
A.fu DAPDC : VK-FSVDSLDELRTISKIAKEVGKE-VEIAFRVNPDVDPKTHPKIATGLRESKFGIPHE--MVREAYEM---ALKLDGVVPVGI : 191
P.ae DAPDC : VHCFNVESGEELERLQRVAAELGVK-APVSLRVNPDVDAQTHPYISTGLKENKFGIAID--EAEAVYAR---AAELDHLEVIGV : 196

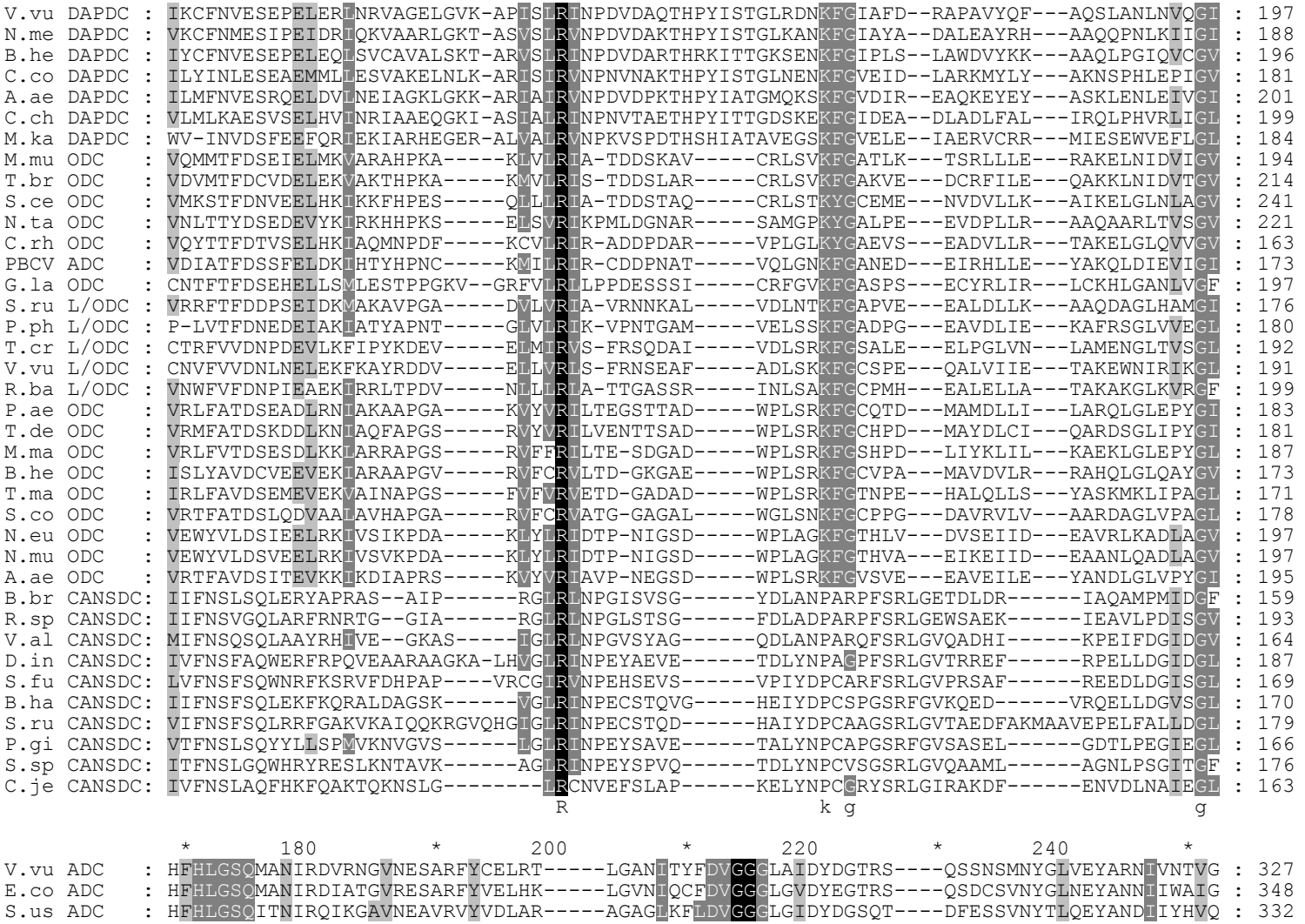
V.vu DAPDC : IKCFNVESEPELERINRVAGELGVK-APISLRINPDVDAQTHPYISTGLRDNKFGIAFD--RAPAVYQF---AQSLANLNVQGI : 197
N.me DAPDC : VKCFNMESIPEIDRIQKVAARLGKT-ASVSLRVNPDVDAKTHPYISTGLKANKFGIAYA--DALEAYRH---AAQQPNLKIIGI : 188
B.he DAPDC : IYCFNVESEPELEQLSVCAVALSKT-ARVSLRINPDVDARTHRKITTGKSENKFGIPLS--LAWDVYKK---AAQLPGIQVCGV : 196
C.co DAPDC : ILYINLESEAEMMLIESVAKELNLK-ARISIRVNPNVNAKTHPYISTGLNENKFGVEID--LARKMYLY---AKNSPHLEPIGV : 181
A.ae DAPDC : ILMFNVESRQELDVLNEIAGKLGKK-ARIAIRVNPDVDPKTHPYIATGMQKSKFGVDIR--EAQKEYEY---ASKLENLEIVGI : 201
C.ch DAPDC : VLMLKAESVSELHVINRIAAEQGKI-ASIALRINPNVTAETHPYITTGDSKEKFGIDEA--DLADLFAL---IRQLPHVRLIGL : 199
M.ka DAPDC : WV-INVDSFEEFQRIEKIARHEGER-ALVALRVNPKVSPDTHSHIATAVEGSKFGVELE--IAERVCRR---MIESEWVEFLGL : 184
M.mu ODC : VQMMTFDSEIELMKVARAHPKA-----KLVLRIA-TDDSKAV-----CRLSVKFGATLK---TSRLLLE---RAKELNIDVIGV : 194
T.br ODC : VDVMTFDCVDELEKVAKTHPKA-----KMVLRIS-TDDSLAR-----CRLSVKFGAKVE---DCRFILE---QAKKLNIDVTGV : 214
S.ce ODC : VMKSTFDNVEELHKIKKFHPES-----QLLLRIA-TDDSTAQ-----CRLSTKYGCEME---NVDVLLK---AIKELGLNLAGV : 241
N.ta ODC : VNLTTYDSEDEVYKIRKHHPKS-----ELSVRIKPMLDGNAR-----SAMGPKYGALPE---EVDPLLR---AAQAARLTVSGV : 221
C.rh ODC : VQYTTFDTVSELHKIAQMNPDF-----KCVLRIR-ADDPDAR-----VPLGLKYGAEVS---EADVLLR---TAKELGLQVVGV : 163
PBCV ADC : VDIATFDSSFELDKIHTYHPNC-----KMILRIR-CDDPNAT-----VQLGNKFGANED---EIRHLLE---YAKQLDIEVIGI : 173
G.la ODC : CNTFTFDSEHELLSMLESTPPGKV--GRFVLRLLPPDESSSI-----CRFGVKFGASPS---ECYRLIR---LCKHLGANLVGF : 197
S.ru L/ODC : VRRFTFDDPSEIDKMAKAVPGA-----DVLVRIA-VRNNKAL-----VDLNTKFGAPVE---EALDLLK---AAQDAGLHAMGI : 176
P.ph L/ODC : P-LVTFDNEDEIAKIATYAPNT-----GLVLRIK-VPNTGAM-----VELSSKFGADPG---EAVDLIE---KAFRSGLVVEGL : 180
T.cr L/ODC : CTRFVVDNPDEVLKFIPYKDEV-----ELMIRVS-FRSQDAI-----VDLSRKFGSALE---ELPGLVN---LAMENGLTVSGL : 192
V.vu L/ODC : CNVFVVDNLNELEKFKAYRDDV-----ELLVRLS-FRNSEAF-----ADLSKKFGCSPE---QALVIIE---TAKEWNIRIKGL : 191
R.ba L/ODC : VNWFVFDNPIEAEKIRRLTPDV-----NLLLRLA-TTGASSR-----INLSAKFGCPMH---EALELLA---TAKAKGLKVRGF : 199
P.ae ODC : VRLFATDSEADLRNIAKAAPGA-----KVYVRILTEGSTTAD-----WPLSRKFGCQTD---MAMDLLI---LARQLGLEPYGI : 183
T.de ODC : VRMFATDSKDDLKNIAQFAPGS-----RVYVRILVENTTSAD-----WPLSRKFGCHPD---MAYDLCI---QARDSGLIPYGI : 181
M.ma ODC : VRLFVTDSESDLKKIARRAPGS-----RVFFRILTE-SDGAD-----WPLSRKFGSHPD---LIYKLIL---KAEKLGLEPYGL : 187
B.he ODC : ISLYAVDCVEEVEKIARAAPGV-----RVFCRVLTD-GKGAE-----WPLSRKFGCVPA---MAVDVLR---RAHQLGLQAYGV : 173
T.ma ODC : IRLFAVDSEMEVEKVAINAPGS-----FVFVRVETD-GADAD-----WPLSRKFGTNPE---HALQLLS---YASKMKLIPAGL : 171
S.co ODC : VRTFATDSLQDVAAIAVHAPGA-----RVFCRVATG-GAGAL-----WGLSNKFGCPPG---DAVRVLV---AARDAGLVPAGL : 178
N.eu ODC : VEWYVLDSIEELRKIVSIKPDA-----KLYLRIDTP-NIGSD-----WPLAGKFGTHLV---DVSEIID---EAVRLKADLAGV : 197
N.mu ODC : VEWYVLDSVEELRKIVSVKPDA-----KLYLRIDTP-NIGSD-----WPLAGKFGTHVA---EIKEIID---EAANLQADLAGV : 197
A.ae ODC : VRTFAVDSITEVKKIKDIAPRS-----KVYVRIAVP-NEGSD-----WPLSRKFGVSVE---EAVEILE---YANDLGLVPYGI : 195
B.br CANSDC: IIFNSLSQLERYAPRAS--AIP------RGLRLNPGISVSG------YDLANPARPFSRLGETDLDR------IAQAMPMIDGF : 159
R.sp CANSDC: IIFNSVGQLARFRNRTG--GIA------RGLRLNPGLSTSG------FDLADPARPFSRLGEWSAEK------IEAVLPDISGV : 193
V.al CANSDC: MIFNSQSQLAAYRHIVE--GKAS-----IGLRLNPGVSYAG------QDLANPARQFSRLGVQADHI------KPEIFDGIDGV : 164
D.in CANSDC: IVFNSFAQWERFRPQVEAARAAGKA-LHVGLRINPEYAEVE------TDLYNPACPFSRLGVTRREF------RPELLDGIDGL : 187
S.fu CANSDC: LVFNSFSQWNRFKSRVFDHPAP----VRCGIRVNPEHSEVS------VPIYDPCARFSRLGVPRSAF------REEDLDGISGL : 169
B.ha CANSDC: IIFNSFSQLEKFKQRALDAGSK------VGLRINPECSTQVG-----HEIYDPCSPGSRFGVKQED------VRQELLDGVSGL : 170
S.ru CANSDC: VIFNSFSQLRRFGAKVKAIQQKRGVQHGIGLRINPECSTQD------HAIYDPCAAGSRLGVTAEDFAKMAAVEPELFALLDGL : 179
P.gi CANSDC: VTFNSLSQYYLLSPMVKNVGVS------LGLRINPEYSAVE------TALYNPCAPGSRFGVSASEL------GDTLPEGIEGL : 166
S.sp CANSDC: ITFNSLGQWHRYRESLKNTAVK------AGLRINPEYSPVQ------TDLYNPCVSGSRLGVQAAML------AGNLPSGITGF : 176
C.je CANSDC: IVFNSLAQFHKFQAKTQKNSLG--------LRCNVEFSLAP------KELYNPCGRYSRLGIRAKDF------ENVDLNAIEGL : 163
R k g g
* 180 * 200 * 220 * 240 *
V.vu ADC : HFHLGSQMANIRDVRNGVNESARFYCELRT-----LGANITYFDVGGGLAIDYDGTRS----QSSNSMNYGLVEYARNIVNTVG : 327
E.co ADC : HFHLGSQMANIRDIATGVRESARFYVELHK-----LGVNIQCFDVGGGLGVDYEGTRS----QSDCSVNYGLNEYANNIIWAIG : 348
S.us ADC : HFHLGSQITNIRQIKGAVNEAVRVYVDLAR-----AGAGLKFLDVGGGLGIDYDGSQT----DFESSVNYTLQEYANDIIYHVQ : 332

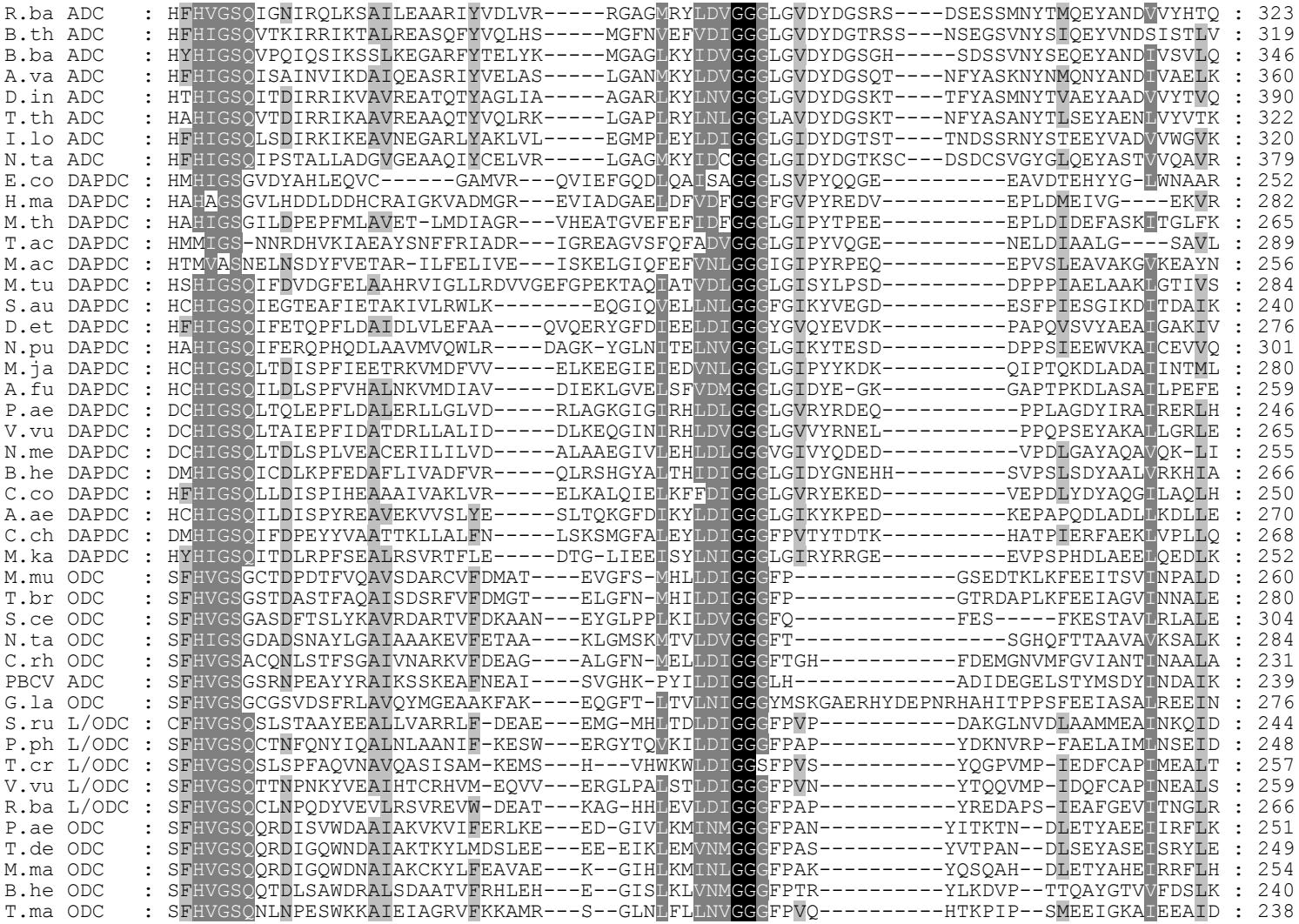
R.ba ADC : HFHVGSQIGNIRQLKSAILEAARIYVDLVR-----RGAGMRYLDVGGGLGVDYDGSRS----DSESSMNYTMQEYANDVVYHTQ : 323
B.th ADC : HFHIGSQVTKIRRIKTALREASQFYVQLHS-----MGFNVEFVDIGGGLGVDYDGTRSS---NSEGSVNYSIQEYVNDSISTLV : 319
B.ba ADC : HYHIGSQVPQIQSIKSSLKEGARFYTELYK-----MGAGLKYIDVGGGLGVDYDGSGH-----SDSSVNYSEQEYANDIVSVLQ : 346
A.va ADC : HFHIGSQISAINVIKDAIQEASRIYVELAS-----LGANMKYLDVGGGLGVDYDGSQT----NFYASKNYNMQNYANDIVAELK : 360
D.in ADC : HTHIGSQITDIRRIKVAVREATQTYAGLIA-----AGARLKYLNVGGGLGVDYDGSKT----TFYASMNYTVAEYAADVVYTVQ : 390
T.th ADC : HAHIGSQVTDIRRIKAAVREAAQTYVQLRK-----LGAPLRYLNLGGGLAVDYDGSKT----NFYASANYTLSEYAENIVYVTK : 322
I.lo ADC : HFHIGSQLSDIRKIKEAVNEGARLYAKLVL-----EGMPLEYLDIGGGLGIDYDGTST----TNDSSRNYSTEEYVADVVWGVK : 320
N.ta ADC : HFHIGSQIPSTALLADGVGEAAQIYCELVR-----LGAGMKYIDCGGGLGIDYDGTKSC---DSDCSVGYGLQEYASTVVQAVR : 379
E.co DAPDC : HMHIGSGVDYAHLEQVC------GAMVR---QVIEFGQDLQAISAGGGLSVPYQQGE----------EAVDTEHYYG-LWNAAR : 252
H.ma DAPDC : HAHAGSGVLHDDLDDHCRAIGKVADMGR---EVIADGAELDFVDFGGGFGVPYREDV----------EPLDMEIVG----EKVR : 282
M.th DAPDC : HAHIGSGILDPEPFMLAVET-LMDIAGR---VHEATGVEFEFIDFGGGLGIPYTPEE----------EPLDIDEFASKITGLFK : 265
T.ac DAPDC : HMMIGS-NNRDHVKIAEAYSNFFRIADR---IGREAGVSFQFADVGGGLGIPYVQGE----------NELDIAALG----SAVL : 289
M.ac DAPDC : HTMVASNELNSDYFVETAR-ILFELIVE---ISKELGIQFEFVNLGGGIGIPYRPEQ----------EPVSLEAVAKGVKEAYN : 256
M.tu DAPDC : HSHIGSQIFDVDGFELAAHRVIGLLRDVVGEFGPEKTAQIATVDLGGGLGISYLPSD----------DPPPIAELAAKLGTIVS : 284
S.au DAPDC : HCHIGSQIEGTEAFIETAKIVLRWLK--------EQGIQVELLNLGGGFGIKYVEGD----------ESFPIESGIKDITDAIK : 240
D.et DAPDC : HFHIGSQIFETQPFLDAIDLVLEFAA----QVQERYGFDIEELDIGGGYGVQYEVDK----------PAPQVSVYAEAIGAKIV : 276
N.pu DAPDC : HAHIGSQIFERQPHQDLAAVMVQWLR----DAGK-YGLNITELNVGGGLGIKYTESD----------DPPSIEEWVKAICEVVQ : 301
M.ja DAPDC : HCHIGSQLTDISPFIEETRKVMDFVV-----ELKEEGIEIEDVNLGGGLGIPYYKDK----------QIPTQKDLADAIINTML : 280
A.fu DAPDC : HCHIGSQILDLSPFVHALNKVMDIAV-----DIEKLGVELSFVDMGGGLGIDYE-GK----------GAPTPKDLASAILPEFE : 259
P.ae DAPDC : DCHIGSQLTQLEPFLDALERLLGLVD-----RLAGKGIGIRHLDLGGGLGVRYRDEQ-----------PPLAGDYIRAIRERLH : 246
V.vu DAPDC : DCHIGSQLTAIEPFIDATDRLLALID-----DLKEQGINIRHLDVGGGLGVVYRNEL-----------PPQPSEYAKALLGRLE : 265
N.me DAPDC : DCHIGSQLTDLSPLVEACERILILVD-----ALAAEGIVLEHLDLGGGVGIVYQDED----------VPDLGAYAQAVQK-LI : 255
B.he DAPDC : DMHIGSQICDLKPFEDAFLIVADFVR-----QLRSHGYALTHIDIGGGLGIDYGNEHH----------SVPSLSDYAALVRKHIA : 266
C.co DAPDC : HFHIGSQLLDISPIHEAAAIVAKLVR-----ELKALQIELKFFDIGGGLGVRYEKED----------VEPDLYDYAQGILAQLH : 250
A.ae DAPDC : HCHIGSQILDISPYREAVEKVVSLYE-----SLTQKGFDIKYLDIGGGLGIKYKPED----------KEPAPQDLADLLKDLLE : 270
C.ch DAPDC : DMHIGSQIFDPEYYVAATTKLLALFN-----LSKSMGFALEYLDIGGGFPVTYTDTK----------HATPIERFAEKLVPLLQ : 268
M.ka DAPDC : HYHIGSQITDLRPFSEALRSVRTFLE-----DTG-LIEEISYLNIGGGLGIRYRRGE----------EVPSPHDLAEELQEDLK : 252
M.mu ODC : SFHVGSGCTDPDTFVQAVSDARCVFDMAT----EVGFS-MHLLDIGGGFP-------------GSEDTKLKFEEITSVINPALD : 260
T.br ODC : SFHVGSGSTDASTFAQAISDSRFVFDMGT----ELGFN-MHILDIGGGFP-------------GTRDAPLKFEEIAGVINNALE : 280
S.ce ODC : SFHVGSGASDFTSLYKAVRDARTVFDKAAN---EYGLPPLKILDVGGGFQ-------------FES-----FKESTAVLRLALE : 304
N.ta ODC : SFHIGSGDADSNAYLGAIAAAKEVFETAA----KLGMSKMTVLDVGGGFT----------------SGHQFTTAAVAVKSALK : 284
C.rh ODC : SFHVGSACQNLSTFSGAIVNARKVFDEAG----ALGFN-MELLDIGGGFTGH-----------FDEMGNVMFGVIANTINAALA : 231
PBCV ADC : SFHVGSGSRNPEAYYRAIKSSKEAFNEAI----SVGHK-PYILDIGGGLH-------------ADIDEGELSTYMSDYINDAIK : 239
G.la ODC : SFHVGSGCGSVDSFRLAVQYMGEAAKFAK----EQGFT-LTVLNIGGGYMSKGAERHYDEPNRHAHITPPSFEEIASALREEIN : 276
S.ru L/ODC : CFHVGSQSLSTAAYEEALLVARRLF-DEAE---EMG-MHLTDLDIGGGFPVP-----------DAKGLNVDLAAMMEAINKQID : 244
P.ph L/ODC : SFHVGSQCTNFQNYIQALNLAANIF-KESW---ERGYTQVKILDIGGGFPAP-----------YDKNVRP-FAELAIMLNSEID : 248
T.cr L/ODC : SFHVGSQSLSPFAQVNAVQASISAM-KEMS---H---VHWKWLDIGGSFPVS-----------YQGPVMP-IEDFCAPIMEALT : 257
V.vu L/ODC : SFHVGSQTTNPNKYVEAIHTCRHVM-EQVV---ERGLPALSTLDIGGGFPVN-----------YTQQVMP-IDQFCAPINEALS : 259
R.ba L/ODC : SFHVGSQCLNPQDYVEVLRSVREVW-DEAT---KAG-HHLEVLDIGGGFPAP-----------YREDAPS-IEAFGEVITNGLR : 266
P.ae ODC : SFHVGSQQRDISVWDAAIAKVKVIFERLKE---ED-GIVLKMINMGGGFPAN----------YITKTN--DLETYAEEIIRFLK : 251
T.de ODC : SFHVGSQQRDIGQWNDAIAKTKYLMDSLEE---EE-EIKLEMVNMGGGFPAS----------YVTPAN--DLSEYASEISRYLE : 249
M.ma ODC : SFHVGSQQRDIGQWDNAIAKCKYLFEAVAE---K--GIHLKMINLGGGFPAK----------YQSQAH--DLETYAHEIRRFLH : 254
B.he ODC : SFHVGSQQTDLSAWDRALSDAATVFRHLEH---E--GISLKLVNMGGGFPTR----------YLKDVP--TTQAYGTVVFDSLK : 240
T.ma ODC : SFHVGSQNLNPESWKKAIEIAGRVFKKAMR---S--GLNLFLLNVGGGFPVQ----------HTKPIP--SMEEIGKAIEEAID : 238

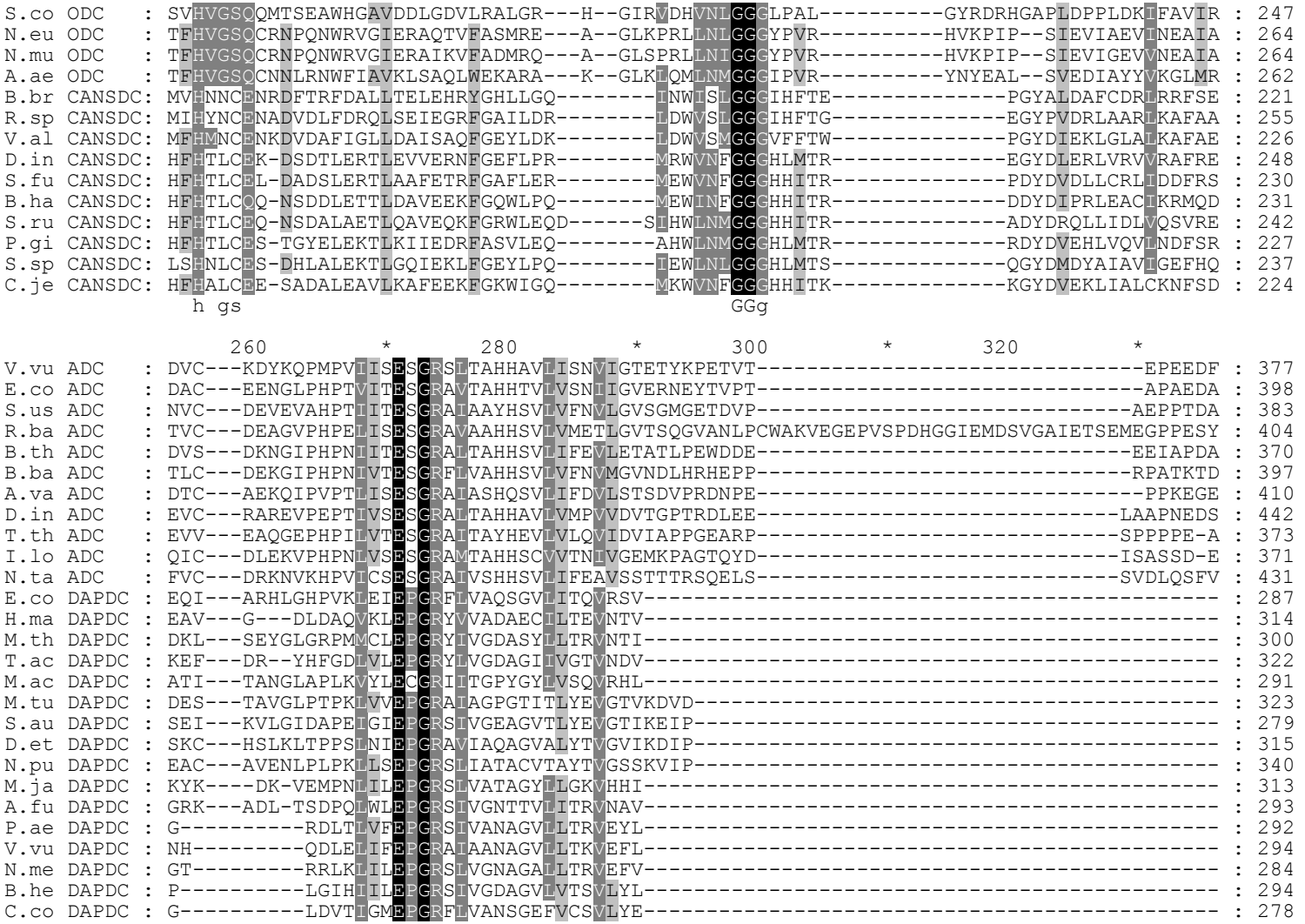
S.co ODC : SVHVGSQQMTSEAWHGAVDDLGDVLRALGR---H--GIRVDHVNLGGGLPAL----------GYRDRHGAPLDPPLDKIFAVIR : 247
N.eu ODC : TFHVGSQCRNPQNWRVGIERAQTVFASMRE---A--GLKPRLLNLGGGYPVR----------HVKPIP--SIEVIAEVINEAIA : 264
N.mu ODC : TFHVGSQCRNPQNWRVGIERAIKVFADMRQ---A--GLSPRLLNIGGGYPVR----------HVKPIP--SIEVIGEVVNEAIA : 264
A.ae ODC : TFHVGSQCNNLRNWFIAVKLSAQLWEKARA---K--GLKLQMLNMGGGIPVR----------YNYEAL--SVEDIAYYVKGLMR : 262
B.br CANSDC: MVHNNCENRDFTRFDALLTELEHRYGHLLGQ--------INWISLGGGIHFTE----------PGYALDAFCDRLRRFSE : 221
R.sp CANSDC: MIHYNCENADVDLFDRQLSEIEGRFGAILDR--------LDWVSLGGGIHFTG----------EGYPVDRLAARLKAFAA : 255
V.al CANSDC: MFHMNCENKDVDAFIGLLDAISAQFGEYLDK--------LDWVSMGGGVFFTW----------PGYDIEKLGLALKAFAE : 226
D.in CANSDC: HFHTLCEK-DSDTLERTLEVVERNFGEFLPR--------MRWVNFGGGHLMTR----------EGYDLERLVRVVRAFRE : 248
S.fu CANSDC: HFHTLCEL-DADSLERTLAAFETRFGAFLER--------MEWVNFGGGHHITR----------PDYDVDLLCRLIDDFRS : 230
B.ha CANSDC: HFHTLCQQ-NSDDLETTLDAVEEKFGQWLPQ--------MEWINFGGGHHITR----------DDYDIPRLEACIKRMQD : 231
S.ru CANSDC: HFHTLCEQ-NSDALAETLQAVEQKFGRWLEQD------SIHWLNMGGGHHITR----------ADYDRQLLIDLVQSVRE : 242
P.gi CANSDC: HFHTLCES-TGYELEKTLKIIEDRFASVLEQ--------AHWLNMGGGHLMTR----------RDYDVEHLVQVLNDFSR : 227
S.sp CANSDC: LSHNLCES-DHLALEKTLGQIEKLFGEYLPQ--------IEWLNLGGGHLMTS----------QGYDMDYAIAVLGEFHQ : 237
C.je CANSDC: HFHALCEE-SADALEAVLKAFEEKFGKWIGQ--------MKWVNFGGGHHITK----------KGYDVEKLIALCKNFSD : 224
h gs GGg
260 * 280 * 300 * 320 *
V.vu ADC : DVC---KDYKQPMPVIISEIGRSLTAHHAVLISNVIGTETYKPETVT----------EPEEDF : 377
E.co ADC : DAC---EENGLPHPTVITESGRAVTAHHTVLVSNIIGVERNEYTVPT----------APAEDA : 398
S.us ADC : NVC---DEVEVAHPTIITESGRAIAAYHSVLVFNVLGVSGMGETDVP----------AEPPTDA : 383
R.ba ADC : TVC---DEAGVPHPELISESGRAVAAHHSVLVMETLGVTSQGVANLPCWAKVEGEPVSPDHGGIEMDSVGAIETSEMEGPPESY : 404
B.th ADC : DVS---DKNGIPHPNIITESGRALTAHHSVLIFEVLETATLPEWDDE----------EEIAPDA : 370
B.ba ADC : TLC---DEKGIPHPNIVTESGRFLVAHHSVLVFNVMGVNDLHRHEPP----------RPATKTD : 397
A.va ADC : DTC---AEKQIPVPTIISESGRAIASHQSVLIFDVLSTSDVPRDNPE----------PPKEGE : 410
D.in ADC : EVC---RAREVPEPTIVSESGRALTAHHAVLVMPVVDVTGPTRDLEE----------LAAPNEDS : 442
T.th ADC : EVV---EAQGEPHPILVTESGRAITAYHEVLVLQVIDVIAPPGEARP----------SPPPPE-A : 373
I.lo ADC : QIC---DLEKVPHPNIVSESGRAMTAHHSCVVTNIVGEMKPAGTQYD----------ISASSD-E : 371
N.ta ADC : FVC---DRKNVKHPVICSESGRAIVSHHSVLIFEAVSSTTTRSQELS----------SVDLQSFV : 431
E.co DAPDC : EQI---ARHLGHPVKIEIEPGRFLVAQSGVLITQVRSV---------- : 287
H.ma DAPDC : EAV---G---DLDAQVKLEPGRYVVADAECILTEVNTV---------- : 314
M.th DAPDC : DKL---SEYGLGRPMMCLEPGRYIVGDASYLLTRVNTI---------- : 300
T.ac DAPDC : KEF---DR--YHFGDLVLEPGRYLVGDAGIIVGTVNDV---------- : 322
M.ac DAPDC : ATI---TANGLAPLKVYLECGRIITGPYGYLVSQVRHL---------- : 291
M.tu DAPDC : DES---TAVGLPTPKIVVEPGRAIAGPGTITLYEVGTVKDVD---------- : 323
S.au DAPDC : SEI---KVLGIDAPEIGIEPGRSIVGEAGVTLYEVGTIKEIP---------- : 279
D.et DAPDC : SKC---HSLKLTPPSLNIEPGRAVIAQAGVALYTVGVIKDIP---------- : 315
N.pu DAPDC : EAC---AVENLPLPKLLSEPGRSLIATACVTAYTVGSSKVIP---------- : 340
M.ja DAPDC : KYK----DK-VEMPNLILEPGRSLVATAGYLLGKVHHI---------- : 313
A.fu DAPDC : GRK---ADL-TSDPQLWLEPGRSIVGNTTVLITRVNAV---------- : 293
P.ae DAPDC : G----------RDLTLVFEPGRSIVANAGVLLTRVEYL---------- : 292
V.vu DAPDC : NH---------QDLEIIFEPGRAIAANAGVLLTKVEFL---------- : 294
N.me DAPDC : GT---------RRLKLILEPGRSLVGNAGALLTRVEFV---------- : 284
B.he DAPDC : P----------LGIHIILEPGRSIVGDAGVLVTSVLYL---------- : 294
C.co DAPDC : G----------LDVTIGMEPGRFLVANSGEFVCSVLYE---------- : 278

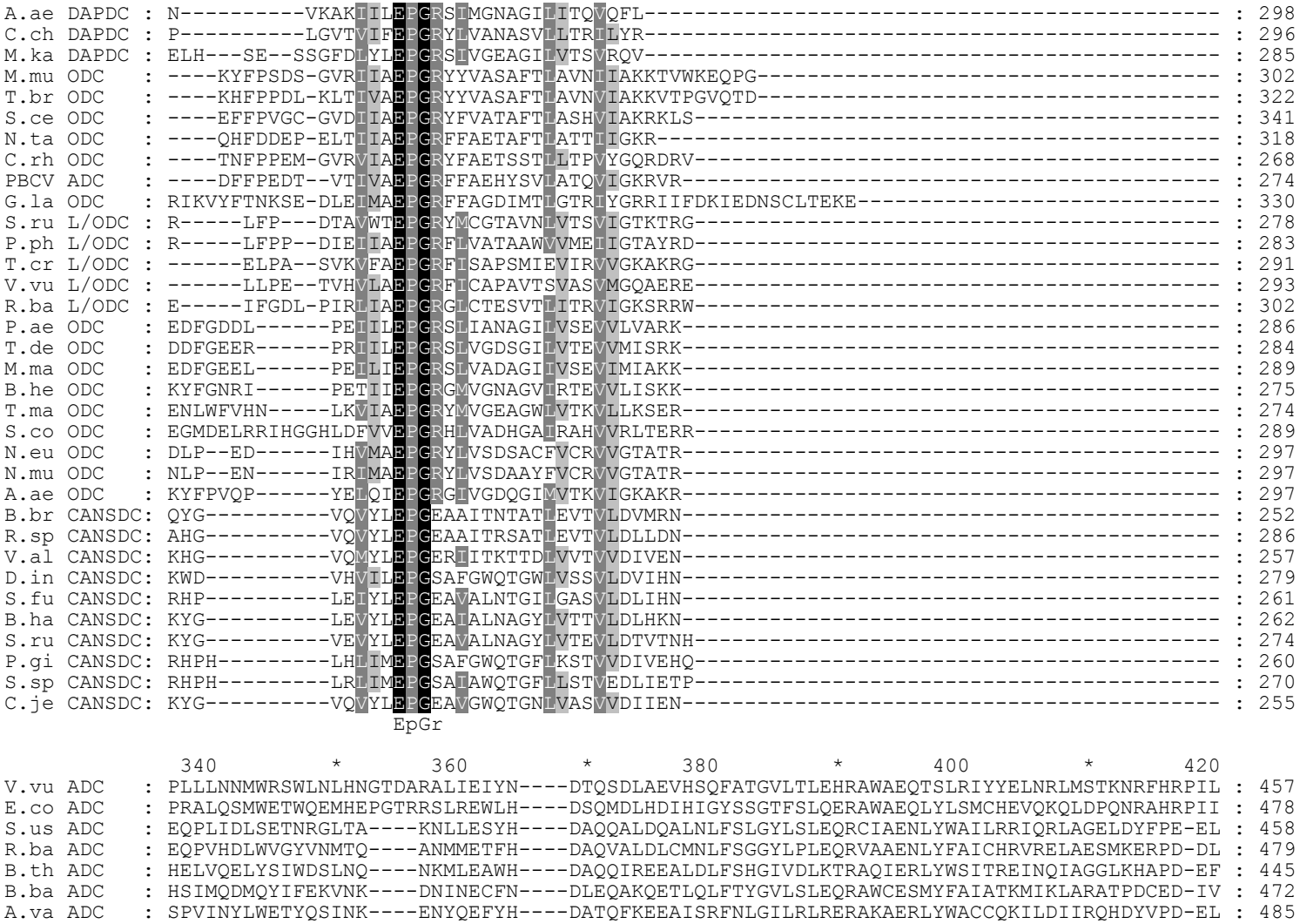
A.ae DAPDC : N----------VKAKIILEPGRSIMGNAGILITQVQFL---------- : 298
C.ch DAPDC : P----------LGVTVIFEPGRYLVANASVLLTRILYR---------- : 296
M.ka DAPDC : ELH---SE--SSGFDLYLEPGRSIVGEAGILVTSVRQV---------- : 285
M.mu ODC : ----KYFPSDS-GVRIIAEPGRYYVASAFTLAVNIIAKKTVWKEQPG---------- : 302
T.br ODC : ----KHFPPDL-KLTIVAEPGRYYVASAFTLAVNVIAKKVTPGVQTD---------- : 322
S.ce ODC : ----EFFPVGC-GVDIIAEPGRYFVATAFTLASHVIAKRKLS---------- : 341
N.ta ODC : ----QHFDDEP-ELTIIAEPGRFFAETAFTLATTIIGKR---------- : 318
C.rh ODC : ----TNFPPEM-GVRVIAEPGRYFAETSSTLLTPVYGQRDRV---------- : 268
PBCV ADC : ----DFFPEDT--VTIVAEPGRFFAEHYSVLATQVIGKRVR---------- : 274
G.la ODC : RIKVYFTNKSE-DLEIMAEPGRFFAGDIMTLGTRIYGRRIIFDKIEDNSCLTEKE---------- : 330
S.ru L/ODC : R-----LFP---DTAVWTEPGRYMCGTAVNLVTSVIGTKTRG---------- : 278
P.ph L/ODC : R-----LFPP--DIEIIAEPGRFLVATAAWVVMEIIGTAYRD---------- : 283
T.cr L/ODC : ------ELPA--SVKVFAEPGRFISAPSMIEVIRVVGKAKRG---------- : 291
V.vu L/ODC : ------LLPE--TVHVLAEPGRFICAPAVTSVASVMGQAERE---------- : 293
R.ba L/ODC : E-----IFGDL-PIRLIAEPGRGLCTESVTLITRVIGKSRRW---------- : 302
P.ae ODC : EDFGDDL------PEIILEPGRSLIANAGILVSEVVLVARK---------- : 286
T.de ODC : DDFGEER------PRIILEPGRSLVGDSGILVTEVVMISRK---------- : 284
M.ma ODC : EDFGEEL------PEILIEPGRSLVADAGIIVSEVIMIAKK---------- : 289
B.he ODC : KYFGNRI------PETIIEPGRGMVGNAGVIRTEVVLISKK---------- : 275
T.ma ODC : ENLWFVHN-----LKVIAEPGRYMVGEAGWLVTKVLLKSER---------- : 274
S.co ODC : EGMDELRRIHGGHLDFVVEPGRHLVADHGAIRAHVVRLTERR---------- : 289
N.eu ODC : DLP--ED------IHVMAEPGRYLVSDSACFVCRVVGTATR---------- : 297
N.mu ODC : NLP--EN------IRIMAEPGRYLVSDAAYFVCRVVGTATR---------- : 297
A.ae ODC : KYFPVQP------YELQIEPGRGIVGDQGIMVTKVIGKAKR---------- : 297
B.br CANSDC: QYG----------VQVYLEPGEAAITNTATLEVTVLDVMRN---------- : 252
R.sp CANSDC: AHG----------VQVYLEPGEAAITRSATLEVTVLDLLDN---------- : 286
V.al CANSDC: KHG----------VQMYLEPGERIITKTTDLVVTVVDIVEN---------- : 257
D.in CANSDC: KWD----------VHVILEPGSAFGWQTGWLVSSVLDVIHN---------- : 279
S.fu CANSDC: RHP----------LEIYLEPGEAVALNTGILGASVLDLIHN---------- : 261
B.ha CANSDC: KYG----------LEVYLEPGEAIALNAGYLVTTVLDLHKN---------- : 262
S.ru CANSDC: KYG----------VEVYLEPGEAVALNAGYLVTEVLDTVTNH---------- : 274
P.gi CANSDC: RHPH---------LHLIMEPGSAFGWQTGFLKSTVVDIVEHQ---------- : 260
S.sp CANSDC: RHPH---------LRLIMEPGSAIAWQTGFLLSTVEDLIETP---------- : 270
C.je CANSDC: KYG----------VQVYLEPGEAVGWQTGNLVASVVDIIEN---------- : 255
EpGr
340 * 360 * 380 * 400 * 420
V.vu ADC : PLLLNNMWRSWLNLHNGTDARALIEIYN----DTQSDLAEVHSQFATGVLTLEHRAWAEQTSLRIYYELNRLMSTKNRFHRPIL : 457
E.co ADC : PRALQSMWETWQEMHEPGTRRSLREWLH----DSQMDLHDIHIGYSSGTFSLQERAWAEQLYLSMCHEVQKQLDPQNRAHRPII : 478
S.us ADC : EQPLIDLSETNRGLTA----KNLLESYH----DAQQALDQALNLFSLGYLSLEQRCIAENLYWAILRRIQRLAGELDYFPE-EL : 458
R.ba ADC : EQPVHDLWVGYVNMTQ----ANMMETFH----DAQVALDLCMNLFSGGYLPLEQRVAAENLYFAICHRVRELAESMKERPD-DL : 479
B.th ADC : HELVQELYSIWDSLNQ----NKMLEAWH----DAQQIREEALDLFSHGIVDLKTRAQIERLYWSITREINQIAGGLKHAPD-EF : 445
B.ba ADC : HSIMQDMQYIFEKVNK----DNINECFN----DLEQAKQETLQLFTYGVLSLEQRAWCESMYFAIATKMIKLARATPDCED-IV : 472
A.va ADC : SPVINYLWETYQSINK----ENYQEFYH----DATQFKEEAISRFNLGILRLRERAKAERLYWACCQKILDIIRQHDYVPD-EL : 485

```
D.in ADC   : HQIVKDLEDILVNISS----RNYREMYN----DAVGDKQTLHNLFDLGYVTLNDRARGEALFNAILRKIAKLIQGEKYVPD-EL : 517
T.th ADC   : HPLVKELWESLQSLSP----KNFQEVYH----DAFADKETLQTLYDLGLVSLRDRALAEEIFYHIARRVQAIAQNLPYVPD-EL : 448
I.lo ADC   : HILVKNMRELHSSGDQ----FHPQERYN----DAAGYKQNAYEAFKLGILSLNEMAKLDTMYWQILADIHHSLDKDTYVMQ-EL : 446
N.ta ADC   : EKLNDDARADYRNLSA----AAIRGEYDTCVLYADQLKQRCVEQFKDGDLDIEQLAAVDGICDFVSKAIGASDP---------- : 501
E.co DAPDC : ---------------------------------------------------------------------------------- :   -
H.ma DAPDC : ---------------------------------------------------------------------------------- :   -
M.th DAPDC : ---------------------------------------------------------------------------------- :   -
T.ac DAPDC : ---------------------------------------------------------------------------------- :   -
M.ac DAPDC : ---------------------------------------------------------------------------------- :   -
M.tu DAPDC : ---------------------------------------------------------------------------------- :   -
S.au DAPDC : ---------------------------------------------------------------------------------- :   -
D.et DAPDC : ---------------------------------------------------------------------------------- :   -
N.pu DAPDC : ---------------------------------------------------------------------------------- :   -
M.ja DAPDC : ---------------------------------------------------------------------------------- :   -
A.fu DAPDC : ---------------------------------------------------------------------------------- :   -
P.ae DAPDC : ---------------------------------------------------------------------------------- :   -
V.vu DAPDC : ---------------------------------------------------------------------------------- :   -
N.me DAPDC : ---------------------------------------------------------------------------------- :   -
B.he DAPDC : ---------------------------------------------------------------------------------- :   -
C.co DAPDC : ---------------------------------------------------------------------------------- :   -
A.ae DAPDC : ---------------------------------------------------------------------------------- :   -
C.ch DAPDC : ---------------------------------------------------------------------------------- :   -
M.ka DAPDC : ---------------------------------------------------------------------------------- :   -
M.mu ODC   : ------------------------------------------------------------------------------SDD : 305
T.br ODC   : -----------------------------------------------------------------------------VGA : 325
S.ce ODC   : ---------------------------------------------------------------------------------- :   -
N.ta ODC   : ---------------------------------------------------------------------------------- :   -
C.rh ODC   : ---------------------------------------------------------------------------------- :   -
PBCV ADC   : ---------------------------------------------------------------------------------- :   -
G.la ODC   : ---------------------------------------------------------------------------IME : 333
S.ru L/ODC : ---------------------------------------------------------------------------------- :   -
P.ph L/ODC : ---------------------------------------------------------------------------------- :   -
T.cr L/ODC : ---------------------------------------------------------------------------------- :   -
V.vu L/ODC : ---------------------------------------------------------------------------------- :   -
R.ba L/ODC : ---------------------------------------------------------------------------------- :   -
P.ae ODC   : ---------------------------------------------------------------------------------- :   -
T.de ODC   : ---------------------------------------------------------------------------------- :   -
M.ma ODC   : ---------------------------------------------------------------------------------- :   -
B.he ODC   : ---------------------------------------------------------------------------------- :   -
T.ma ODC   : ---------------------------------------------------------------------------------- :   -
S.co ODC   : ---------------------------------------------------------------------------------- :   -
N.eu ODC   : ---------------------------------------------------------------------------------- :   -
N.mu ODC   : ---------------------------------------------------------------------------------- :   -
A.ae ODC   : ---------------------------------------------------------------------------------- :   -
```

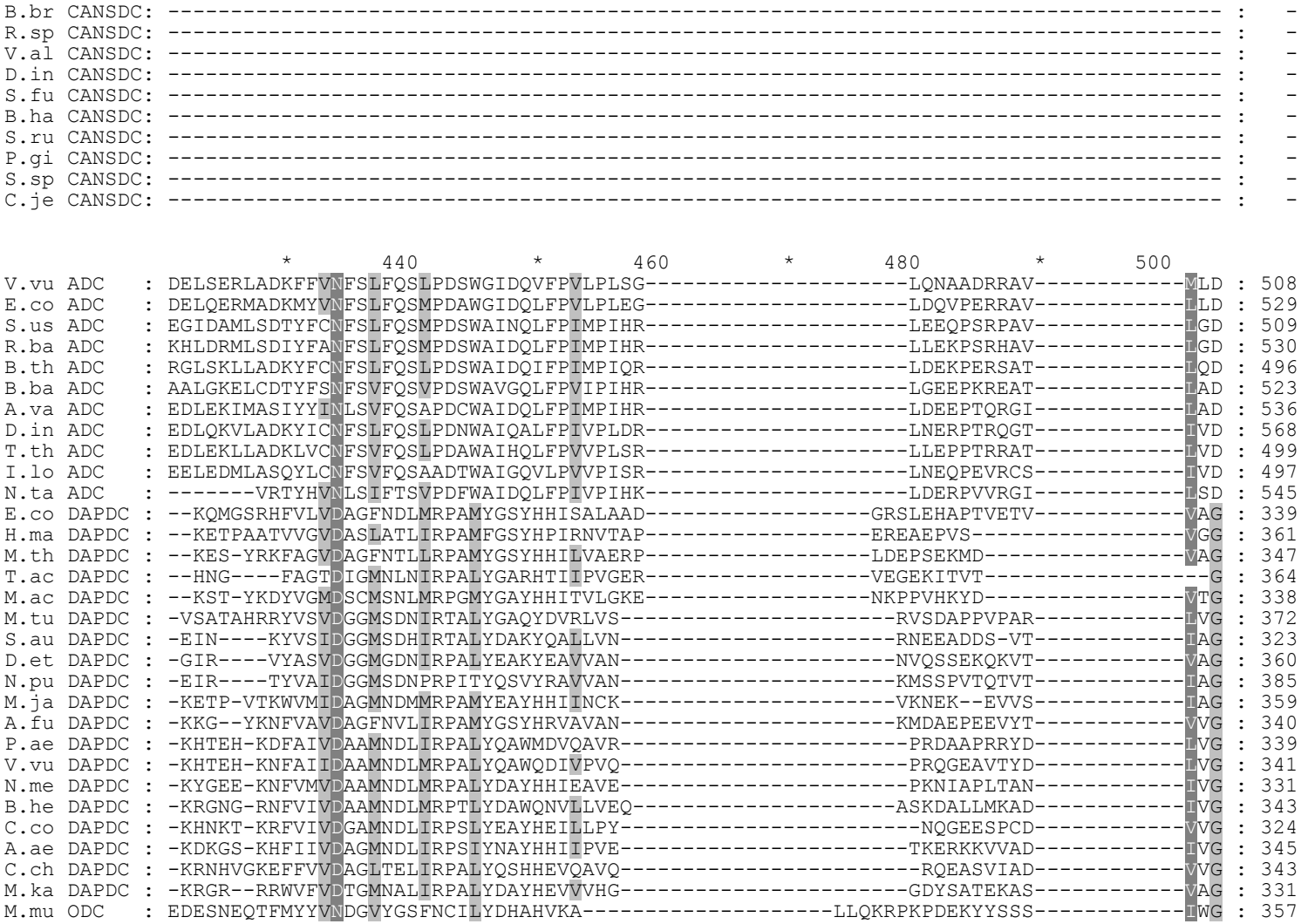
B.br CANSDC: ---------- : -
R.sp CANSDC: ---------- : -
V.al CANSDC: ---------- : -
D.in CANSDC: ---------- : -
S.fu CANSDC: ---------- : -
B.ha CANSDC: ---------- : -
S.ru CANSDC: ---------- : -
P.gi CANSDC: ---------- : -
S.sp CANSDC: ---------- : -
C.je CANSDC: ---------- : -
* 440 * 460 * 480 * 500
V.vu ADC : DELSERLADKFFVNFSLFQSLPDSWGIDQVFPVLPLSG----------LQNAADRRAV----------MLD : 508
E.co ADC : DELQERMADKMYVNFSLFQSMPDAWGIDQLFPVLPLEG----------LDQVPERRAV----------LLD : 529
S.us ADC : EGIDAMLSDTYFCNFSLFQSMPDSWAINQLFPIMPIHR----------LEEQPSRPAV----------LGD : 509
R.ba ADC : KHLDRMLSDIYFANFSLFQSMPDSWAIDQLFPIMPIHR----------LLEKPSRHAV----------LGD : 530
B.th ADC : RGLSKLLADKYFCNFSLFQSLPDSWAIDQIFPIMPIQR----------LDEKPERSAT----------LQD : 496
B.ba ADC : AALGKELCDTYFSNFSVFQSVPDSWAVGQLFPVIPIHR----------LGEEPKREAT----------LAD : 523
A.va ADC : EDLEKIMASIYYINLSVFQSAPDCWAIDQLFPIMPIHR----------LDEEPTQRGI----------LAD : 536
D.in ADC : EDLQKVLADKYICNFSLFQSLPDNWAIQALFPIVPLDR----------LNERPTRQGT----------IVD : 568
T.th ADC : EDLEKLLADKLVCNFSVFQSLPDAWAIHQLFPVVPLSR----------LLEPPTRRAT----------IVD : 499
I.lo ADC : EELEDMLASQYLCNFSVFQSAADTWAIGQVLPVVPISR----------LNEQPEVRCS----------IVD : 497
N.ta ADC : -------VRTYHVNLSIFTSVPDFWAIDQLFPIVPIHK----------LDERPVVRGI----------LSD : 545
E.co DAPDC : --KQMGSRHFVLVDAGFNDLMRPAMYGSYHHISALAAD----------GRSLEHAPTVETV----------VAG : 339
H.ma DAPDC : --KETPAATVVGVDASLATLIRPAMFGSYHPIRNVTAP----------EREAEPVS----------VGG : 361
M.th DAPDC : --KES-YRKFAGVDAGFNTLLRPAMYGSYHHILVAERP----------LDEPSEKMD----------VAG : 347
T.ac DAPDC : --HNG----FAGTDIGMNLNIRPALYGARHTIIPVGER----------VEGEKITVT----------G : 364
M.ac DAPDC : --KST-YKDYVGMDSCMSNLMRPGMYGAYHHITVLGKE----------NKPPVHKYD----------VTG : 338
M.tu DAPDC : -VSATAHRRYVSVDGGMSDNIRTALYGAQYDVRLVS----------RVSDAPPVPAR----------IVG : 372
S.au DAPDC : -EIN----KYVSIDGGMSDHIRTALYDAKYQALLVN----------RNEEADDS-VT----------IAG : 323
D.et DAPDC : -GIR----VYASVDGGMGDNIRPALYEAKYEAVVAN----------NVQSSEKQKVT----------VAG : 360
N.pu DAPDC : -EIR----TYVAIDGGMSDNPRPITYQSVYRAVVAN----------KMSSPVTQTVT----------IAG : 385
M.ja DAPDC : -KETP-VTKWVMIDAGMNDMMRPAMYEAYHHIINCK----------VKNEK--EVVS----------IAG : 359
A.fu DAPDC : -KKG--YKNFVAVDAGFNVLIRPAMYGSYHRVAVAN----------KMDAEPEEVYT----------VVG : 340
P.ae DAPDC : -KHTEH-KDFAIVDAAMNDLIRPALYQAWMDVQAVR----------PRDAAPRRYD----------IVG : 339
V.vu DAPDC : -KHTEH-KNFAIIDAAMNDLMRPALYQAWQDIVPVQ----------PRQGEAVTYD----------IVG : 341
N.me DAPDC : -KYGEE-KNFVMVDAAMNDLMRPALYDAYHHIEAVE----------PKNIAPLTAN----------IVG : 331
B.he DAPDC : -KRGNG-RNFVIVDAAMNDLMRPTLYDAWQNVLLVEQ----------ASKDALLMKAD----------IVG : 343
C.co DAPDC : -KHNKT-KRFVIVDGAMNDLIRPSLYEAYHEILLPY----------NQGEESPCD----------VVG : 324
A.ae DAPDC : -KDKGS-KHFIIVDAGMNDLIRPSIYNAYHHIIPVE----------TKERKKVVAD----------IVG : 345
C.ch DAPDC : -KRNHVGKEFFVVDAGLTELIRPALYQSHHEVQAVQ----------RQEASVIAD----------VVG : 343
M.ka DAPDC : -KRGR--RRWVFVDTGMNALIRPALYDAYHEVVVHG----------GDYSATEKAS----------VAG : 331
M.mu ODC : EDESNEQTFMYYVNDGVYGSFNCILYDHAHVKA----------LLQKRPKPDEKYYSSS----------IWG : 357

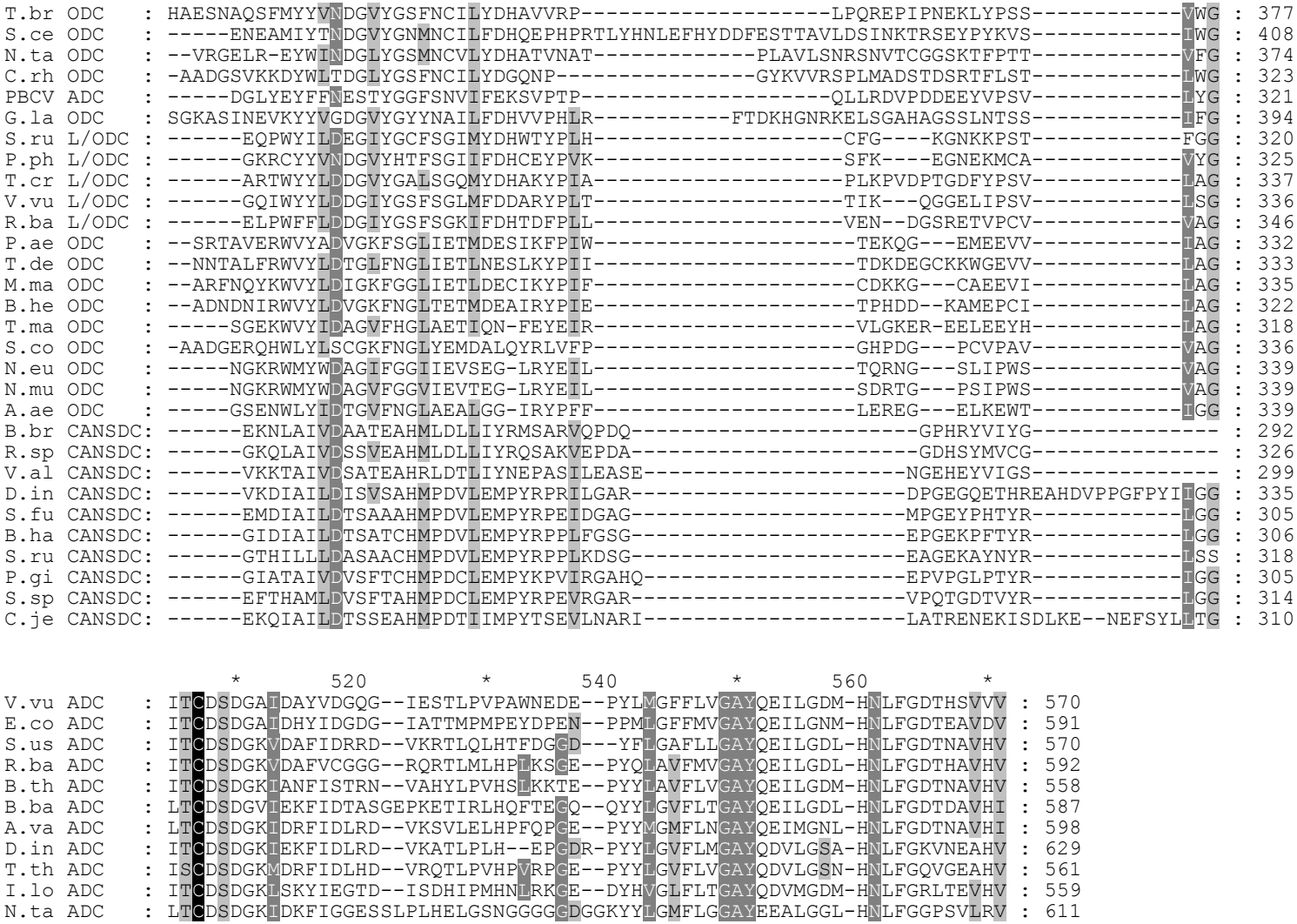
T.br ODC : HAESNAQSFMYYVNDGVYGSFNCILYDHAVVRP----------LPQREPIPNEKLYPSS----------VWG : 377
S.ce ODC : -----ENEAMIYTNDGVYGNMNCILFDHQEPHPRTLYHNLEFHYDDFESTTAVLDSINKTRSEYPYKVS----------IWG : 408
N.ta ODC : --VRGELR-EYWINDGLYGSMNCVLYDHATVNAT----------PLAVLSNRSNVTCGGSKTFPTT----------VFG : 374
C.rh ODC : -AADGSVKKDYWLTDGLYGSFNCILYDGQNP----------GYKVVRSPLMADSTDSRTFLST----------LWG : 323
PBCV ADC : -----DGLYEYFFNESTYGGFSNVIFEKSVPTP----------QLLRDVPDDEEYVPSV----------LYG : 321
G.la ODC : SGKASINEVKYYVGDGVYGYYNAILFDHVVPHLR----------FTDKHGNRKELSGAHAGSSLNTSS----------IFG : 394
S.ru L/ODC : ------EQPWYILDEGIYGCFSGIMYDHWTYPLH----------CFG----KGNKKPST----------FGG : 320
P.ph L/ODC : ------GKRCYYVNDGVYHTFSGIIFDHCEYPVK----------SFK----EGNEKMCA----------VYG : 325
T.cr L/ODC : ------ARTWYYLDDGVYGALSGQMYDHAKYPIA----------PLKPVDPTGDFYPSV----------LAG : 337
V.vu L/ODC : ------GQIWYYLDDGIYGSFSGLMFDDARYPLT----------TIK---QGGELIPSV----------LSG : 336
R.ba L/ODC : ------ELPWFFLDDGIYGSFSGKIFDHTDFPLL----------VEN--DGSRETVPCV----------VAG : 346
P.ae ODC : --SRTAVERWVYADVGKFSGLIETMDESIKFPIW----------TEKQG---EMEEVV----------IAG : 332
T.de ODC : --NNTALFRWVYLDTGLFNGLIETLNESLKYPII----------TDKDEGCKKWGEVV----------LAG : 333
M.ma ODC : --ARFNQYKWVYLDIGKFGGLIETLDECIKYPIF----------CDKKG---CAEEVI----------LAG : 335
B.he ODC : --ADNDNIRWVYLDVGKFNGLTETMDEAIRYPIE----------TPHDD--KAMEPCI----------LAG : 322
T.ma ODC : -----SGEKWVYIDAGVFHGLAETIQN-FEYEIR----------VLGKER-EELEEYH----------LAG : 318
S.co ODC : -AADGERQHWLYLSCGKFNGLYEMDALQYRLVFP----------GHPDG---PCVPAV----------VAG : 336
N.eu ODC : -----NGKRWMYWDAGIFGGIIEVSEG-LRYEIL----------TQRNG---SLIPWS----------VAG : 339
N.mu ODC : -----NGKRWMYWDAGVFGGVIEVTEG-LRYEIL----------SDRTG---PSIPWS----------VAG : 339
A.ae ODC : -----GSENWLYIDTGVFNGLAEALGG-IRYPFF----------LEREG---ELKEWT----------IGG : 339
B.br CANSDC: ------EKNLAIVDAATEAHMLDLLIYRMSARVQPDQ----------GPHRYVIYG---------- : 292
R.sp CANSDC: ------GKQLAIVDSSVEAHMLDLLIYRQSAKVEPDA----------GDHSYMVCG---------- : 326
V.al CANSDC: ------VKKTAIVDSATEAHRLDTLIYNEPASILEASE----------NGEHEYVIGS---------- : 299
D.in CANSDC: ------VKDIAILDISVSAHMPDVLEMPYRPRILGAR----------DPGEGQETHREAHDVPPGFPYIIGG : 335
S.fu CANSDC: ------EMDIAILDTSAAAHMPDVLEMPYRPEIDGAG----------MPGEYPHTYR----------LGG : 305
B.ha CANSDC: ------GIDIAILDTSATCHMPDVLEMPYRPPLFGSG----------EPGEKPFTYR----------LGG : 306
S.ru CANSDC: ------GTHILLLDASAACHMPDVLEMPYRPPLKDSG----------EAGEKAYNYR----------LSS : 318
P.gi CANSDC: ------GIATAIVDVSFTCHMPDCLEMPYKPVIRGAHQ----------EPVPGLPTYR----------IGG : 305
S.sp CANSDC: ------EFTHAMLDVSFTAHMPDCLEMPYRPEVRGAR----------VPQTGDTVYR----------LGG : 314
C.je CANSDC: ------EKQIAILDTSSEAHMPDTIIMPYTSEVLNARI----------LATRENEKISDLKE--NEFSYLLTG : 310
* 520 * 540 * 560 *
V.vu ADC : ITCDSDGAIDAYVDGQG--IESTLPVPAWNEDE--PYLMGFFLVGAYQEILGDM-HNLFGDTHSVVV : 570
E.co ADC : ITCDSDGAIDHYIDGDG--IATTMPMPEYDPEN--PPMLGFFMVGAYQEILGNM-HNLFGDTEAVDV : 591
S.us ADC : ITCDSDGKVDAFIDRRD--VKRTLQLHTFDGGD---YFLGAFLLGAYQEILGDL-HNLFGDTNAVHV : 570
R.ba ADC : ITCDSDGKVDAFVCGGG--RQRTLMLHPLKSGE--PYQLAVFMVGAYQEILGDL-HNLFGDTHAVHV : 592
B.th ADC : ITCDSDGKIANFISTRN--VAHYLPVHSLKKTE--PYYLAVFLVGAYQEILGDM-HNLFGDTNAVHV : 558
B.ba ADC : LTCDSDGVIEKFIDTASGEPKETIRLHQFTEGQ--QYYLGVFLTGAYQEILGDL-HNLFGDTDAVHI : 587
A.va ADC : LTCDSDGKIDRFIDLRD--VKSVLELHPFQPGE--PYYMGMFLNGAYQEIMGNL-HNLFGDTNAVHI : 598
D.in ADC : ITCDSDGKIEKFIDLRD--VKATLPLH--EPGDR-PYYLGVFLMGAYQDVLGSA-HNLFGKVNEAHV : 629
T.th ADC : ISCDSDGKMDRFIDLHD--VRQTLPVHPVRPGE--PYYLGVFLVGAYQDVLGSN-HNLFGQVGEAHV : 561
I.lo ADC : ITCDSDGKLSKYIEGTD--ISDHIPMHNLRKGE--DYHVGLFLTGAYQDVMGDM-HNLFGRLTEVHV : 559
N.ta ADC : LTCDSDGKIDKFIGGESSLPLHELGSNGGGGGDGGKYYLGMFLGGAYEEALGGL-HNLFGGPSVLRV : 611

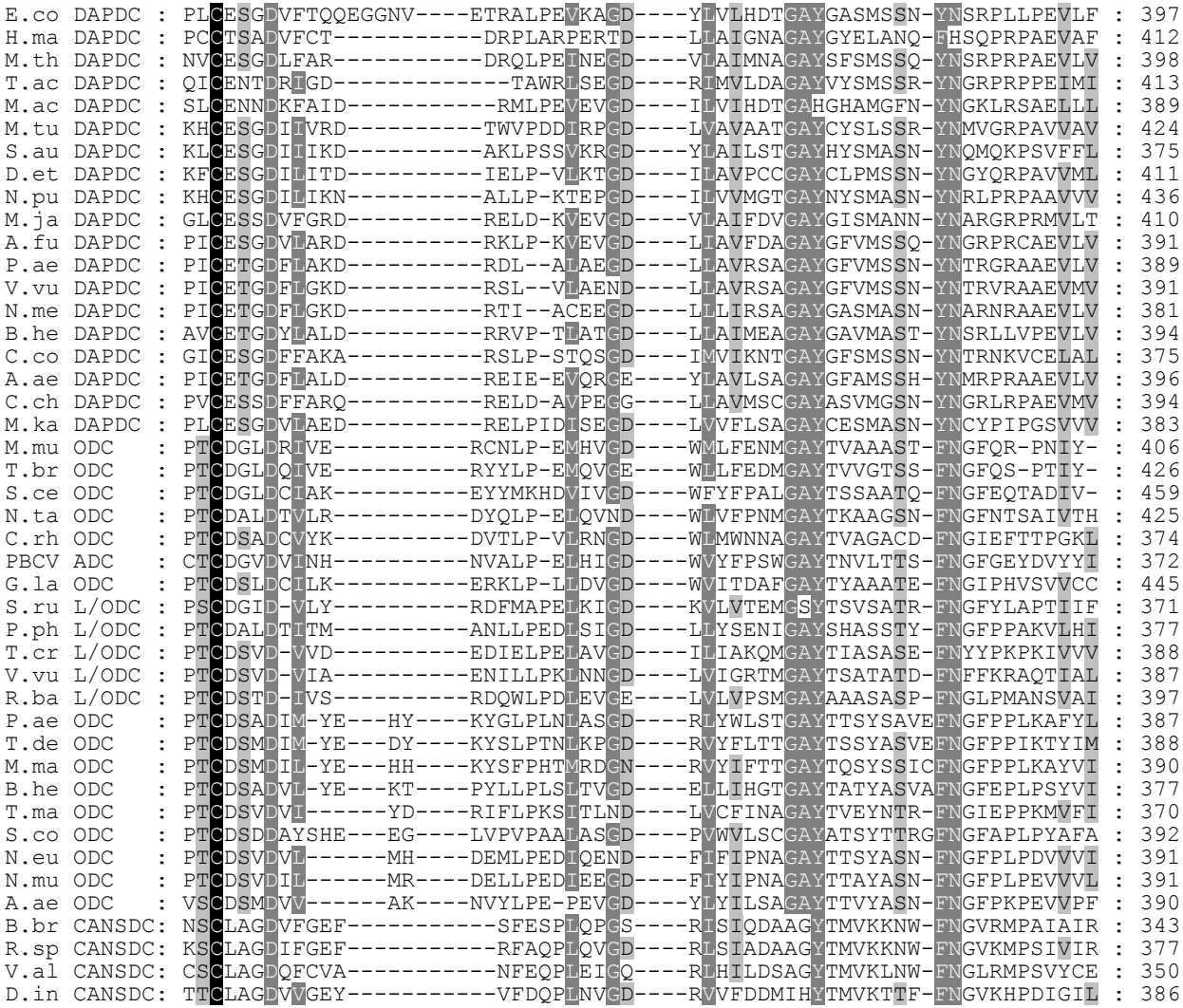
E.co DAPDC : PLCESGDVFTQQEGGNV----ETRALPEVKAGD----YLVLHDTGAYGASMSSN-YNSRPLLPEVLF : 397
H.ma DAPDC : PCCTSADVFCT-----------DRPLARPERTD----LLAIGNAGAYGYELANQ-FHSQPRPAEVAF : 412
M.th DAPDC : NVCESGDLFAR-----------DRQLPEINEGD----VLAIMNAGAYSFSMSSQ-YNSRPRPAEVLV : 398
T.ac DAPDC : QICENTDRIGD-------------TAWRLSEGD----RIMVLDAGAYVYSMSSR-YNGRPRPPEIMI : 413
M.ac DAPDC : SLCENNDKFAID-----------RMLPEVEVGD----ILVIHDTGAHGHAMGFN-YNGKLRSAELLL : 389
M.tu DAPDC : KHCESGDIIVRD----------TWVPDDIRPGD----LVAVAATGAYCYSLSSR-YNMVGRPAVVAV : 424
S.au DAPDC : KLCESGDIIIKD----------AKLPSSVKRGD----YLAILSTGAYHYSMASN-YNQMQKPSVFFL : 375
D.et DAPDC : KFCESGDILITD----------IELP-VLKTGD----ILAVPCCGAYCLPMSSN-YNGYQRPAVVML : 411
N.pu DAPDC : KHCESGDILIKN----------ALLP-KTEPGD----ILVVMGTGAYNYSMASN-YNRLPRPAAVVV : 436
M.ja DAPDC : GLCESSDVFGRD----------RELD-KVEVGD----VLAIFDVGAYGISMANN-YNARGRPRMVLT : 410
A.fu DAPDC : PICESGDVLARD----------RKLP-KVEVGD----LIAVFDAGAYGFVMSSQ-YNGRPRCAEVLV : 391
P.ae DAPDC : PICETGDFLAKD----------RDL--ALAEGD----LLAVRSAGAYGFVMSSN-YNTRGRAAEVLV : 389
V.vu DAPDC : PICETGDFLGKD----------RSL--VLAEND----LLAVRSAGAYGFVMSSN-YNTRVRAAEVMV : 391
N.me DAPDC : PICETGDFLGKD----------RTI--ACEEGD----LLLIRSAGAYGASMASN-YNARNRAAEVLV : 381
B.he DAPDC : AVCETGDYLALD----------RRVP-TLATGD----LLAIMEAGAYGAVMAST-YNSRLLVPEVLV : 394
C.co DAPDC : GICESGDFFAKA----------RSLP-STQSGD----IMVIKNTGAYGFSMSSN-YNTRNKVCELAL : 375
A.ae DAPDC : PICETGDFLALD----------REIE-EVQRGE----YLAVLSAGAYGFAMSSH-YNMRPRAAEVLV : 396
C.ch DAPDC : PVCESSDFFARQ----------RELD-AVPEGG----LLAVMSCGAYASVMGSN-YNGRLRPAEVMV : 394
M.ka DAPDC : PLCESGDVLAED----------RELPIDISEGD----LVVFLSAGAYCESMASN-YNCYPIPGSVVV : 383
M.mu ODC : PTCDGLDRIVE----------RCNLP-EMHVGD----WMLFENMGAYTVAAAST-FNGFQR-PNIY- : 406
T.br ODC : PTCDGLDQIVE----------RYYLP-EMQVGE----WLLFEDMGAYTVVGTSS-FNGFQS-PTIY- : 426
S.ce ODC : PTCDGLDCIAK----------EYYMKHDVIVGD----WFYFPALGAYTSSAATQ-FNGFEQTADIV- : 459
N.ta ODC : PTCDALDTVLR----------DYQLP-ELQVND----WLVFPNMGAYTKAAGSN-FNGFNTSAIVTH : 425
C.rh ODC : PTCDSADCVYK----------DVTLP-VLRNGD----WLMWNNAGAYTVAGACD-FNGIEFTTPGKL : 374
PBCV ADC : CTCDGVDVINH----------NVALP-ELHIGD----WVYFPSWGAYTNVLTTS-FNGFGEYDVYYI : 372
G.la ODC : PTCDSLDCILK----------ERKLP-LLDVGD----WVITDAFGAYTYAAATE-FNGIPHVSVVCC : 445
S.ru L/ODC : PSCDGID-VLY----------RDFMAPELKIGD----KVLVTEMGSYTSVSATR-FNGFYLAPTIIF : 371
P.ph L/ODC : PTCDALDTITM----------ANLLPEDLSIGD----LLYSENIGAYSHASSTY-FNGFPPAKVLHI : 377
T.cr L/ODC : PTCDSVD-VVD----------EDIELPELAVGD----ILIAKQMGAYTIASASE-FNYYPKPKIVVV : 388
V.vu L/ODC : PTCDSVD-VIA----------ENILLPKLNNGD----LVIGRTMGAYTSATATD-FNFFKRAQTIAL : 387
R.ba L/ODC : PTCDSTD-IVS----------RDQWLPDLEVGE----LVLVPSMGAYAAASASP-FNGLPMANSVAI : 397
P.ae ODC : PTCDSADIM-YE---HY----KYGLPLNLASGD----RLYWLSTGAYTTSYSAVEFNGFPPLKAFYL : 387
T.de ODC : PTCDSMDIM-YE---DY----KYSLPTNLKPGD----RVYFLTTGAYTSSYASVEFNGFPPIKTYIM : 388
M.ma ODC : PTCDSMDIL-YE---HH----KYSFPHTMRDGN----RVYIFTTGAYTQSYSSICFNGFPPLKAYVI : 390
B.he ODC : PTCDSADVL-YE---KT----PYLLPLSLTVGD----ELLIHGTGAYTATYASVAFNGFEPLPSYVI : 377
T.ma ODC : PTCDSVDVI------YD----RIFLPKSITLND----LVCFINAGAYTVEYNTR-FNGIEPPKMVFI : 370
S.co ODC : PTCDSDDAYSHE---EG----LVPVPAALASGD----PVWVLSCGAYATSYTTRGFNGFAPLPYAFA : 392
N.eu ODC : PTCDSVDVL------MH----DEMLPEDIQENDD----FIFIPNAGAYTTSYASN-FNGFPLPDVVVI : 391
N.mu ODC : PTCDSVDIL------MR----DELLPEDIEEGD----FIYIPNAGAYTTAYASN-FNGFPLPEVVVL : 391
A.ae ODC : VSCDSMDVV------AK----NVYLPE-PEVGD----YLYILSAGAYTTVYASN-FNGFPKPEVVPF : 390
B.br CANSDC: NSCLAGDVFGEF-----------SFESPLQPGS----RISIQDAAGYTMVKKNW-FNGVRMPAIAIR : 343
R.sp CANSDC: KSCLAGDIFGEF-----------RFAQPLQVGD----RLSIADAAGYTMVKKNW-FNGVKMPSIVIR : 377
V.al CANSDC: CSCLAGDQFCVA----------NFEQPLEIGQ----RLHILDSAGYTMVKLNW-FNGLRMPSVYCE : 350
D.in CANSDC: TTCLAGDVVGEY----------VFDQPLNVGD----RVVFDDMIHYTMVKTTF-FNGVKHPDIGIL : 386

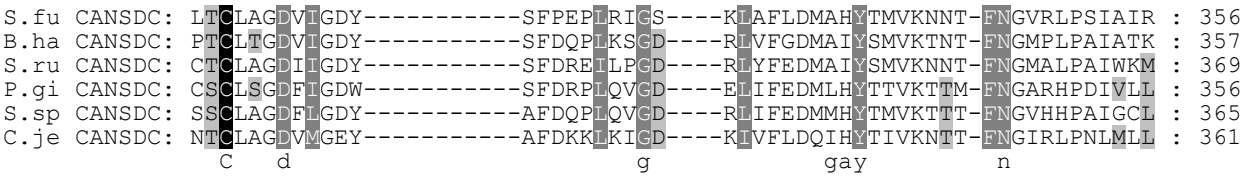

Figure 2.4 ClustalW sequence alignment of the β/α-barrel fold basic amino acid decarboxylases.

1. *Vibrio vulnificus* (γ-Proteobacteria) BAC94750; 2. *Escherichia coli* (γ-Proteobacteria) NP_755399; 3. *Solibacter usitatus* (Fibrobacteres/Acidobacteria) ZP_00527266; 4. *Rhodopirellula baltica* (Planctomycetes) CAD73363; 5. *Bacteriodes thetaiotaomicron* (Bacteriodetes) AAO78500; 6. *Bdellovibrio bacteriovorus* (δ-Proteobacteria) CAE78014; 7. *Anabaena variabilis* (Cyanobacteria) ABA23030; 8. *Deinococcus geothermalis* (Deinococcus-Thermus) ZP_00396333; 9. *Thermus thermophilus* (Deinococcus-Thermus) AAS81619; 10. *Idiomarina loihiensis* (γ-Proteobacteria) AAV82053; 11. *Nicotiana tabacum* (Viridiplantae) BAD06581; 12. *Escherichia coli* (γ-Proteobacteria) ZP_00712553; 13. *Haloarcula marismortui* (*Halobacteria) YP_134965; 14. *Methanothermobacter thermautotrophicus* (*Methanobacteria) AAB85813; 15. *Thermoplasma acidophilum* (*Thermoplasmata) CAC11919; 16. *Methanosarcina acetovirans* (*Methanomicrobia) AAM04166; 17. *Mycobacterium tuberculosis* (Actinobacteria) AAA25361; 18. *Staphylococcus aureus* (Firmicutes) CAB82467; 19. *Dehalococcoides ethenogenes* (Chloroflexi) AAW40184; 20. *Nostoc punctiforme* (Cyanobacteria) ZP_00110395; 21. *Methanocaldococcus jannaschii* (*Methanococci) NP_248090; 22. *Archaeoglobus fulgidus* (*Archaeglobi) AAB90438; 23. *Pseudomonas aeruginosa* (γ-Proteobacteria) NP_253964; 24. *Vibrio vulnificus* (γ-Proteobacteria) AAO09601; 25. *Neisseria meningitidis* (β-Proteobacteria) CAB83764; 26. *Bartonella henselae* (α-Proteobacteria) YP_034310; 27. *Campylobacter coli* (ε-Proteobacteria) ZP_00367584; 28. *Aquifex aeolicus* (Aquificae) AAC07209; 29. *Chlorobium chlorochromatii* (Chlorobi) ABB28371; 30. *Methanopyrus kandleri* (*Methanopyri) AAM01698; 31. *Mus musculus* (Metazoa) P00860; 32. *Trypanosoma brucei* (Euglenozoa) AAA30218; 33. *Saccharomyces cerevisiae* (Fungi) NP_012737; 34. *Nicotiana tabacum* (Viridiplantae) BAA83427; 35. *Chlamydomonas reinhardtii* (Viridiplantae) CAE46410; 36. Chlorella Virus PBCV-1 (Chlorovirus) NP_048554; 37. *Giardia lamblia* (Diplomonadida) XP_778717; 38. *Selenomonas ruminantium* (Firmicutes) O50657; 39. *Pelodictyon phaeoclathratiforme* (Chlorobi) ZP_00589758; 40. *Thiomicrospira crunogena* (γ-Proteobacteria) YP_390544; 41. *Vibrio vulnificus* (γ-Proteobacteria) NP_762948; 42. *Rhodopirellula baltica* (Planctomycetes) NP_868377; 43. *Pseudomonas aeruginosa* (γ-Proteobacteria) NP_253209; 44. *Treponema denticola* (Spirochaetes) NP_971717; 45. *Methanosarcina mazei* (*Methanomicrobia) NP_635209; 46. *Bartonella henselae* (α-Proteobacteria) YP_034014; 47. *Thermotoga maritima* (Thermotogae) NP_229669; 48. *Streptomyces coelicolor* (Actinobacteria) CAA19247; 49. *Nitrosomonas europaea* (β-

Proteobacteria) NP_840983; 50. *Nitrospira multiformis* (Nitrospirae) ABB75259; 51. *Aquifex aeolicus* (Aquificae) NP_213500; 52. *Bordetella bronchiseptica* (β-Proteobacteria) CAE34481; 53. *Rhodobacter sphaeroides* (α-Proteobacteria) ZP_00916901; 54. *Vibrio alginolyticus* (γ-Proteobacteria) BAA06561; 55. *Deinococcus geothermalis* (Deinococcus-Thermus) ZP_00395795; 56. *Syntrophobacter fumaoxidans* (δ-Proteobacteria) ZP_00668139; 57. *Bacillus halodurans* (Firmicutes) BAB07677; 58. *Selenomonas ruminantium* (Firmicutes) BAD86639; 59. *Porphyromonas gingivalis* (Bacteriodetes) AAQ65393; 60. *Synechocystis sp. PCC6803* (Cyanobacteria) BAA17602; 61. *Campylobacter jejuni* (ε-Proteobacteria) AAW36121

CHAPTER 3

STRUCTURAL STUDY ON THE DUAL SUBSTRATE SPECIFICITY ENZYME, LYSINE/ORNITHINE DECARBOXYLASE FROM *VIBRIO VULNIFICUS*

A. Introduction

β/α-Barrel fold decarboxylases function as homodimers and each dimer is composed of two monomers with N-terminal domain of β/α-barrel and C-terminal domain of β-sheet. The structures of the β/α-barrel fold decarboxylases with different substrate specificities provided insights into the structural basis of the substrate specificity difference. Comparison of the structures of enzymes with different substrate preferences (ODC, DAPDC and *cv*ADC) identified the 3_{10}-helix that contains Asp332 as a key specificity element (Shah et al., 2007). Amino acid residues that project from the 3_{10}-helix interact with substrate, and both the amino acid composition of the helix and its position are variable. Substrates of different size are accommodated by changes in the distance from the 3_{10}-helix to PLP, whereas changes in amino acid composition of the 3_{10}-helix allow specific interactions to occur with the full range of substrates.

As described in the Chapter Two, we identified a distinct group of prokaryotic ODCs and a subclade containing the dual function L/ODCs. The *Selenomonas* L/ODC is highly homologous to the eukaryotic ODCs (sequence identity ~35%) and has the same active site residues including Asp332 and Asp361. Eukaryotic ODCs prefer L-ornithine over L-lysine with a specificity preference of 100-fold based on k_{cat}/K_m. However *Selenomonas* L/ODC is equally active toward L-lysine and L-ornithine. While the structures of the eukaryotic ODCs have been extensively studied as previously described,

no solved structures of the prokaryotic enzymes with activity on L-ornithine had been determined and the structural basis of the dual substrate specificity was not known. In the previous study we identified another dual specificity enzyme from *V.vulnificus* that is evolutionarily distant from *S.ruminantium* within the dual specificity enzyme subclade in the phylogenetic tree (Figure 2.1). Therefore I solved the X-ray structure of the dual function enzyme from *V. vulnificus* (*Vv*L/ODC) representing the first determined structure of prokaryotic β/α-barrel fold decarboxylase with activity on L-ornithine. This structure provided insight into the structural basis for the dual specificity. Comparison of the sequence alignment with the available X-ray structures allowed us to identify amino acid motifs in the 3_{10}-helix that are predictive for the function of the bacterial and eukaryotic ornithine and diaminopimelate specific decarboxylases.

B. Experimental Procedures

1. Materials

L-ornithine, L-lysine, pyridoxal 5'-phosphate (PLP), and all other reagents were purchased from Sigma (St. Louis, MO) unless noted otherwise.

2. Crystallization of the *V.vulnificus* L/ODC and Data Collection

Initial crystallization conditions were identified in Hampton Research crystallization screens using the hanging drop method (Riverside, CA). Clusters of thick plate crystals formed upon mixing equal volumes (1.5 μl) of reservoir buffer (0.1 M Tris·HCl pH 8.5, 30% PEG-4000, 0.2 M $MgCl_2$) with *Vv*L/ODC (10 mg/ml) in buffer (0.1 M HEPES pH 7.5, 0.3 M NaCl, 0.5 mM EDTA, 10% w/v glycerol, 0.03% w/v

Brij35 and 1 mM DTT) plus 10 mM L-ornithine at 16ºC. Indexing of the resulting crystals demonstrated that they had a large unit cell dimension (6~8 molecules per asymmetric unit). To search for a crystal condition that would yield a smaller unit cell additive screening was performed using Hampton Research Additive Screen^{TM} kit. The inclusion of n-octyl-β-D-glucoside (0.5%) yielded single rod crystals of *Vv*L/ODC-putrescine. Diffraction to 2.0 Å revealed the space group $P2_12_12_1$ with only 2 molecules per asymmetric unit. Diffraction quality *Vv*L/ODC-putrescine crystals were obtained with microseeding at 4ºC by incubation of *Vv*L/ODC (1.5 µl of 10 mg/ml) pre-incubated with 20 mM L-ornithine, 1.5µl reservoir buffer (0.1 M Tris·HCl pH 8.4, 35% PEG-4000, 0.2 M $MgCl_2$) and 0.3 µl of 5% w/v n-octyl-β-D-glucoside for one week. *Vv*L/ODC-cadaverine crystals formed without microseeding by mixing 1.5 µl of 20 mg/ml protein pre-incubated with L-lysine (20 – 30 mM), 1.5µl of the reservoir buffer (except 30% PEG-4000 was used instead of 35%) and 0.3 µl of 5% w/v n-octyl-β-D-glucoside The crystals were flash-frozen and stored in liquid N_2 until data collection. Diffraction data for the crystals of *Vv*L/ODC-putrescine at 1.7 Å resolution and *Vv*L/ODC-cadaverine at 1.65 Å and 2.15 Å resolution were collected at 19BM beamline of Advanced Photon Source (Argonne National Laboratory, Argonne, IL). Data were processed and scaled using the HKL3000 package (Minor et al., 2006). The statistics are listed in Table III.

3. Phasing and Refinement of the *Vv*L/ODC

Crystals of putrescine-bound *Vv*L/ODC and cadaverine-bound *Vv*L/ODC were formed in the $P2_12_12_1$ space group with slightly different unit cell parameters (*a*=82.08 Å,

b=88.68 Å, *c*=111.84 Å, $\alpha=\beta=\gamma=90°$ for *Vv*L/ODC-putrescine and *a*=84.02 Å, *b*=88.30 Å, *c*=100.10 Å, $\alpha=\beta=\gamma=90°$ for *VvL/*ODC-cadaverine), indicating one dimer per asymmetric unit in both structures. A monomer of the *T. brucei* ODC (PDB entry 1F3T) with putrescine removed was modified by Chainsaw (Schwarzenbacher et al., 2004) and used as the search model in the MolRep (Vagin A, 1997) program of the CCP4-6.0 package. This analysis yielded initial solutions with R-factors of 52% and 55% and correlation coefficients of 34% and 33% for *Vv*L/ODC-putrescine and *Vv*L/ODC-cadaverine, respectively. Phases were improved by refinement using REFMAC5 (Murshudov et al., 1997) resulting in density-modified maps of decent quality. The initial models for the *Vv*L/ODC-putrescine and *Vv*L/ODC-cadaverine were built by ARP/wARP (Morris et al., 2003). Strong electron density for the product putrescine bound to the PLP cofactor was observed in the $2F_o$-F_c map of *Vv*L/ODC-putrescine structure. Crystals were grown in the presence of the substrates L-ornithine and L-lysine, however the substrates were efficiently decarboxylated during the time frame of the crystallization and the ligand electron density that is observed in both structures is for the decarboxylated products putrescine and cadaverine. Putrescine-PLP was modeled into the *Vv*L/ODC-putrescine structure and the model was rebuilt manually in Coot (Emsley and Cowtan, 2004), followed by refinement using REFMAC5. Water molecules were automatically added by ARP/warp during the early stages of refinement, and additional waters were added during manual refinement. TLS parameters were applied in the final rounds of refinement, resulting in a final model with a working R-factor of 18.2 % and an R_{free} of 21.3 % for *Vv*L/ODC-putrescine structure. Electron density for the product cadaverine bound to PLP appeared only in one active site in the map of *Vv*L/ODC-cadaverine structure. The 1.65

Å-resolution data set of *Vv*L/ODC-cadaverine was collected from a crystal that was incubated with 10 mM cadaverine in the final drop. A second data set at lower resolution (2.15 Å) was also obtained from a crystal that was incubated with 15 mM cadaverine. It had very similar unit cell parameters (a=88.24 Å, b=88.03 Å, c=99.27 Å, $\alpha=\beta=\gamma$=90°) to the 1.65 Å dataset. The model of 1.65 Å was applied to 2.15 Å dataset and rebuilt in Coot. Electron density for the cadaverine-PLP was observed in both active sites. A good quality model was produced after several rounds of manual model building in Coot, followed by REFMAC5 refinement. In the final rounds, TLS parameters were applied for refinement, yielding the final model with a working R-factor of 17.5 % and an R_{free} of 24.0 % for *Vv*L/ODC-cadaverine structure. For both structures, PROCHECK (Laskowski RA, 1993) confirmed excellent stereochemistry. The modeling statistics are reported in Table 3.1.

The final refined model of *Vv*L/ODC-putrescine contains two monomers (chain A and B) in the asymmetric unit. Good electron density is observed for PLP-putrescine in both active sites, and for all amino acid residues in the protein with the following exceptions: chain A, residues 12-15, 155-163 and chain B, residues 155-163, 325-326, are missing. The final refined structure contains 614 water molecules. The *Vv*L/ODC-cadaverine structure also contains two monomers in the asymmetric unit, with good electron density observed for PLP-cadaverine in both chains, and for all amino acid residues, except that chain A, residues 11-17, 155-164 and chain B, residues 155-163, are missing. The structure contains 352 bound water molecules.

4. Molecular Modeling

Structures were displayed using the graphics program PyMol (DeLano, 2003). All RMSD calculations were based on structural alignment of the monomers by PyMol and calculated within the program.

C. Results

1. Solved Structures of the *V. vulnificus* L/ODC in Complex with Putrescine and Cadaverine

The X-ray structure of *Vv*L/ODC was solved in the presence of the reaction products putrescine and cadaverine to 1.7 and 2.15 Å, respectively (Table 3.1 and Figure 3.2A). Crystals in both conditions formed in the $P2_12_12_1$ space group with a single dimer present in the asymmetric unit. Overall the structure of *Vv*L/ODC is similar to that observed in previous structures of mammalian and *T. brucei* ODC (Grishin et al., 1999; Kern et al., 1999) (Figure 3.2A). The N-terminal domain is composed of a β/α-barrel (residues 42 – 279) and the C-terminal domain is a β-barrel (residues 280 – 387).

As found in all other members of this structural fold, two identical active sites were formed at the dimer interface between the N-terminal domain from one monomer and the C-terminal domain from the other (Figure 3.2A). Good electron density was observed for both ligands in the active sites (Figure 3.1). In the *Vv*L/ODC-putrescine structure PLP is observed in a gem-diamine structure bound to both K66 (equivalent to K69 in mouse ODC) and putrescine, while for the *Vv*L/ODC-cadaverine structure PLP forms a Schiff base with the ligand and K66 is displaced away from the ligand (Figure 3.4). A gem-diamine structure has not been previously observed in a wild-type ODC

homolog, however a carbinolamine has been observed for the PLP in the unliganded *cv*ADC structure (Shah et al., 2007) and a gem-diamine was observed between D-Orn and *T. brucei* ODC in the K294A mutant (Jackson et al., 2004). The active site lid (residues 153-170), which was observed for the first time in the closed position in the *cv*ADC structure (Shah et al., 2007), is partially disordered (residues 155-163) in the *Vv*L/ODC structure (Figure 3.3), similar to what has been observed in the structures of *T. brucei* ODC.

2. Structural Basis on the Dual Substrate Specificity of the *V. vulnificus* L/ODC

Active site structures of the *Vv*L/ODC bound to putrescine and cadaverine were compared to gain insight into the structural basis for the dual substrate specificity (Figures 3.2B). Structures were aligned by a single monomer and the RMSD (= 0.25Å) was calculated for the dimer demonstrating that no significant structural rearrangements were induced by the different ligands. The active site structures are nearly identical, with the exceptions that 1) K66 sits in a somewhat different position reflective of the fact that it participates in a gem-diamine in the putrescine-bound structure but not in the cadaverine-bound structure, and 2) a water molecule (W5 in Figure 3.1 and scheme 3.1) is observed in the *Vv*L/ODC-putrescine structure, positioned between the δ-amino group of putrescine and Asp340 (equivalent to Asp361 in *T. brucei* ODC). In contrast, in the *Vv*L/ODC cadaverine bound structure the ε-amino group of cadaverine makes a direct interaction with Asp340 and W5 is missing from the structure. The distance between W5 in the *Vv*L/ODC-putrescine structure and the ε-amino group of cadaverine in the

*Vv*L/ODC-cadaverine structure is only 1.6Å, suggesting that a water molecule in this position is displaced from the cadaverine bound active site because of steric hindrance.

*Vv*L/ODC complexed to putrescine and cadaverine were compared to the structures of *T. brucei* ODC bound to putrescine and to *cv*ADC bound to agmatine (Figure 3.2B). Alignment of the *Vv*L/ODC and *T. brucei* ODC (pdb 1F3T) or of *cv*ADC (pdb 2NVA) monomers gave RMSD values of 1.26 and 1.3 Å calculated for the overall dimer structure. Several helices and loops towards the surface of the structure assume somewhat different positions between these structures, but the changes do not have an apparent influence on the active site structure. With respect to the active site, the most significant difference between the three structures is the position of the 3_{10}-helix (residues 309 – 313 in *Vv*L/ODC), which sits at the back of the substrate-binding pocket and serves to position key residues involved in substrate interactions (e.g. Asp314 in *Vv*L/ODC). This helix is shifted furthest back in the *cv*ADC structure allowing the larger agmatine ligand to be accommodated. It is positioned in an intermediate position in *Vv*L/ODC, between that observed for *T. brucei* ODC and *cv*ADC (the distances between C4′ of PLP and the Cα of D314, D332 and E296 from *Vv*L/ODC, *T.brucei* ODC and *cv*ADC, respectively are 10.8 Å, 9.7 Å and 12.1 Å).

D. Discussion

The structural basis for the dual function of *Vv*L/ODC was analyzed by X-ray structure determination of the enzyme in complex with both products putrescine and cadaverine. Overall the structures are similar to the eukaryotic ODC structures that have been previously determined (e.g. *T. brucei* (Grishin et al., 1999), mouse (Kern et al.,

1999) and human (Almrud et al., 2000)). The active site lid was found disordered in both structures similar to the eukaryotic ODCs. The Two structures in complex with putrescine and cadaverine are almost identical to each other except at the active site, where they assume different chemical states. PLP forms Schiff base with the ligand cadaverine in the *Vv*L/ODC-cadaverine wheras PLP was observed in a gem-diamine structure interacting with Lys-66 and the ligand putrescine in *Vv*L/ODC-putrescine. The active sites were remarkably similar to the eukaryotic ODC structures with the exception of the position of the 3_{10}-helix (specificity element) at the back of the binding pocket. This helix sits slightly further away from the PLP cofactor in the *Vv*L/ODC structure compared to *T. brucei* ODC, thus accommodating the larger L-lysine side chain. Key contacts between ligand and the conserved Asp at position 332 (Asp314 *Vv*L/ODC) are however preserved. The ability of *Vv*L/ODC to also efficiently interact with L-ornithine despite this enlarged pocket appears to result from the positioning of a bridging water molecule that participates in the binding of the shorter putrescine ligand but which is absent in the cadaverine bound structure. The resolution of *Vv*L/ODC-cadaverine structure is slightly lower than the putrescine-bound structure (2.15 Å versus 1.7 Å), resulting in the lower number of water molecules (352) built in the structure compared to *Vv*L/ODC-putrescine structure with 614 water molecules. However the electron density map of the active site at the cadaverine-bound structure showed good, interpretable density for the other four water molecules (W1 – W4 in Figure 3.1), which excludes the possibility that the absence of W5 in the *Vv*L/ODC-cadaverine structure is due to the lower resolution of the structure. A water molecule was previously implicated in the catalysis of multiple substrates by the protease trypsin (Kossiakoff, 1987). Trypsin

hydrolyzes both lysine-containing peptide ligands, where a water forms a bridge between the ε-amino group and Asp189, and arginine-containing peptides where the water has been displaced and the substrate interacts directly with the substrate binding pocket.

To understand how the bacterial ODCs function on L-ornithine despite the absence of key substrate binding residues, the amino acid sequence alignments of the prokaryotic ODCs were compared with the available structural data (e.g. the eukaryotic ODCs, *Vv*L/ODC, the bacterial DAPDCs and *cv*ADC). This analysis identified consensus sequences within the 3_{10}-helix that are predictive of the function of these enzymes (Figure 1.3). Asp332 is an invariant residue in the eukaryotic ODCs and the L/ODCs, but does not appear to be important in the prokaryotic ODCs where it is substituted with Glu, Gly or Asn (Figure 1.3). However, in the prokaryotic ODCs an invariant Glu at position 328 is present instead. While the equivalent residue (Cys328) in the eukaryotic ODCs does not contact ligand, the structures of both *cv*ADC and DAPDC demonstrate that ligand binding residues may originate from different positions within the 3_{10}-helix. In *cv*ADC the residue at position 328 (Asn292 *cv*ADC) forms a H-bond with the guanidinium group of the bound product agmatine, and in DAPDC an invariant Arg residue in position 327 interacts with the carboxylate of the *meso* substrate (Shah et al., 2007). These data suggest that in the prokaryotic ODCs, Glu328 replaces the function of Asp332 in the eukaryotic ODCs despite originating from a different position in the 3_{10}-helix specificity element. Finally, while the L/ODCs and the eukaryotic ODCs both have an invariant Asp at position 332, the eukaryotic ODC consensus is Asn/Cys at positions 327/328 and the dual function L/ODCs contain Ser/Gly.

In summary X-ray structure of *Vv*L/ODC was solved for the first time among the β/α-barrel fold dual specificity enzymes. The enzyme structures in complex with both products putrescine and cadaverine provided insights into the structural basis for the dual function of VvL/ODC.

	*Vv*L/ODC-Putrescine	*Vv*L/ODC-Cadaverine
(a) Data Collection and Processing		
Data source	19BM	19BM
Wavelength (Å)	0.979	0.979
Space group	$P2_12_12_1$	$P2_12_12_1$
Unit cell dimensions	*A*=82.08 Å, *B*=88.68 Å, *C*=111.84 Å	*A*=88.24 Å, *B*=88.03 Å, *C*=99.27 Å
Resolution	20.0 - 1.7	26.8 - 2.15
Total Reflections	633221	159450
Unique reflections	90404	37184
Completeness (%)	99.9	90.6
Redundancy	7.0	4.4
Intensities I/σ (last shell)	35.9 (2.5)	14.6 (2.0)
R_{merge} (last shell)	0.074 (0.63)	0.107 (0.43)
(b) Refinement		
No. of non-hydrogen atoms	6406	6064
No. of water molecules	614	352
R_{work}	18.2	17.5
R_{free}	21.3	24.0
R.m.s.d. bond lengths (Å)	0.014	0.014
R.m.s.d. bond angles (deg)	1.4	1.5
average B-value ($Å^2$)	20.9	26.2

Table 3.1. Statistical summary for the *V. vulnificus* dual specificity enzyme (*VvL/ODC)* structural analysis

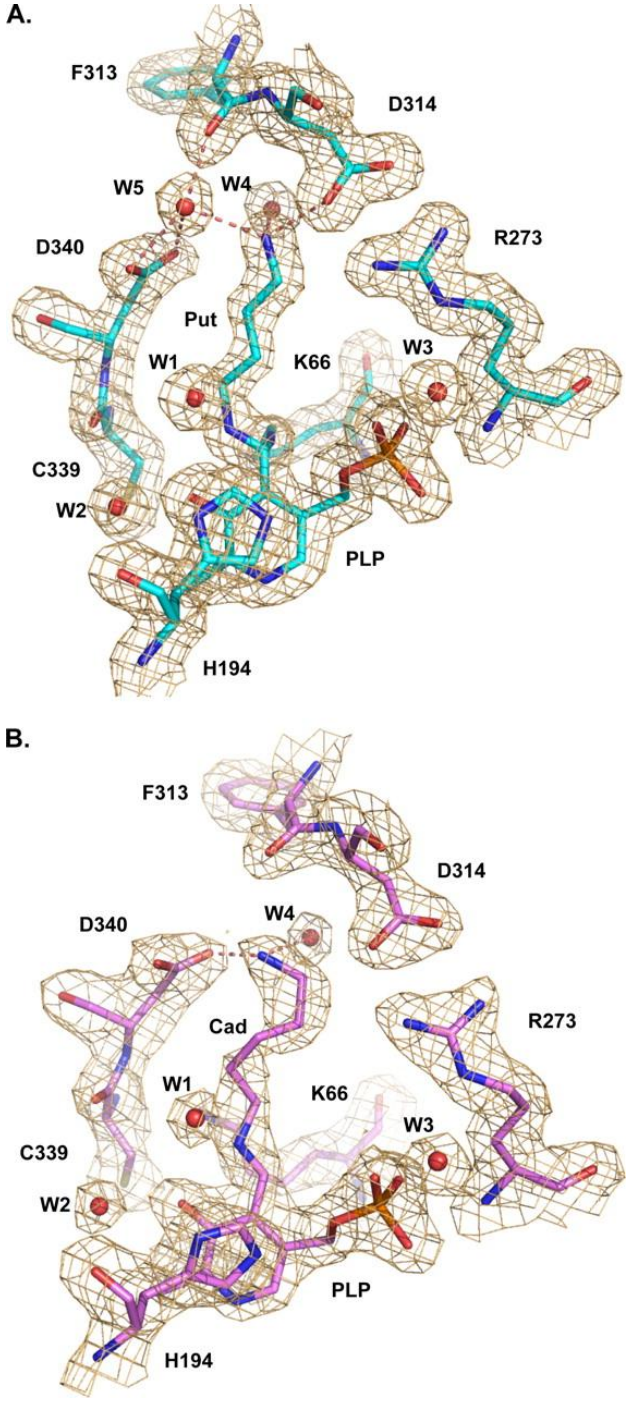

Figure 3.1 Electron density maps ($2F_o$-F_c) of the active sites of *Vv*L/ODC bound with putrescine (A) and cadaverine (B). The contour level is 1.0σ.

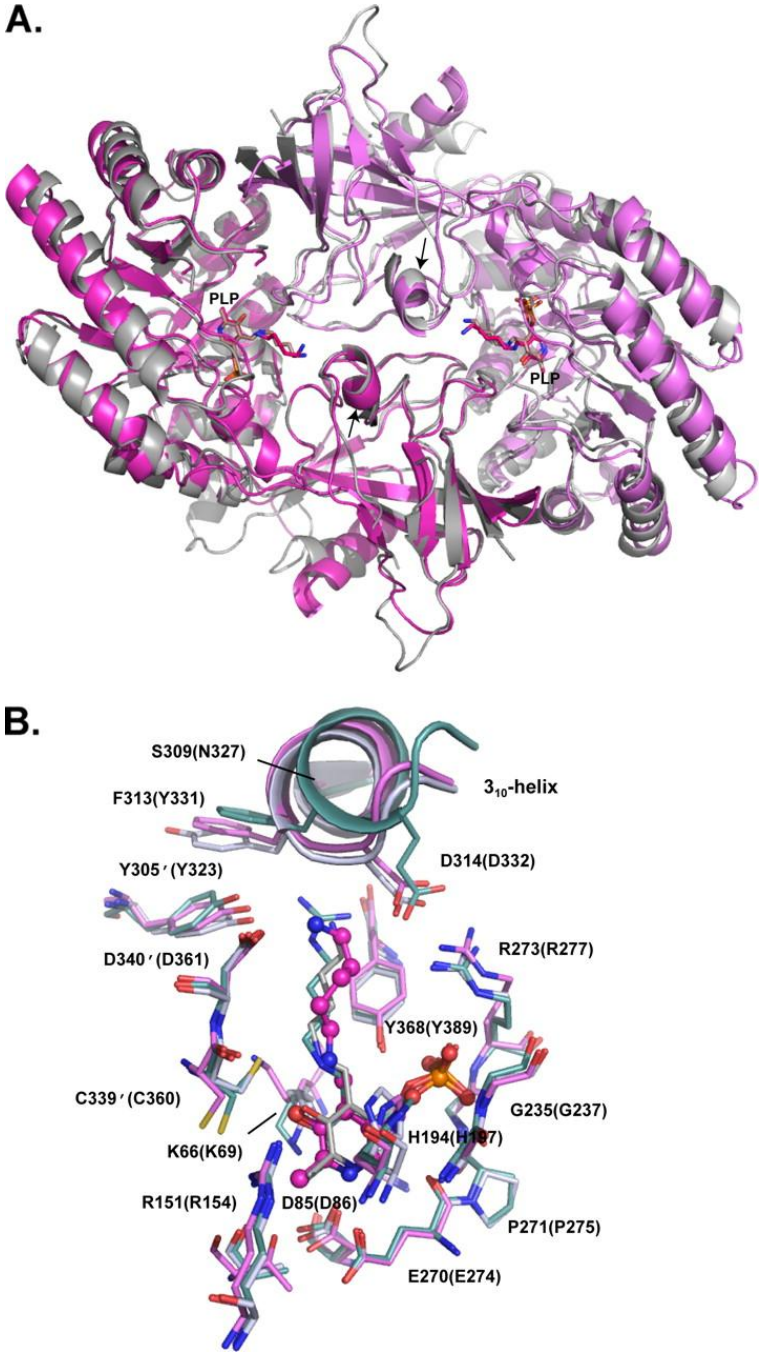

Figure 3.2 Comparison of the *Vv*L/ODC structure with *T.brucei* ODC and *cv*ADC

A. Comparison of the overall fold. The monomer of *Vv*L/ODC (violet) was superimposed on a monomer of *T. brucei* ODC (gray), and the dimer is displayed. The individual

monomers within each species are displayed in different shades. Arrows indicate the 3_{10}-helices. B. Overlay of product-bound structures of *Vv*L/ODC (violet), *T.brucei* ODC (gray) and *cv*ADC (pale green) at the active sites. The bound PLP-cadaverine in the *Vv*L/ODC structure is displayed in ball and stick. Residues are numbered based on the *Vv*L/ODC sequence, with the equivalent *T. brucei* ODC numbers in parenthesis. This figure was created by PyMol (DeLano, 2003).

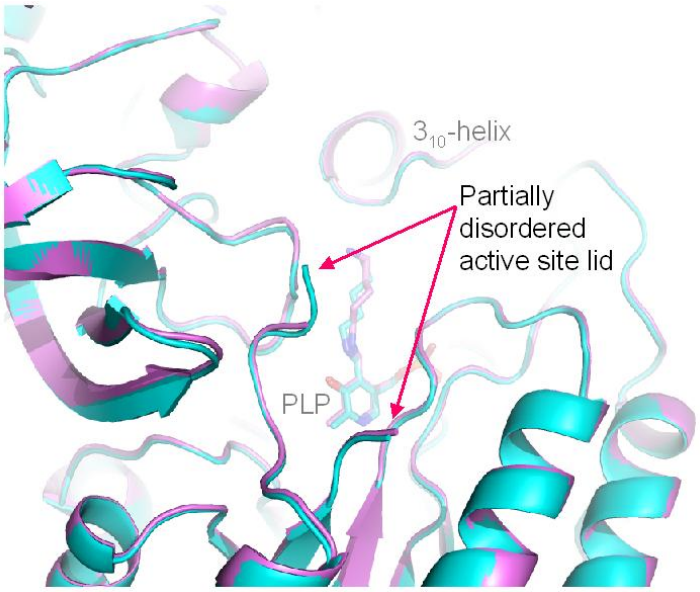

Figure 3.3 Partially disordered active site lids of *Vv*L/ODC in complex with putrescine (cyan) and cadaverine (violet). Arrows indicate disordered region (residues 155-163). This figure was created by PyMol (DeLano, 2003).

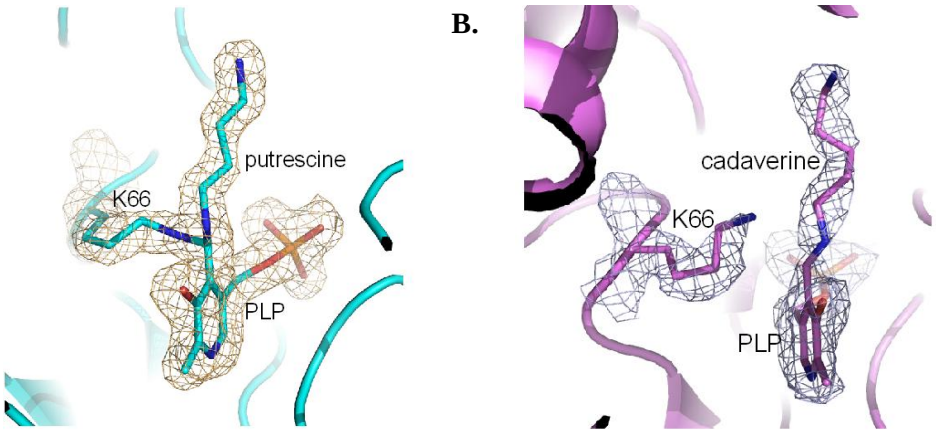

Figure 3.4 Two different chemical states of the *V. vulnificus* L/ODC structures bound with putrescine (A) and cadaverine (B). PLP is observed in a gem-diamine structure with K66 and putrescine in the putrescine-bound structure (A) whereas PLP forms a Schiff base with cadaverine in the cadaverine-bound structure (B). The contour level is 1.0σ. This figure was created by PyMol (DeLano, 2003).

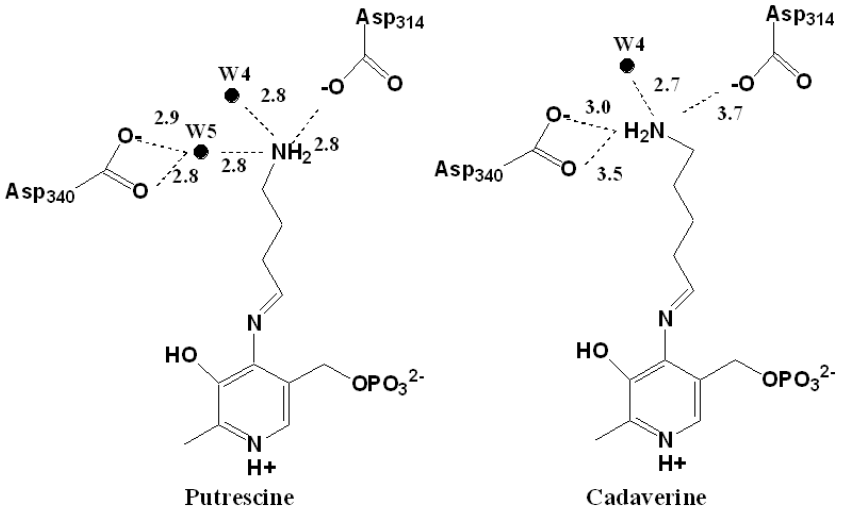

Scheme 3.1 Schematic active site comparison of *Vv*L/ODC bound to putrescine or cadaverine showing the distances (Å) to the bound water molecules.

CHAPTER 4

DETERMINATION OF NORSPERMIDINE/SPERMIDINE BIOSYNTHETIC PATHWAY IN *VIBRIO CHOLERAE*

A. Introduction

In most eukaryotic and prokaryotic organisms, *S*-adenosylmethionine decarboxylase (AdoMetDC) plays a crucial role in polyamine biosynthesis because it produces decarboxylated *S*-adenosylmethionine (dcAdoMet), which serves as a propylamine moiety donor for higher polyamines (Pegg and McCann, 1992; Tabor and Tabor, 1984). However a few previous studies suggested some organisms possess unusual polyamine pathways that are independent of AdoMetDC (Tait, 1976). *Lathyrus sativus* (grass pea) seedlings were reported to contain both an alternative pathway in which L-aspartic β-semialdehyde (ASA) is used to produce spermidine from putrescine, and the classical dcAdoMet pathway (Srivenugopal and Adiga, 1980). Some species of the genus *Vibrio* in which norspermidine is one of the major polyamines also lack AdoMetDC and spermidine synthase activities. Norspermidine is a structural homolog of spermidine and is one carbon shorter than spermidine in length. A series of papers on the three partially purified enzyme activities, diaminobutyrate decarboxylase (DABA DC), carboxynorspermidine synthase and carboxynorspermidine decarboxylase (CANSDC) from *V.alginolyticus* (Nakao et al., 1991; Yamamoto et al., 1994; Yamamoto et al., 1992) led to the hypothesis that the three enzymes comprise a novel pathway for norspermidine biosynthesis (Figure 1.4). These studies showed 1, 3-diaminopropane (DAP) which subsequently is produced from 2, 4-diaminobutyrate (DABA) by DABA DC, condenses

with ASA through the reductive action of carboxynorspermidine synthase, producing carboxynorspermidine, which is then decarboxylated to norspermidine by CANSDC. ASA is originally produced from L-aspartate, which was found to be incorporated into norspermidine in *V.alginolyticus* (Yamamoto et al., 1986a). However no direct proof of this hypothesis has been reported and the recombinant enzymes have never been characterized, thus this alternative polyamine biosynthetic pathway has not been validated.

Recently with the expansion of the genomic sequence database, we were able to identify these putative polyamine biosynthetic enzymes in a number of genomes. The protein sequences of DABA DC, which was originally characterized in *V.alginolyticus*, are found in many bacteria including *Vibrio* species. The sequence of carboxynorspermidine synthase is now annotated as carboxynorspermidine dehydrogenase (CANSDH). In all sequenced *Vibrio* species, the three genes *daba dc*, *cansdh* and *cansdc* are clustered together, suggesting that they function as an operon. Consistent with the previous reports on the *Vibrio* species showing that they lack AdoMetDC activity, no AdoMetDC sequences were identified in the *Vibrio* species. CANSDH and CANSDC are often found clustered in a variety of bacteria besides the genus *Vibrio*. These observations led us to hypothesize that the alternative polyamine biosynthetic pathway that utilizes ASA as a propylamine moiety donor instead of dcAdoMet through the actions of CANSDH and CANSDC, is wide spread among many bacteria. In this study, *V.cholerae*, an important human pathogen, was used as a model organism to study this putative alternative pathway. *V.cholerae* causes cholera characterized by severe watery diarrhea in humans. Therefore if this alternative pathway

proves to be effective and responsible for its major polyamine production, it could be targeted for development of selective treatment for cholera, because the pathway is absent in humans. The enzymatic decarboxylating activities of the cloned DABA DC and CANSDC from *V.cholerae* were tested on various substrates and the norspermidine biosynthesis pathway was extensively defined by *in vivo* gene reconstitution in *E.coli* and genetic knockout studies in *V.cholerae*.

B. Experimental Procedures

1. Materials and Bacterial Strains

Chemical synthesis of carboxynorspermidine and carboxyspermidine was carried out by Dr. Doug Frantz (University of Texas Southwestern Medical Center, Dallas, TX). Polyamine standards used for HPLC analysis, spermidine, norspermidine, 1,3-diaminopropane, putrescine, cadaverine and 1,7-diaminoheptane were purchased from Sigma. All other chemical reagents were purchased from Sigma unless noted otherwise. Infinity™ carbon dioxide detection reagent was from Thermo Electron Corp. (Louisville, CO). The AccQ-Fluor reagent kit for labeling amino acids was purchased from Waters (Milford, MA). Genomic DNA from *V. vulnificus* CMCP6 was kindly provided by Dr. Joon Haeng Rhee (Chonnam University, Gwangju, Korea). Genomic DNA from the wild type *V.cholerae* c6709 (Roberts, 1992), which is naturally resistant to streptomycin, was prepared from 5 ml culture using the protocol as described in Current Protocols in Molecular Biology (1997) (Wilson, 1997).

2. Media and Growth Conditions

E. coli was grown at 37 °C in Luria-Bertani (LB) broth and *V.cholerae* was grown at 37 °C or 30 °C in LB or M9-minimal medium (M9MM). The M9MM contained 0.4 % glycerol as a carbon source instead of glucose because glucose is a repressor for the P_{BAD} promoter that controls gene expression of *cansdc* and *cansdh* in the genetically complemented strains c_cansdcKO and c_cansdhKO, respectively. When needed, the antibiotics streptomycin (Sm), chloramphenicol (Cm), kanamycin (Kn), ampicillin (Ap) and carbenicillin (Cb) were added at the concentrations of 30 μg/ml, 10 μg/ml, 50 μg/ml, 50 μg/ml and 50 μg/ml, respectively. L-arabinose was added at 0.2 % w/v in the culture for protein induction under the P_{BAD} promoter.

3. Cloning of the Putative Norspermidine Biosynthetic Genes in the Protein Expression Vectors

The ORF of *cansdc* was amplified by PCR from the genomic DNA of *V.vulnificus* CMCP6 using primers VvCANSDC_F and VvCANSDC_R (Table 4.3) and cloned into pET-15b (Novagen) at *NdeI* and *XhoI* sites, resulting a plasmid pET15:*Vv*CANSDC (Table 4.2).

The *XbaI* site of pET-15b was mutated to *SalI* by QuickChange™ site directed mutagenesis kit (Stratagene, La Jolla, CA) using the primers QpET15F and QpET15R to generate qpET-15b vector. The ORF of *cansdc* (locus vc1623) was PCR amplified from the genomic DNA of *V.cholerae* c6709 using primers pET1623F and pET1623R and cloned into qpET-15b (Novagen) at the *NdeI* and *XhoI* sites, yielding a plasmid qpET15:1623. The *cansdc* gene contained an *NdeI* site that was removed by QuickChange™ mutagenesis using the primers Q1623F and Q1623R before the final

cloning step. The amplified genes of *daba at/dc* (locus vc1625, primers pET1625F and pET1625R) and *cansdh* (locus vc1624, primers pET1624F and pET1624R) from the genomic DNA of *V.cholerae* c6709 were cloned into qpET-15b at the *NdeI* and *XhoI* sites and produced the plasmids qpET15:1625 and qpET15:1624, respectively. The cloned gene of *daba at/dc* was cut out of qpET15:1625 at *NdeI* and *BamHI* and pasted into pET28a (Novagen), resulting pET28:1625. The *SalI* and *XhoI* sites of qpET15:1624 were changed into *BamHI* and *SacI* sites by amplifying the *cansdh* gene with the preceding ribosome binding site (rbs) using the primers 1624BamHI and 1624SacI and the plasmid qpET15:1624 as the template. The amplified product was pasted into pET28:1625 at *BamHI* and *SacI* sites, resulting in pET28:1625/1624. Lastly qpET15:1623 was disgested with *SalI* and *XhoI* to release the rbs followed by the *cansdc* gene, both of which were then cloned into pET28:1625/1624 at *SalI* and *XhoI*, yielding a plasmid pET28:1625/1624/1623. These two co-expression plasmids pET28:1625/1624 and pET28:1625/1624/1623 were under control of a single T7 RNA polymerase promoter and a single T7 terminator with a rbs preceding each gene.

4. Construction of Knockout Mutants

Construction of two knockout mutant strains of *V.cholerae* was carried out by replacing the target gene with an antibiotic resistance cassette as described below. The *cansdc* gene (locus vc1623) was replaced with the *cat* gene (chloramphenicol resistance cassette) and the *cansdh* (locus vc1624) with the *aphA-3* gene (kanamycin resistance cassette). Two flanking upstream (primers vc1623A and vc1623B) and downstream (primers vc1623C and vc1623D) regions of vc1623 were amplified and the *cat* gene was

amplified from plasmid pACYC184 using primers CmF and CmR. The three amplified fragments were assembled in pBluescript II SK+ (Stratagene) and were cloned into the suicide vector pCVD422 (Donnenberg and Kaper, 1991), resulting in the *cansdc* knockout plasmid pCVD1623. Similarly, the nonpolar *cansdh* knockout mutant was constructed by use of the pCVD422 vector to produce a knockout plasmid pCVD1624 that carried two amplified flanking upstream (primers vc1624A and vc1624B) and downstream (primers vc1624C and vc1624D) regions of vc1624 and *aphA-3* cassette amplified from plasmid pUC18K using primers KanF and KanR (Table 4.2). Plasmids pCVD1623 and pCVD1624 were introduced into *V.cholerae* by conjugation with *E.coli* SM10λPir (for conjugation, see below) and integrants were confirmed by PCR from chromosomal DNA using primers VC1623IF and VC1624D for the *cansdc* gene and VC1624IF and VC1624R for the *cansdh* gene. The resulting knockout strains (Δ*cansdc* and Δ*cansdh*) were named cansdcKO and cansdhKO, respectively (Table 4.1).

5. Conjugation

Overnight LB cultures of *E.coli* SM10λPir transformed with pCVD1623 or pCVD1624 as a donor and wild type *V.cholerae* as a recipient were diluted in LB 1:10 and 1:100, respectivley and grown without antibiotics for 1 hour. An equal volume of *E.coli* and *V.cholerae* culture was mixed, inoculated on LB-agar plates, and incubated for 8 hours at 37 °C for conjugation. Conjugated cells were plated on LB containing no NaCl + 5 % sucrose + streptomycin + either chlormaphenicol (Δ*cansdc*) or kanamycin (Δ*cansdh*) and incubated at 30 °C until colonies grew big enough for patching on

ampicillin plates, which were used for selection of ampicillin-sensitive mutants with gene replacement.

6. Genetic Complementation of the Mutants

Complementation was carried out by introduction of the *cansdc* and *cansdh* genes under P_{BAD} promoter control. The *cansdc* (primers pBAD1623F and pBAD1623R) and *cansdh* (primers pBAD1624F and pBAD1624R) genes were PCR amplified from *V.cholerae* genomic DNA and cloned into a relatively low copy number plasmid pBAD/Myc-HisA at *XhoI* and *HindIII* sites. The resulting plasmids pBAD1623 and pBAD1624 were electroporated in cansdcKO and cansdhKO, respectively and the resulting complemented mutant strains were named c_cansdcKO and c_cansdhKO (Table 4.1).

7. Protein Expression and Purification of the Putative Norspermidine Biosynthetic Enzymes

E.coli BL21(DE3) cells were transformed with the protein expression vectors, pET15:*Vv*CANSDC and pET28:1625 to prepare enzymes *V.vulnificus* CANSDC and *V.cholerae* DABA AT/DC, respectively. They were grown to exponential phase at 37°C in LB medium containing ampicillin (pET15:*Vv*CANSDC) or kanamycin (pET28:1625). Expression of the recombinant proteins was induced by 200 μM of isopropyl-1-thio-β-D-galactopyranoside (IPTG) at 16°C overnight. Recombinant *Vv*CANSDC and *Vc*DABA AT/DC were purified to homogeneity using Ni^{2+}-affinity and gel filtration chromatography as described (Osterman et al., 1994; Osterman et al., 1995). Protein

purity was analyzed by SDS-PAGE and the protein concentration was determined by absorbance measurements at 280 nm. All enzyme preparations were used in assays without cleavage of the His_6-tag.

E.coli BL21(DE3) were transformed with a single expression plasmid pET28:1625 that expresses *Vc*DABA AT/DC, and co-expression plasmids, pET28:1625/1624 that co-expresses *Vc*DABA AT/DC and *Vc*CANSDH, and pET28:1625/1624/1623 that co-expresses *Vc*DABA AT/DC, *Vc*CANSDH and *Vc*CANSDC. An empty pET28a vector was used as a negative control vector for transformation. The transformed cells were grown at 37°C in LB medium containing kanamycin and over-expression of the recombinant proteins under T7 promoter was induced by 200 μM IPTG at 16°C overnight to facilitate soluble protein production. Over-expression of the proteins in soluble form was confirmed by comparing total cell lysate and soluble fraction in SDS-PAGE analysis.

8. Measurement of Cellular Polyamine Contents in the Transformed *E.coli* and *V.cholerae* by HPLC

Absorbance at 600nm of overnight cell cultures grown in LB or M9 minimal medium was read and approximately same number of cells from each sample were pelleted at 4000 x *g*. The cell pellets were washed in 1 ml of 1x phosphate-buffered saline (pH 7.4; 137 mM NaCl, 2.7 mM KCl, 10 mM Na_2HPO_4, 1.8 mM KH_2PO_4) three times and resuspended in 25 μl of lysis buffer (20 mM MOPS, pH 8.0, 10 mM NaCl, 4 mM $MgCl_2$). The resuspended cells were lysed by freezing in liquid nitrogen and thawing in a 37 °C water bath three times. 7.5 μl of 40 % trichloroacetic acid (TCA) was added and

the proteins precipitated on ice for 5 min. The cell lysate was cleared of cell debris by centrifugation at 13,000 x *g* for 3 min at room temperature and stored at –20ºC until analysis.

Cellular polyamines were labeled with AccQ-Tag Reagent Kit (Waters, Milford, MA), the fluorescent reagent (6-aminoquinolyl-*n*-hydroxysuccinimidyl in acetonitrile) in 5% sodium tetraborate as described previously (Grishin et al., 1999). Labeled polyamines were analyzed by HPLC using AccQ-Tag C_{18} column (Waters) with fluorescence detection. Briefly, 5 μL of polyamine containing sample was reacted with 20 μL of the fluorescent reagent in 100 μL reaction at 55 ˚C. Cleared culture media were also analyzed to measure secreted polyamines. Six different labeled polyamines (carboxynorspermidine, 1,3-diaminopropane, putrescine, cadaverine, norspermidine and spermidine) and 1,7-diaminoheptane as an internal standard were clearly separated in the following gradient system with the buffer A: 450 mM sodium acetate (diluted from 1M stock pH4.5), 17 mM TEA, pH adjusted to 4.75 with NaOH and the buffer B: 60 % acetonitrile and 0.01 % acetone: 1 – 5 min 0 – 20 % B; 5 – 50 min 20 – 50 %; 50 – 55 min 50 – 100 %; 55 – 57 min 100%.

C. Results

1. Biochemical Characterization of Polyamine Biosynthetic Enzymes from *Vibrio* Species

Recombinant CANSDC from *V.vulnificus* (*Vv*CANSDC) was purified and characterized to determine its substrate specificity. Carboxynorspermidine was the primary substrate (k_{cat}/K_m = 7.4 x 10^4 $M^{-1}s^{-1}$) and was decarboxylated 20-fold more

efficiently than carboxyspermidine (k_{cat}/K_m = 3.2 x 10^3 $M^{-1}s^{-1}$) (Table 4.4). *Vv*CANSDC was also slightly active on L-ornithine (K_m ~ 40 mM, k_{cat} ~ 0.08 s^{-1}) but showed no activity on the other basic amino acid substrates of the following: L-arginine, L-lysine and *meso*-diaminopimelate. The substrate specificity of *Vv*CANSDC is slightly different from that of *V.alginolyticus* CANSDC, which was reported to be equally active on carboxynorspermidine and carboxyspermidine (Nakao, 1990).

The DABA DC from *V.alginolyticus* is found as a fusion of a diaminobutyrate decarboxylase (DC) domain and an aminotransferase (AT) domain. Based on the sequence homology, the AT domain is predicted to be diaminobutyrate aminotransferase (DABA AT, aka, pyruvate transaminase), which was reported in *Acinetobacter baumannii* to transfer an amino group from a donor such as glutamate to an acceptor ASA, producing DABA (Ikai and Yamamoto, 1997). All other sequenced *Vibrio* species also exhibit this type of fusion enzyme (AT domain followed by DC domain, DABA AT/DC).

The full length DABA AT/DC enzyme from *V.cholerae* (*Vc*DABA AT/DC) was cloned and purified. It showed decarboxylating activity on 2, 4-diaminobutyrate and L-ornithine among the tested substrates and had an absolute preference for 2, 4-diaminobutyrate over L-ornithine by 1000-fold (k_{cat}/K_m = 4.9 x 10^4 $M^{-1}s^{-1}$ and 4.9 x 10^1 $M^{-1}s^{-1}$ for 2, 4-diaminobutyrate and L-ornithine, respectively) (Table 4.4). The catalytic efficiency of *Vc*DABA AT/DC as a decarboxylase in this study is comparable to the previously reported value (k_{cat}/K_m ~ 9.9 x 10^4 $M^{-1}s^{-1}$) for *V.alginolyticus* DABA AT/DC (Nakao et al., 1989). Whereas the decarboxylase could be directly measured, its aminotransferase activity could not be tested because the transamination product of the

AT domain, DABA would be further catalyzed to DAP by the decarboxylating activity of the DC domain.

2. Proposal of Polyamine Biosynthetic Pathway in *V.cholerae* Based on Sequenced Genomes

It was previously speculated that DABA AT/DC, CANSDH and CANSDC are responsible for norspermidine biosynthesis in *Vibrio* species although direct proof is lacking. In addition to these three enzymes, *V.cholerae* contains sequences for ADC and ODC, both of which produce putrescine, but it does not contain AdoMetDC and spermidine synthase sequences that are required for spermidine biosynthesis in the classical pathway. This led me to hypothesize that norspermidine and spermidine are synthesized in the same way through CANSDH and CANSDC from DAP and putrescine, respectively in *V.cholerae* (Figure 4.1). ASA, the propylamine group donor to DAP and putrescine is also predicted to be a precursor for L-2, 4-diaminobutyrate (DABA) through the aminotransferase action of the fusion enzyme *Vc*DABA AT/DC based on the report that *A.baumannii* DABA AT transferred an amino group to ASA, forming DABA (Figure 4.1).

3. *In vivo* Reconstitution of Norspermidine/Spermidine Biosynthetic Pathway of *V.cholerae* in *E.coli*

Our proposed polyamine pathway in *V.cholerae* predicted that three genes *daba at/dc, cansdh* and *cansdc* would be sufficient to produce norspermidine in *E.coli*, an organism which does not normally make norspermidine. To test this hypothesis the three

genes were cloned individually or together into pET28a vector for protein over-expression, resulting a single protein expression plasmid pET28:1625 and two co-expression plasmids pET28:1625/1624 and pET28:1625/1624/1623 (Table 4.2). The three proteins could be over-expressed in *E.coli* BL21(DE3) transformed with pET28:1625/1624/1623 as soluble protein based on the SDS-PAGE analysis (Figure 4.2A). HPLC analysis of the cellular polyamine contents of *E.coli* transformed with the empty vector pET28a showed that *E.coli* produces putrescine and spermidine as its major polyamines (data not shown). When *E.coli* was transformed with pET28:1625 expressing *Vc*DABA AT/DC, however, it exhibited a new peak corresponding to DAP (Figure 4.2B, peak 1 in top window), which is a reaction product of *Vc*DABA AT/DC. *E.coli* transformed with pET:1625/1624/1623 in which the *Vibrio* norspermidine biosynthetic pathway is reconstituted revealed a novel peak, which corresponded to norspermidine (Figure 4.2B, peak 3 in bottome window). These findings supported our predicted pathway for norspermidine biosynthesis, but not for spermidine since spermidine is a naturally occurring polyamine in *E.coli*. Carboxynorspermidine was expected to be detected in *E.coli* transformed with pET28:1625/1624 that over-expresses *Vc*DABA AT/DC and *Vc*CANSDH, however it was not observed. Another possible product carboxyspermidine which would be produced in case *Vc*CANSDH uses putrescine instead of DAP for condensation with ASA, was not separable from putrescine in our HPLC condition and therefore it could not be experimentally demonstrated.

4. Confirmation of Norspermidine/Spermidine Biosynthetic Pathway in *V.cholerae* by Genetic Analysis

Putrescine, norspermidine and spermidine were observed as the major polyamines in the wild type *V.cholerae* cells grown in the rich medium LB (data not shown). In contrast, the wild type cells grown in M9MM showed no significant spermidine content, while putrescine and norspermidine were present in similar concentration to that found in LB (Figure 4.3A, top window). I generated two knockout mutants of *V.cholerae*, cansdcKO and cansdhKO, from which *cansdc* and *cansdh* genes were knocked out, respectively. Similar to the wild type cells, the two knockout mutants contained spermidine when grown in LB (data not shown), however spermidine was not observed when the knockout cells were grown in M9MM.

Based on our proposed pathway the cansdcKO mutant should produce DAP, putrescine and carboxynorspermidine but not norspermidine or spermidine, because it lacks the *cansdc* gene (Figure 4.1). HPLC analysis of the cansdcKO mutant growin in LB showed that it contained DAP and carboxynorspermidine as well as putrescine and spermidine (Figure 4.3B, bottom window) and as expected spermidine and norspermidine were absent when cansdcKO was cultured in M9MM (Figure 4.3A, middle window). The cansdhKO mutant was expected to produce only DAP and putrescine. As anticipated, cansdhKO samples from culture in M9MM did not have spermidine or norspermidine but contained a large amount of DAP (Figure 4.3A, bottom window and Figure 4.4).

Genetically complemented cansdcKO and cansdhKO mutants (c_cansdcKO and c_cansdhKO, respectively) were also examined for polyamine content. Interestingly, both c_cansdcKO and c_cansdhKO cells grown in M9MM contained significant levels of spermidine (Figure 4.3B, top and middle windows and Figure 4.4) while their levels of norspermidine were similar to wild type. The intracellular levels of DAP showed

differences among the cells: c_cansdcKO contained about 3-fold higher DAP compared to the wild type similar to the two knockout cells, while DAP was almost depleted in c_cansdhKO. An unidentified peak (*′ on the left) increased and a new peak (*′ on the right) appeared in the c_cansdcKO sample (Figure 4.3B, top window). Another novel peak (*′ on the right) also showed up in the c_cansdhKO sample (Figure 4.3B, middle window). Cleared media of wild type and mutant cultures were also analyzed for secreted polyamine detection. No significant amounts of polyamines were detected in these samples but a novel peak was detected in the medium from cansdhKO and c_cansdhKO (data not shown). All of these unknown peaks remain to be identified.

D. Discussion

We have directly shown the enzymatic activities of *Vv*CANSDC and *Vc*DABA AT/DC on various substrates using cloned proteins. *Vv*CANSDC displayed similar kinetic parameters on carboxynorspermidine compared to the CANSDC from *V.alginolyticus*. It showed 20-fold lower catalytic efficiency on carboxyspermidine and this is slightly different from Nakao et al.'s report claiming that carboxyspermidine also served as efficient as carboxynorspermidine (Nakao, 1990). DC domain of *Vc*DABA AT/DC preferred DABA as its primary substrate similar to the *V.alginolyticus* enzyme although *Vc*DABA AT/DC also showed low activity toward L-ornithine that was not reported for the *V.alginolyticus* enzyme (Nakao, 1990).

A novel norspermidine biosynthetic pathway was proposed previously based on the activities of partially purified DABA AT/DC, CANSDH and CANSDC from *V.alginolyticus*. I reconstituted this predicted pathway in *E.coli* by introducing the three

genes from *V.cholerae* in *E.coli*. The transformed *E.coli* was able to produce norspermidine in addition to its native polyamines, confirming the validity of this alternative pathway for norspermidine biosynthesis in *V.cholerae*. My finding that *Vv*CANSDC can produce norspermidine and spermidine with comparable catalytic efficiencies on carboxynorspermidine and carboxyspermidine, together with the observation that AdoMetDC sequence is absent in the genome of *Vibrio* species suggested that spermidine might also be produced by this same pathway as norspermidine. However this could not be tested in *E.coli* system because of naturally occurring spermidine in *E.coli*.

We further investigated the polyamine biosynthetic pathway in *V.cholerae*, an important human pathogen, as a representative species among the *Vibrio* genus. We established two mutants in which *cansdc* or *cansdh* gene is knocked out from chromosome (Figure 4.1) and two mutants in which the knockout was genetically complemented. The finding that carboxynorspermidine was built up in the cansdcKO confirmed that CANSDH produces carboxynorspermidine, providing the first evidence for the CANSDH function in vivo (Figure 4.3B, bottom window). Norspermidine was not observed in either the cansdcKO or cansdhKO mutants grown in either LB or M9MM. This supports our proposed norspermidine biosynthetic pathway. To our surprise, wild type *V.cholerae* culture in M9MM contained no spermidine whereas a significant level of spermidine was detected from the culture in LB. All knockout mutants also exhibited similar level of spermidine to the wild type grown in LB whereas they produced no spermidine in M9MM. It is likely that spermidine detected in cells in LB is transported into the cells, as LB is a rich source of spermidine but not norspermidine. Altogether we

propose that wild type *V.cholerae* does not actively synthesize spermidine but transports it from the environment. Nakao et al. claimed that putrescine was much less active as a substrate for the *V.alginolyticus* CANSDH than DAP (Nakao et al., 1991) and our data suggest that DAP would also be used more efficiently than putrescine by CANSDH, explaining the lack of spermidine biosynthesis in these cells.

Genetic complementation of the mutant knockout cells did not restore polyamine pool profiles to the wild type cells (Figure 4.4). Complemented Δ*cansdc* (c_cansdcKO) and Δ*cansdh* (c_cansdhKO) mutants regained the ability to produce norspermidine, showing the complemented genes were effectively expressed in the mutants. However c_cansdcKO and c_cansdhKO mutants produced high levels of spermidine in M9MM cultures (Figure 4.3B, top and middle windows). This is proof that our proposed polyamine biosynthetic pathway is also effective for spermidine synthesis in *V.cholerae*, although the wild type did not produce significant level of spermidine in the minimal growth condition. In addition to spermidine, unidentified compounds that were in insignificant levels in the other samples showed up in c_cansdcKO and c_cansdhKO cells. The unnatural polyamine pools found in the complemented cells could be explained by over-expression of the complementing genes under the P_{BAD} promoter. For example, over-expressed CANSDH depleted DAP to produce carboxynorspermidine and also accepted putrescine as a substrate to produce carboxyspermidine, yielding production of spermidine in c_cansdhKO (Figure 4.4). Similarly the overwhelming high activity of over-expressed CANSDC seemed to produce unusual compounds, which remain to be identified.

Overall we have shown that norspermidine and spermidine are produced from CANSDH and CANSDC in *V.cholerae*. Sequenced genome information suggests that many *Vibrio* species are likely to possess very similar polyamine pathways to *V.cholerae* and a number of bacteria from different genuses also contain *cansdh* and *cansdc* genes in a cluster. These data suggest that this alternative CASNDH/CANSDC polyamine biosynthetic pathway that does not require AdoMetDC is wide spread in many bacteria. Therefore this alternative pathway could be targeted to develop selective therapeutic agents against those bacteria because the pathway is absent in humans.

Strain	Description	Reference/source
E.coli DH5α	Cloning purpose	Laboratory
E.coli BL21(DE3)	Expression of recombinant protein from pET-derived plasmids	Laboratory
E.coli SM10λPir	Conjugation (donor)	V.Sperandio (Miller and Mekalanos, 1988)
E.coli S17-1	Preparation of pCVD422 plasmid	V.Sperandio (R. Simon, 1983)
V.cholerae c6709	Wild type (O1 El Tor); Sm^r	V.Sperandio (Roberts, 1992)
cansdcKO	*V.cholerae* Δ*cansdc*::*cat*; Sm^r, Cm^r	This study
cansdhKO	*V.cholerae* Δ*cansdh*::*aph-3*, Sm^r, Kan^r	This study
c_cansdcKO	cansdcKO::pBAD1623, Sm^r, Cm^r, Ap^r	This study
c_cansdhKO	cansdhKO::pBAD1624, Sm^r, Kan^r, Ap^r	This study

Table 4.1 Bacterial strains used in this study

Plasmid	Description	Reference/source
pBluescript II SK+	Cloning (assembly of KO construct), Ap^r	Stratagene
pUK18K	Amplification of *aphA-3* gene, Kn^r	V.Sperandio (Menard et al., 1993)
pBAD/Myc-HisA	Genetic complementation, Ap^r	Invitrogen
pACYC184	Amplification of *cat* gene, Kn^r,Cm^r	New England Biolabs
pET-15b	Expression plasmid, Ap^r	Novagen
qpET-15b	Expression plasmid, Ap^r	This study
pET28a	Expression plasmid, Kn^r	Novagen
pCVD422	Suicide vector, Ap^r	V.Sperandio (Donnenberg and Kaper, 1991)
pET15:*Vv*CANSDC	pET-15b - *Vv*CANSDC, Ap^r	This study
qpET15:1623	qpET-15b - *Vc*CANSDC, Ap^r	This study
qpET15:1624	qpET-15b - *Vc*CANSDH, Ap^r	This study
qpET15:1625	qpET-15b - *Vc*DABA AT/DC, Ap^r	This study
pET28:1625	pET28a - *Vc*DABA AT/DC, Kn^r	This study
pET28:1625/1624	pET28a - *Vc*DABA AT/DC - *Vc*CANSDH, Kn^r	This study
pET28:1625/1624/1623	pET28a - *Vc*DABA AT/DC - *Vc*CANSDH - *Vc*CANSDC, Kn^r	This study
pCVD1623	*cansdc* KO construct, Ap^r,Cm^r	This study

pCVD1624	*cansdh* KO construct, Ap^r, Kn^r	This study
pBAD1623	pBAD/Myc-HisA - *Vc*CANSDC , complementation, Ap^r	This study
pBAD1624	pBAD/Myc-HisA - *Vc*CANSDH, complementation, Ap^r	This study

Table 4.2 Plasmids used and constructed in this study

Oligonucleotide	Oligonucleotide sequence (5' to 3') *	Purpose
QpET15F QpET15R	gtgagcggataacaattccccgtcgacaataattttgtttaac gttaaacaaaattattgtcgacggggaattgttatccgctcac	Site directed mutagenesis of pET-15b vector
VvCANSDC_F VvCANSDC_R	cagttaaagtgatgatacatatgaacaaagagcaattg ctgctcttatctatatagctcgagttactgtaccgaccatag	Cloning of *cansdc* gene from *V.vulnificus*
pET1623F pET1623R	gatatttgccatcacaagcacatatggaaacattgcag gagtccagacaaaatatgctcgagctactcaattgaccataaag	Cloning of *cansdc* gene from *V.cholerae*
Q1623F Q1623R	ggcgtgatgttccacatgaactgtgaaaataaagac gtctttattttcacagttcatgtggaacatcacgcc	Site directed mutagenesis of *cansdc* gene
pET1625F pET1625R	catctcaaggggaaaacatatgagtacagcctttg gaatagacatagttcctctcgagttagttcgctagctcagc	Cloning of *daba at/dc* gene from *V.cholerae*
pET1624F pET1624R	cgaactaaaggtaaaggacatatgtctattctacagattgg ggttttcactctcagctcgagttatttcaccacttg	Cloning of *cansdh* gene from *V.cholerae*
1624BamHI 1624SacI	ggataacaattccccggatccaataattttgtttaac gttagcagccggatcgagctcttatttcaccacttg	Cloning of rbs and *cansdh* gene into pET28a
VC1623A VC1623B VC1623C VC1623D	acacttcagtgccaacacca gctctagaacgcgtaccttgccatactc aagcttgtctggactcgaagcggtga gtcgacggtgatgagtacgactatcg	*cansdc* knockout construct
VC1624A VC1624B VC1624C VC1624D	ccggaattccaaccaacaccgcctgcacc gtcgacgagtatgcggacaaactgcg cgcggatccgatcggtctaggctgggatg gctctagatagagctgaacagcgtgacg	*cansdh* knockout construct
CmF CmR	gtgacggaagatcacttcgca gcgtttaagggcaccaataactgcc	Amplification of the *cat* gene

KanF KanR	ccatgattacgaattcgagctcggtaccc cgactctagaggatcccgggtgac	Amplification of the *aphA-3* gene
VC1623IF VC1624IF VC1624R	gatcttcaactcacaatcgcaactggc cgcgacaaatttaagcaagccggtatc ggctcaataagccaatatcacgcatc	Confirmation of gene replacement
pBAD1623F pBAD1623R	gatatttgccatcacactcgagaatggaaacattgcag gacaaaatatgtacaagcttctcaattgaccataaag	Genetic complementation of cansdcKO
pBAD1624F pBAD1624R	ctggtgccgcgcggctcgagtatgtctattctacag gttagcagccggatcaagctttttatttcaccacttg	Genetic complementation of cansdhKO

*Engineered restriction sites are underlined.

Table 4.3 Oligonucleotides used in this study

Enzyme	Substrate	k_{cat} (s^{-1})	K_m (mM)	k_{cat}/K_m ($M^{-1}s^{-1}$)
*Vv*CANSDC	Carboxynorspermidine	20.1 ± 0.3	0.27 ± 0.03	7.4×10^4
	Carboxyspermidine	3.2 ± 1.0	1.0 ± 0.1	3.2×10^3
*Vc*DABA AT/DC	L-2, 4-diaminobutyrate	8.3 ± 0.6	0.17 ± 0.04	4.9×10^4
	L-Ornithine	0.54 ± 0.02	11.1 ± 0.9	4.9×10^1

Table 4.4 Kinetic parameters of decarboxylating activities of *Vv*CANSDC and *Vc*DABA AT/DC on various substrates.

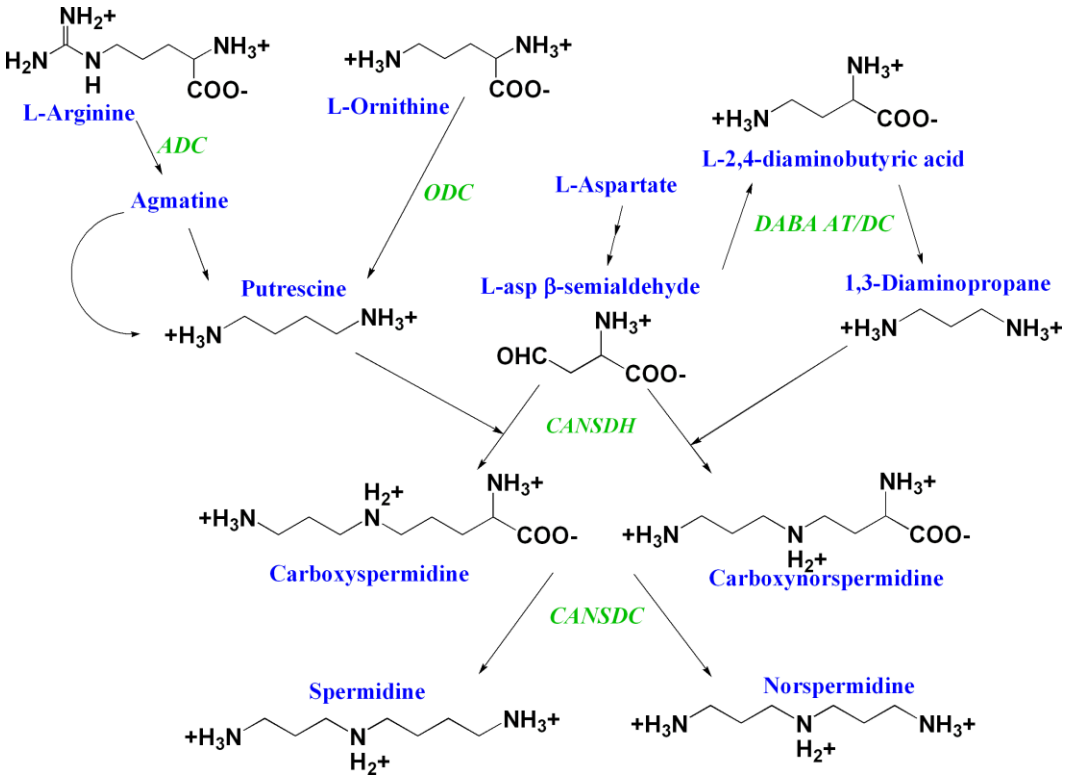

Figure 4.1 Proposed polyamine biosynthetic pathways in *Vibrio cholerae*. ADC, arginine decarboxylase; ODC, ornithine decarboxylase; DABA AT/DC, diaminobutyrate aminotransferase/decarboxylase; CANSDH, carboxynorspermidine dehydrogenase; CANSDC, carboxynorspermidine decarboxylase.

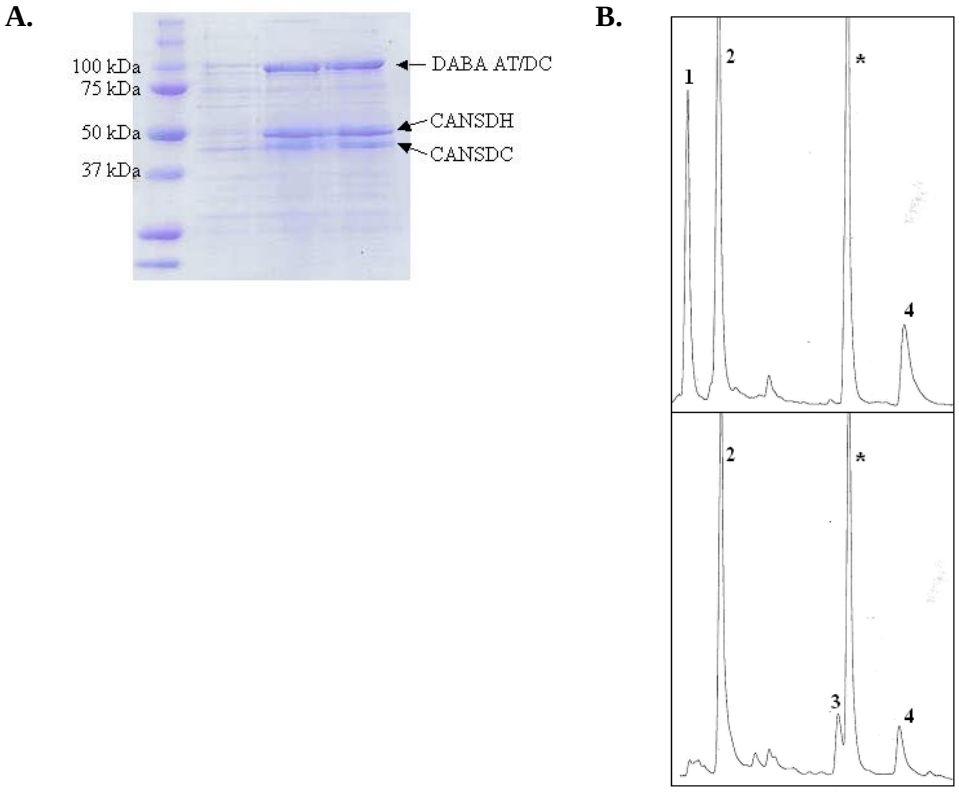

Figure 4.2 Analysis of *E.coli* transformed with alternative pathway enzymes. A. SDS-PAGE analysis of over-expressed proteins from *E.coli* transformed with pET28:1625/1624/1623: Lane 1, molecular markers; Lane 2, total cell lysate before induction of protein over-expression; Lane 3, total cell lysate after induction; Lane 4, cleared supernatant of cell lysate after induction. Expected molecular weights of diaminobutyrate aminotransferase/decarboxylase (DABA AT/DC), carboxynorspermidine dehydrogenase (CANSDH) and carboxynorspermidine decarboxylase (CANSDC) are 105 kDa, 46 kDa and 43 kDa, respectively. B. HPLC chromatograms of polyamines from *E.coli* transformed with pET28:1625 (top panel) and with pET28:1625/1624/1623 (bottom panel): 1, 1,3-diaminopropane; 2, putrescine; 3, norspermidine; 4, spermidine; *, unidentified background peak. Over-expression of recombinant proteins was induced by 200 μM IPTG at 16 ˚C overnight. For the polyamine labeling and HPLC conditions, see Experimental Procedures.

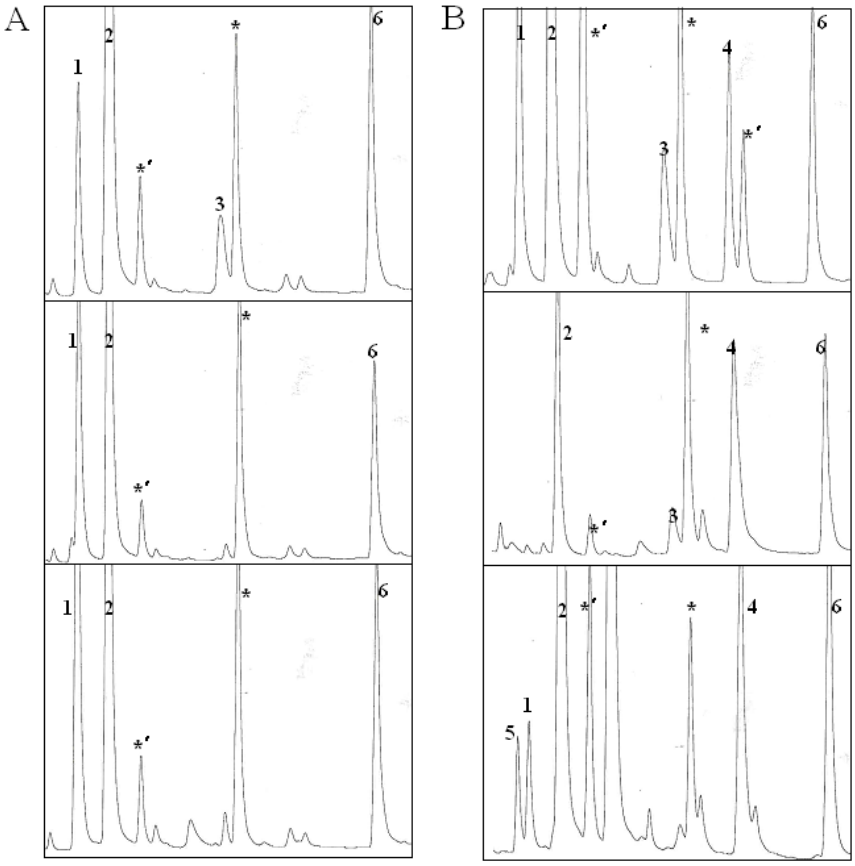

Figure 4.3 HPLC chromatograms of cellular polyamines from wild type and mutant *V.cholerae*. Wild type (panel A, top), cansdcKO (panel A, middle), cansdhKO (panel A, bottom), c_cansdcKO (panel B, top) and c_cansdhKO (panel B, middle) were grown in M9-minimal medium at 37°C overnight. cansdcKO was grown in LB medium (panel B, bottom) at 37°C overnight to detect carboxynorspermidine. 1, 1,3-diaminopropane; 2, putrescine; 3, norspermidine; 4, spermidine; 5, carboxynorspermidine; 6, 1,7-diaminoheptane (internal standard); *, unidentified peak coming from background; *′unidentified peaks. For the polyamine labeling and HPLC conditions, see Experimental Procedures.

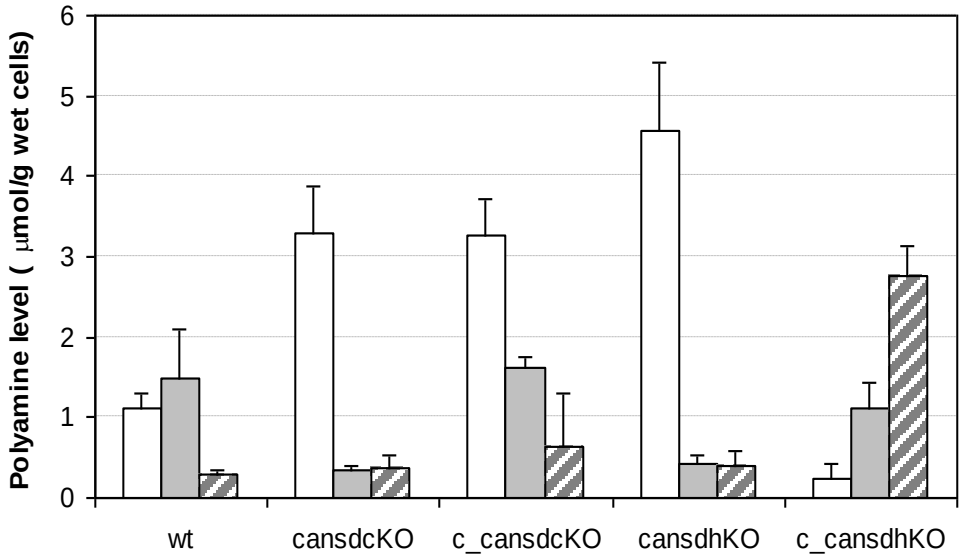

Figure 4.4 Polyamine pools of *V.cholerae*. Intracellular levels of 1,3-diaminopropane (open white), norspermidine (gray) and spermidine (striped) were measured from the same number of cells (based on OD_{600}) grown in M9-minimal medium at 37°C overnight. Putrescine was also observed in all strains but is not displayed in this figure. Error bars indicate the standard deviations of three independent cultures.

CHAPTER 5

BIOLOGICAL ROLES OF NORSPERMIDINE/SPERMIDINE IN *V.CHOLERAE*

A. Introduction

V.cholerae can grow planktonically or in biofilm in the natural aquatic environment. Evidence suggests that biofilm development provides *V.cholerae* with persistence in the environment (Watnick and Kolter, 1999; Watnick et al., 2001; Yildiz and Schoolnik, 1999) and also plays an essential role in the cholera epidemic probably by delivering higher dose of bacteria concentrated in biofilm (Purevdorj, 2004). The formation of biofilm requires an exopolysaccharide termed VPS (*Vibrio* polysaccharide). VPS is synthesized by a number of proteins encoded by two *vps* operons, *vpsA ~ vpsK* and *vpsL ~ vpsQ* (Wai et al., 1998; Watnick and Kolter, 1999; Yildiz and Schoolnik, 1999). The *vps* gene transcription and biofilm formation are regulated by many environmental signals such as surfaces and quorum sensing (QS). QS is a bacterial cell-cell communication measuring cell population density using autoinducer (AI) molecules that are produced and detected by bacteria (Waters and Bassler, 2005). At low cell density, the QS response regulator LuxO is phosphorylated, activating transcription of four redundant Quorum Regulatory small RNAs (*qrr*1-4 sRNAs) (Figure 5.3, left pannel) (Lenz et al., 2004). Expressed Qrr1-4 repress translation of HapR, the master QS transcription factor that represses biofilm and virulence genes (Hammer and Bassler, 2003; Jobling and Holmes, 1997). At high cell density, LuxO is dephosphorylated and inactivated, leading to termination of *qrr*1-4 expression and allowing HapR to regulate its target genes (Lenz et al., 2004) (Figure 5.3, right panel). Another chemical signaling

system using the intracellular second messenger molecule 3´, 5´-cyclic diguanylic acid (c-di-GMP) is involved in the regulation of biofilm formation. At high levels of c-di-GMP, biofilm formation is activated whereas virulence factor expression and motility are repressed in *V.cholerae* (Beyhan et al., 2006; Tischler and Camilli, 2004, 2005) (Figure 5.3, bottom of left panel). Environmental norspermidine is also a signaling molecule that activates biofilm formation in *V.cholerae* through interaction with the periplasmic norspermidine sensor protein NspS (locus VC0704) (Karatan et al., 2005). A neighboring protein MbaA (locus VC0703), an integral membrane protein containing GGDEF and EAL domains is a repressor of biofilm formation and is predicted to function as a phosphodiesterase, degrading c-di-GMP (Bomchil et al., 2003). Therefore it was proposed that norspermidine sensed by NspS interrupts the function of MbaA, which increases the level of c-di-GMP, resulting in elevated biofilm formation. Norspermidine is also found as a building molecule of vibriobactin, the only siderophore produced by *V.cholerae*. However its relevance to iron acquisition has not been examined.

Our previous study showed that *Vibrio* speicies employ an alternative polyamine biosynthetic pathway that is not dependent on AdoMetDC. This polyamine pathway is absent in humans and the resulting norspermidine is not found in humans as well. Similar polyamine pathways seem to occur in a number of bacterial species based on their genome sequence (see Chapter 4). Therefore norspermidine-producing enzymes such as *cansdc* and *cansdh* could be potential drug targets to develop selective cures for bacterial infectious diseases if they are essential for cell viability or associated with virulence. Previously we had established two knockout mutants, cansdcKO and cansdhKO that cannot make norspermidine and spermidine in *V.cholerae*. This allowed us to examine

the biological roles of norspermidine and spermidine in *V.cholerae* including their effects on cell growth and biofilm formation. Our study showed that norspermidine and spermidine are not essential for cell growth and norspermidine is important for biofilm formation in *V.cholerae*. Our preliminary real-time RT PCR analysis suggests that the intracellular level of norspermidine/spermidine may also be associated with QS. Based on our current observations, we propose that both intracellular and extracellular norspermidine is involved in more than one regulatory signaling pathways for biofilm formation: extracellular norspermidine affects the MbaA-dependent pathway via NspS and intracellular norspermidine plays a role in an unknown signaling pathway probably related to QS.

B. Experimental Procedures

1. Strains and Growth Conditions

Five strains of *V.cholerae* established in the previous study (see Chapter 4) were used in this study: *V.cholerae* c6709 (wild type, O1 El Tor, Sm^r), cansdcKO (*V.cholerae* Δ*cansdc*::*cat*, Sm^r, Cm^r), 1624 KO (*V.cholerae* Δ*cansdc*::*aph-3*, Sm^r, Kn^r), c_cansdcKO (cansdcKO::pBAD1623, Sm^r, Cm^r, Ap^r) and c_cansdhKO (cansdhKO::pBAD1624, Sm^r, Kn^r, Ap^r). *V.cholerae* was grown at 37 °C and 30 °C in Luria-Bertani (LB) broth and M9-minimal medium (M9MM). The M9MM containing 0.4 % glycerol as a carbon source was used in all experiments except in the growth experiment in which 0.4 % glucose-containing M9MM was used because the complemented strains were not tested. El Tor strains of *V.cholerae* such as the strain *V.cholerae* c6709 that was used in this study do not express cholera toxin in LB but express it in AKI medium (Iwanaga et al., 1986).

Therefore AKI medium was used to prepare total RNA for real time RT-PCR that was exploited to measure virulence gene expressions including the cholera toxin-producing gene. When needed, the antibiotics streptomycin, chloramphenicol, kanamycin, ampicillin and carbenicillin were added at the concentrations of 30 μg/ml, 10 μg/ml, 50 μg/ml, 50 μg/ml and 50 μg/ml, respectively. L-Arabinose was added at 0.2 % w/v in the culture as an inducer under the P_{BAD} promoter.

2. Growth Experiment

Wild type and mutant strains (cansdcKO and cansdhKO) of *V.cholerae* were grown at 37 °C in LB overnight and washed twice in M9-minimal medium (M9MM). They were diluted to an initial OD_{600} of 0.02 in fresh M9MM or LB ± 250 μM spermidine and/or 250 μM norspermidine and incubated at 37 °C with shaking at 250 rpm. The OD_{600} was measured from each sample at the times indicated. 24-hour culture in M9MM was reinoculated in fresh M9MM and observed for growth.

3. Measurement of Static Biofilm Formation by Crystal Violet Staining

Microtiter static biofilm assay was modified from the standard method described by O'Toole et al. (O'Toole et al., 1999). In brief, overnight bacterial cultures were washed twice in M9MM, and diluted 1:100 in LB or M9MM, yielding an initial OD_{600} of 0.02 ~ 0.04. 100 μl of each diluted culture was incubated in quadruplicate wells of a microtiter plate at 30 °C for 24 hrs. After the planktonic cell density was determined by measuring OD_{600} of 80 μl cell culture, planktonic cells were removed and plates were

washed in distilled water. The remaining biofilm was stained with 125 µl of 0.1% crystal violet solution, and washed twice in distilled water. Crystal violet stain was solubilized in 200 µl of DMSO for 10 min and 125 µl of the contents in each well were transferred to a visible flat-bottom 96-well plate for determination of absorbance at 595 nm.

4. RNA Preparation and Real-Time RT-PCR

Overnight cultures of *V.cholerae* strains in LB at 37 °C were diluted 1:200 in freshly prepared AKI medium, and grown to mid-log phase (OD_{600} ~ 0.5). Total RNA from *V.cholerae* was prepared using RiboPure-Bacteria kit (Ambion) according to the manufacturer's protocol. The RNA was stored at –80 °C until use. Reverse transcription (RT) of RNA was carried out using SuperScriptIII One-Step RT-PCR kit (Invitrogen). Two micrograms of total RNA was used for RT in 20 µl reaction, which was incubated at 25 °C for 3 min, 37 °C for 2 hrs and 70 °C for 10 min, and cooled at 4 °C to produce cDNA. The cDNA samples were stored at –80 °C until analysis.

Primers for the five genes of interest, *ctxA*, *tcpA*, *vpsL*, *hapR* and *epsM* and a housekeeping gene *gyrA* were chosen from the Primer 3 program (http://frodo.wi.mit.edu/) or adopted from previously performed real-time PCR reactions (Table 5.1) (Beyhan et al., 2007; Gubala, 2006; Yildiz et al., 2001). The real-time PCR reactions included 8.8 µl of diluted cDNA, 1.2 µl of primers and 10 µl of 2x iTaq SYBR Green Supermix with ROX (BioRad). Reactions were performed in 7500 Real Time PCR System (Applied Biosystems) using the following thermal cycle: 50 °C for 2 min, 95 °C

for 3 min and 40 cycles of 95 °C for 15 s and 60 °C for 1 min, followed by a dissociation stage ranging between 60 °C and 95 °C.

Real-time PCR efficiencies of six different genes were calculated according to the equation $E = 10^{[-1/\text{slope}]}$, in which the slope was determined from the plot of cycle thresholds (Ct) versus cDNA input for each pair of primers (Table 5.1). The Ct values were determined for each sample and the relative quantification of target genes (*ctxA*, *tcpA*, *vpsL*, *hapR* and *epsM*) in comparison to a reference gene (*gyrA*) was calculated according to the equation 5.1 as previously described by Pfaffl (Pfaffl, 2001). It was displayed as an expression ratio based on the real-time PCR efficiencies (*E*) for each target gene and the reference gene and Ct deviation of an unknown sample (knockout mutant) versus a control (wild type).

$$ratio = \frac{(E_{target})^{\Delta Ct_{target}(control-sample)}}{(E_{ref})^{\Delta Ct_{reference}(control-sample)}} \quad \text{(Eq. 5.1)}$$

C. Results

1. Effect of Intracellular Level of Norspermidine and Spermidine on Cell Growth

Two knockout mutants, cansdcKO and cansdhKO that are incapable of producing norspermidine and spermidine were tested for cell growth in comparison to the wild type *V.cholerae*. Our polyamine analysis showed cansdhKO makes 1,3-diaminopropane (DAP) and putrescine and cansdcKO makes carboxynorspermidine in addition to DAP and putrescine (Figure 4.1, see Chapter 4). These two mutants were grown in M9MM that is free of polyamine and LB that is a rich source of spermidine, to test if the norspermidine and spermidine-deficiency affects the cell viability of *V.cholerae*.

Over the first 24 hrs of culture period, cansdcKO and cansdhKO mutants grew in a very similar manner to the wild type in both cultures in M9MM (Figure 5.1) and LB (data not shown). This suggests that intracellular levels of norspermidine and spermidine do not affect the cell growth of *V.cholerae*. When 250 μM norspermidine or spermidine or both were added in the culture medium, they also showed no effect on the growth of wild type or mutant cells (data not shown).

2. Defective Biofilm Formation in Norspermidine, Spermidine - Deficient *V.cholerae* Mutants

Static biofilm formation of cansdcKO and cansdhKO *V.cholerae* were measured in comparison to the wild type using a microtiter assay. It was measured after 24 hrs of incubation in LB and M9MM at 30 ˚C and normalized to the planktonic cell growth. Both mutants failed to form biofilm in M9MM (data not shown) and showed severely defective biofilm formation in LB compared to wild type (Figure 5.2). This defect was rescued almost up to the wild type level by 0.5 mM of norspermidine added in the culture medium, whereas 0.5 mM of spermidine did not change the level of biofilm formation in both mutant cells. In the wild type, added norspermidine increased the level of biofilm formation by about 2-fold in the wild type but spermidine showed no effect on the biofilm level. Biofilm phenotypes of the knockout mutants were not rescued by genetic complemenations: the levels of biofilm in the complemented strains c_cansdcKO and c_cansdhKO were similar to those of the knockout mutants (Figure 5.2). Their defect was not even fully rescued by 0.5 mM of norspermidine and 0.5mM of spermidine showed no effect.

3. Altered Transcriptional Regulation of Virulence and Biofilm Formation Genes in Norspermidine, Spermidine - Deficient *V.cholerae* Mutants

Gene expression levels of biofilm and virulence factors in the wild type and mutant *V.cholerae* cells were measured using real-time RT PCR analysis. Including the genes from two major virulence factors, cholera toxin (CT) and toxin-coregulated pilus (TCP), five genes were selected for analysis: *ctxA* encoding the subunit A of CT, *tcpA* encoding the major subunit of TCP, *vpsL*, the first gene in the second *vps* cluster involved in biofilm formation, *hapR*, encoding the central transcription factor of QS, HapR that links quorum sensing and biofilm formation and *epsM*, extracellular secretion protein gene.

Our preliminary real-time PCR result suggests that transcription of the *vpsL* gene in both mutants is down-regulated (about 2-fold) compared to the wild type while *hapR* expression was increased ~ 2-fold. *epsM* expression appeared unaffected. Analysis of *ctxA* and *tcpA* expression is in progress.

D. Discussion

Polyamines spermidine, spermine and putrescine are essential for cell growth in eukaryotic cells and they play regulatory roles in cell growth in eukaryotic and prokaryotic cells (Gerner and Meyskens, 2004; Igarashi and Kashiwagi, 2006). Our previous study of cansdcKO and cansdhKO *V.cholerae* cells where the polyamine biosynthetic pathway was disrupted by gene replacement of *cansdc* and *cansdh* with antibiotic resistance cassettes showed that these *V.cholerae* mutant cells contain very low

levels of norspermidine and spermidine unless exogenous polyamines are supplied in their growth medium. These two mutants grew normally in liquid culture (M9MM and LB). To exclude the possibility that the residual norspermidine and spermidine found in the mutants by HPLC analysis allowed the mutants to grow normally, the mutants were subcultured serially in fresh M9MM up to four days and they still showed no growth defect (data not shown). This suggests that normal levels norspermidine and spermidine are not essential for normal cell growth of *V.cholerae*.

The ability to form biofilm was greatly diminished (about 10-fold decrease compared to the wild type) in cansdcKO and cansdhKO cells grown in LB and was restored only by exogenous norspermidine. This is similar to the finding from Karatan et al. (Karatan et al., 2005) that biofilm formed in a norspermidine - dependent manner. They proposed that extracellular norspermidine in the culture medium is sensed by NspS, through which norspermidine affects the function of MbaA, resulting in an increased biofilm formation probably through elevating the cellular level of c-di-GMP. Taken together, endogenous norspermidine is likely to be excreted into the culture medium through an unknown excretion mechanism (there is no known mechanism for norspermidine excretion) and norspermidine at the extracellular side affects the NspS-Mba pathway and therefore increases biofilm formation. In Karatan et al.'s study the decreased level of biofilm formation of the Δ*nspS* mutant was still about a half of the wild type (Karatan et al., 2005) whereas Δ*cansdc* and Δ*cansdh* mutants exhibited almost no biofilm compared to the wild type. This implies that intracellular norspermidine could be involed in alternative pathways for biofilm regulation.

Exogenous norspermidine increased *vpsL* gene expression in the wild type consistent with the increased biofilm formation (Karatan et al., 2005). In addition to the c-di-GMP-dependent pathway, biofilm formation is also regulated by QS through the transcription factor HapR. Recently it was found that HapR represses biofilm formation through both the transcriptional control of genes encoding c-di-GMP - synthesizing or degrading proteins and direct repression of the biofilm transcriptional activator, *vpsT* (Waters et al., 2008) (Figure 5.3). Our current preliminary real-time RT-PCR result shows *vpsL* gene expression is down-regulated and *hapR* is up-regulated in the cansdcKO and cansdhKO mutants. This implies that norspermidine may play a role in the QS signaling pathway through *hapR* as well as through the c-di-GMP pathway (Figure 5.3). Qrr sRNAs destabilize the mRNA of *hapR* via the sRNA chaperone Hfq and promotes its degradation (Lenz et al., 2004). sRNAs are regulatory molecules in response to stress or other regulatory signals (Masse et al., 2003). Norspermidine is a intercellular signaling molecule for biofilm formation and majority of polyamines exist as polyamine-RNA complexes in cells (Igarashi and Kashiwagi, 2006). These lead me to hypothesize that norspermidine as a intracellular signaling molecule is involved in the biofilm regulation in accossication with Qrr sRNAs and/or Hfq protein, with which norspermidine regulates the transcription level of *hapR* and therefore target genes including *vps* genes (Figure 5.3). Besides the aspect of biofilm formation, the effect of norspermidine and spermidine on the transcpritional regulation of virulence factors can be assessed when the real-time RT-PCR analysis is completed.

0.5 mM spermidine showed no significant effect on the biofilm formation in wild type and mutants in our study but Karatan et al. claimed that 1mM or higher

concentration of spermidine resulted in decreased biofilm formation in the wild type (Karatan et al., 2005). Genetic complementation did not rescue the biofilm defect of the mutants (c_cansdcKO and c_cansdhKO) and 0.5mM norspermidine failed to fully rescue them in our study. Polyamine profiles of the complemented cells were different from the wild type probably because of the over-expressed CANSDC or CANSDH enzymes. For example, spermidine was found in the complemented cells in M9MM, a culture condition in which wild type did not produce spermidine (Figure 4.4). However it is unlikely that spermidine production in the complemented cells affected biofilm level because the levels of spermidine were generally unaltered in all tested strains including the complemented mutants when they were grown in LB, which was a spermidine containing rich culture medium used for the biofilm measurement. The intracellular level of DAP in c_cansdcKO was about 3-fold higher than that of wild type, while DAP in c_cansdhKO was almost depleted (Figure 4.4). Also the complemented cells contained unusual compounds that remain to be identified. Altogether the disrupted polyamine balance due to the genetic complementation seemed to cause biofilm defect. In fact, the complemented mutants showed a severe growth defect when they were grown in M9MM whereas they grew normally in LB (data not shown), suggesting that the regulation of global polyamine pool is important for cell growth. Some other polyamines such as DAP could be involved in the regulation of biofilm formation in alternative pathways besides norspermidine. Similarly Patel et al. reported that the defective biofilm formation of the *Yersinia pestis* mutant that was unable to produce putrescine and spermidine was not fully rescued by genetic complementation and the polyamine pool of the complemented cells was different from wild type (Patel et al., 2006).

Target gene	Primer	Primer sequence (5’ to 3’)
ctxA (1.94)	ctxAF	cctgccaatccataaccatc
	ctxAR	tatagccactgcacccaaca
tcpA (1.88)	tcpAF	gactaaggctgcgcaaaatc
	tcpAR	tgcagagtttcgtggaaatg
vpsL (1.89)	vpsLF	atcgcaccatagtgaatcgct
	vpsLR	tctgtgcccatccagtaatgc
hapR (1.93)	hapRF	gcgctcgagtatggacgcatcaatcgaaaaacg
	hapRR	cactgttgcaacggagactt
epsM (1.93)	epsMF	tggttgatcgcttggcgcatc
	epsMR	atggcagcctttgagtgag
gyrA (1.95)	gyrAF	gttatcgtgggtcgtgctct
	gyrAR	ctaccacacgggcagatttt

Table 5.1 Sequences of the primers used for real-time PCR. Efficiency (*E*) of real-time PCR for each gene is indicated in parenthesis. Efficiency was calculated according to the equation $E = 10^{[-1/\text{slope}]}$, in which the slope was determined from the plot of cycle thresholds (Ct) versus cDNA input for each pair of primers.

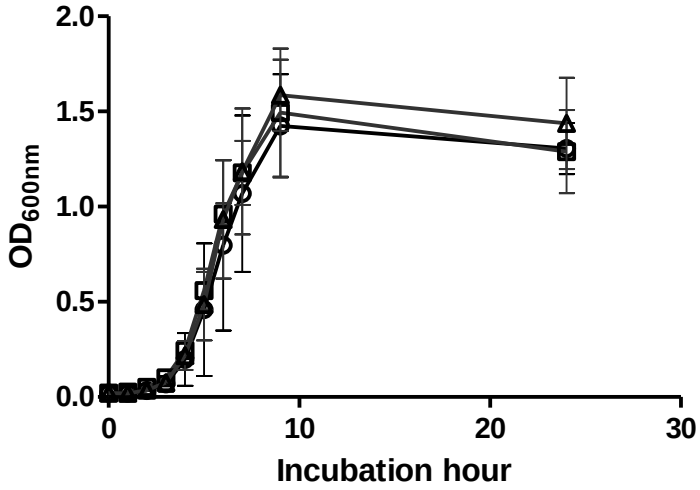

Figure 5.1 Growth profiles of wild type and mutant *V.cholerae*. Wild type (○), cansdcKO (□) and cansdhKO (Δ) cells were grown at 37 °C in a M9 minimal medium containing 0.4 % glucose as a carbon source over the time periods indicated. Cell growth was measured upon the absorbance at 600nm. Error bars indicate the standard deviations of three independent cultures.

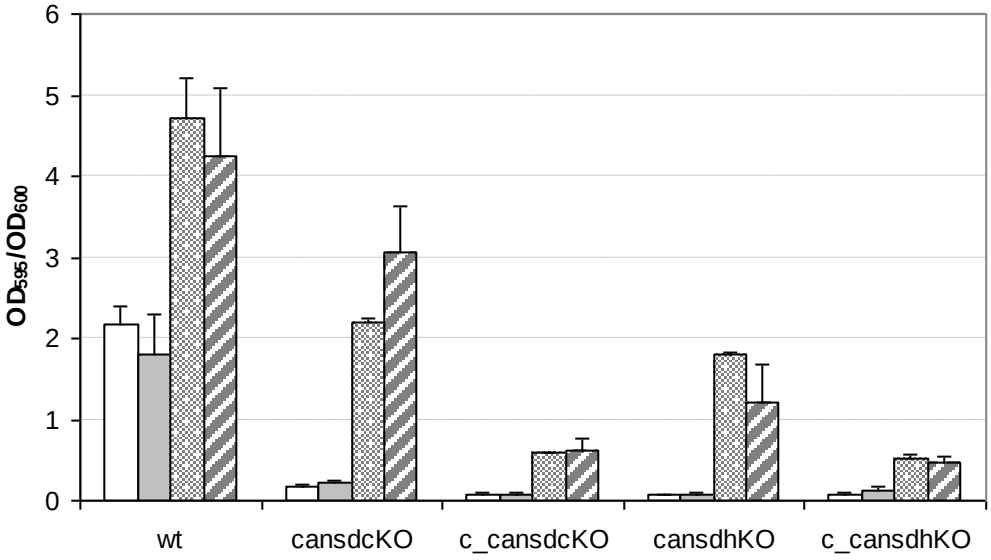

Figure 5.2 Biofilm formations of wild type and mutant *V.cholerae* in LB broth. Static biofilm formed in microtiter plates (OD_{595}) was measured after incubation in LB broth (open white), LB + 0.5 mM spermidine (gray), LB + 0.5 mM norspermidine (dotted) or LB + 0.5 mM spermidine and 0.5 mM norspermidine (striped) at 30 ºC for 24 hrs by staining with 0.1 % crystal violet and standardized upon planktonic cell growth (OD_{600}). Error bars indicate standard deviations from quadruplicate samples.

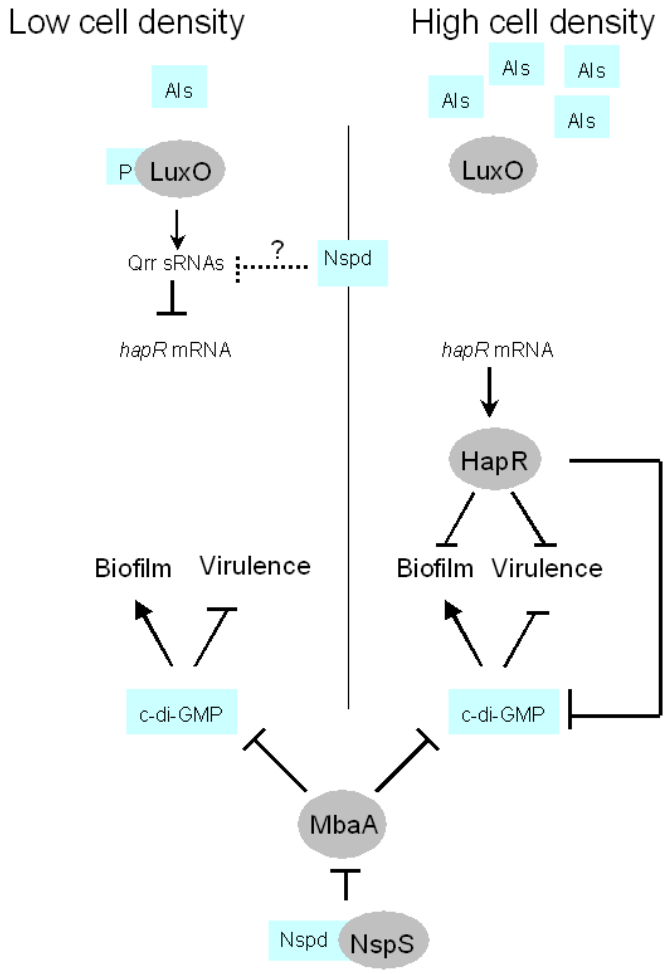

Figure 5.3 Proposed model of the interaction between quorum sensing and c-di-GMP-dependent signaling pathways in the regulation of biofilm and virulence gene expressions in *V.cholerae*. Modified from Waters et al.'s (Waters et al., 2008). At low cell density (left panel), the concentrations of AIs are low and LuxO is phosphorylated. LuxO~P activates the expression of Qrr sRNA-encoding genes, which destabilizes the mRNA of *hapR*. At high cell density (right panel) with high concentrations of AIs, LuxO is dephosphorylated, leading to termination of *qrr* gene expression and production of HapR. HapR represses biofilm and virulence gene expressions, which are also regulated by the intracellular second messenger c-di-GMP. HapR decreases biofilm formation directly by

repressing the expression of biofilm transcriptional activator (*vpsT*) and indirectly by reducing the intracellular level of c-di-GMP that enhances biofilm formation and represses virulence genes through the transcriptional regulation of c-di-GMP-controlling genes. Norspermidine sensed by the NspS sensor protein disrupts MbaA-dependent biofilm repression that is probably achieved by lowering the level of c-di-GMP, resulting in increased biofilm formation.

CHAPTER 6

PERSPECTIVES

Basic amino acid decarboxylation is one of the reactions that are catalyzed by PLP-dependent enzymes and can be catalyzed by two structurally distict groups of enzymes: one group of enzymes that are homolgous to aspartate aminotransferase (AAT-fold decarboxylase) and another that are homologous to alanine racemase (β/α-barrel fold decarboxylase). β/α-barrel fold decarboxylases are functionally and phylogenetically diverse.

Based on the solved structures of eukaryotic ODCs, chlorella virus ADC and bacterial DAPDCs, it was previously proposed that amino acid composition at the active site and the specificity element, the 3_{10}-helix at the active site pocket, were the key determinant of different substrate specificities. Chlorella virus ADC contains a D to E change at the 332 position which was proposed to be one of the key residues for specificity determination. I found that newly identified bacterial sequences of β/α-barrel fold decarboxylases that are close homologs of eukaryotic ODCs have Glu-332 similar to the chlorella virus ADC. My biochemical study on these bacterial enzymes showed that despite this amino acid change these enzymes were all L-ornithine-specific. This shows that chlorella virus ADC is an unusual example of rapid evolution of substrate specificity in this family.

I solved the structures of *V.vulnificus* L/ODC in the presence of two reaction products, putrescine and cadaverine. Comparison of this enzyme structure with *T.brucei* ODC and chlorella virus ADC showed a conservation of catalytic and PLP-binding residues consistant with a common ancestor. My data show that the different substrate preferences of the 3 enzymes are accomodated by change in the position of the 3_{10}-helix at the back of the substrate binding pocket, and by changes in amino acid composition in the pocket.

Polyamines are essential for cell growth and cell proliferation. This allows the polyamine biosynthetic pathway to be a potential drug target for hyperproliferative diseases, such as cancer. Polyamine biosynthetic pathways are described well in eukaryotes including mammalian cells and higher plants, and prokaryotes represented by *E.coli*. The main difference between eukaryotes and prokaryotes is found in how putrescine is produced and higher polyamines such as spermidine and spermine are produced in a similar way that is dependent on S-adenosylmethionine decarboxylase (AdoMetDC). Recently a number of genome sequences from bacteria became available, and it was found that many bacteria do not contain AdoMetDC sequences. *V.cholerae*, which was investigated in this study, also lacks AdoMetDC sequence. Based on the genome information and previously reported facts, I predicted an alternative pathway for norspermidine and spermidine biosynthesis in *V.cholerae* and confirmed it by in vivo reconstitution and genetic knockout study. Instead of using decarboxylated S-adenosylmethionine, *V.cholerae* employed L-aspartic β-semialdehyde as a propylamine group donor: it produced norspermidine and spermidine by carboxynorspermidine dehydrogenase (CANSDH) and carboxynorspermidine decarboxylase (CANSDC). Bioinformatics shows that many bacteria possess clustered CANSDH and CANSDC sequences in their genomes, suggesting that this pathway represents an AdoMetDC-independent alternative polyamine biosynthetic pathway that apprears to be wide spread in bacteria.

My gene knockout study in *V.cholerae* allowed identification of some biological roles of spermidine and norspermidine. Normal levels of spermidine and norspermidine were not essential for cell survival. Reduction of norspermidine by ~70% led to no growth effects. I was able to show however that norspermidine was important for biofilm formation. Previously it was reported that norspermidine functions as an intercellular signaling molecule for biofilm formation. My study on the knockout mutants that cannot produce endogenous norspermidine supports this hypothesis. Further analysis of the transcriptional levels of virulence and quorum sensing genes in the polyamine-deficient mutants will evaluate the effect of norspermidine and/or spermidine on the transcriptional regulation of those genes. Current preliminary data on the intestinal colonization

experiment in infant mouse model shows that Δ*cansdh* mutant is attenuated by ~3-fold in intestinal colonization in comparison to wild type *V.cholerae*. This proposes the possibility that internal level of polyamines is associated with intestinal colonization, which is important for virulence in *V.cholerae*.

Most antimicrobials that are currently used are antibiotics that target and inhibit essential cellular processes. This has lead many bacterial strains to develop resistance to available antibiotics. One of alternative approaches to develop new antimicrobials that will not stimulate resistance is to target bacterial virulence (Cegelski et al., 2008). Inhibiting only virulence without endangering their survival could reduce a selection pressure for drug resistance. Some of the possible targets include genes involved in the biofilm formation and quorum sensing. In this study, normal levels of higher polyamines, spermidine and norspermidine, were not essential for cell growth but seemed to be important in other biological processes such as biofilm formation and quorum sensing in *V.cholerae*. CANSDH/CANSDC pathway for polyamine biosynthesis is absent in humans. Therefore, the norspermidine/spermidine biosynthetic pathway could be targeted to develop selective antivirulence therapeutics for cholera.

BIBLIOGRAPHY

Almrud, J.J., Oliveira, M.A., Kern, A.D., Grishin, N.V., Phillips, M.A., and Hackert, M.L. (2000). Crystal structure of human ornithine decarboxylase at 2.1 A resolution: structural insights to antizyme binding. J Mol Biol *295*, 7-16.

Bacchi, C.J., Nathan, H.C., Hutner, S.H., McCann, P.P., and Sjoerdsma, A. (1980). Polyamine metabolism: a potential therapeutic target in trypanosomes. Science *210*, 332-334.

Beyhan, S., Bilecen, K., Salama, S.R., Casper-Lindley, C., and Yildiz, F.H. (2007). Regulation of rugosity and biofilm formation in Vibrio cholerae: comparison of VpsT and VpsR regulons and epistasis analysis of vpsT, vpsR, and hapR. J Bacteriol *189*, 388-402.

Beyhan, S., Tischler, A.D., Camilli, A., and Yildiz, F.H. (2006). Transcriptome and phenotypic responses of Vibrio cholerae to increased cyclic di-GMP level. J Bacteriol *188*, 3600-3613.

Bomchil, N., Watnick, P., and Kolter, R. (2003). Identification and characterization of a Vibrio cholerae gene, mbaA, involved in maintenance of biofilm architecture. J Bacteriol *185*, 1384-1390.

Born, T.L., and Blanchard, J.S. (1999). Structure/function studies on enzymes in the diaminopimelate pathway of bacterial cell wall biosynthesis. Curr Opin Chem Biol *3*, 607-613.

Buch, J.K., and Boyle, S.M. (1985). Biosynthetic arginine decarboxylase in Escherichia coli is synthesized as a precursor and located in the cell envelope. J Bacteriol *163*, 522-527.

Casero, R.A., Jr., and Marton, L.J. (2007). Targeting polyamine metabolism and function in cancer and other hyperproliferative diseases. Nat Rev Drug Discov *6*, 373-390.

Cavalier-Smith, T. (2006). Rooting the tree of life by transition analyses. Biol Direct *1*, 19.

Cegelski, L., Marshall, G.R., Eldridge, G.R., and Hultgren, S.J. (2008). The biology and future prospects of antivirulence therapies. Nat Rev Microbiol *6*, 17-27.

Coleman, C.S., Stanley, B.A., and Pegg, A.E. (1993). Effect of mutations at active site residues on the activity of ornithine decarboxylase and its inhibition by active site-directed irreversible inhibitors. The Journal of biological chemistry *268*, 24572-24579.

DeLano, W.L. (2003). PyMol Reference Mannual (San Carlos, CA, DeLano Scientific LLC).

Donnenberg, M.S., and Kaper, J.B. (1991). Construction of an eae deletion mutant of enteropathogenic Escherichia coli by using a positive-selection suicide vector. Infect Immun *59*, 4310-4317.

Eliot, A.C., and Kirsch, J.F. (2004). Pyridoxal phosphate enzymes: mechanistic, structural, and evolutionary considerations. Annu Rev Biochem *73*, 383-415.

Emsley, P., and Cowtan, K. (2004). Coot: model-building tools for molecular graphics. Acta Crystallogr D Biol Crystallogr *60*, 2126-2132.

Faruque, S.M., Albert, M.J., and Mekalanos, J.J. (1998). Epidemiology, genetics, and ecology of toxigenic Vibrio cholerae. Microbiol Mol Biol Rev *62*, 1301-1314.

Fries, D., and Fairlamb, A. (2003). In Burger's Medicinal Chemistry and Drug Discovery, D. Abraham, ed. (New York, John Wiley&Sons, Inc.), pp. 1033-1087.

Galston, A.W., and Sawhney, R.K. (1990). Polyamines in plant physiology. Plant Physiol *94*, 406-410.

Gerner, E.W., and Meyskens, F.L., Jr. (2004). Polyamines and cancer: old molecules, new understanding. Nature reviews *4*, 781-792.

Gillin, F.D., Reiner, D.S., and McCann, P.P. (1984). Inhibition of growth of Giardia lamblia by difluoromethylornithine, a specific inhibitor of polyamine biosynthesis. J Protozool *31*, 161-163.

Gokulan, K., Rupp, B., Pavelka, M.S., Jr., Jacobs, W.R., Jr., and Sacchettini, J.C. (2003). Crystal structure of Mycobacterium tuberculosis diaminopimelate decarboxylase, an essential enzyme in bacterial lysine biosynthesis. The Journal of biological chemistry *278*, 18588-18596.

Graham, D.E., Xu, H., and White, R.H. (2002). Methanococcus jannaschii uses a pyruvoyl-dependent arginine decarboxylase in polyamine biosynthesis. The Journal of biological chemistry *277*, 23500-23507.

Griffiths, G.L., Sigel, S.P., Payne, S.M., and Neilands, J.B. (1984). Vibriobactin, a siderophore from Vibrio cholerae. The Journal of biological chemistry *259*, 383-385.

Grishin, N.V., Osterman, A.L., Brooks, H.B., Phillips, M.A., and Goldsmith, E.J. (1999). X-ray structure of ornithine decarboxylase from Trypanosoma brucei: the native structure and the structure in complex with alpha-difluoromethylornithine. Biochemistry *38*, 15174-15184.

Grishin, N.V., Phillips, M.A., and Goldsmith, E.J. (1995). Modeling of the spatial structure of eukaryotic ornithine decarboxylases. Protein Sci *4*, 1291-1304.

Gubala, A.J. (2006). Multiplex real-time PCR detection of Vibrio cholerae. J Microbiol Methods *65*, 278-293.

Hamana, K., Aizaki, T., Arai, E., Saito, A., Uchikata, K., and Ohnishi, H. (2004). Distribution of norspermidine as a cellular polyamine within micro green algae including non-photosynthetic achlorophyllous Polytoma, Polytomella, Prototheca and Helicosporidium. The Journal of general and applied microbiology *50*, 289-295.

Hamana, K., and Itoh, T. (2001). Polyamines of the hyperthermophilic archaebacteria belonging to the genera Thermococcus and Methanothermus and two new genera Caldivirga and Palaeococcus. Microbios *104*, 105-114.

Hamana, K., and Matsuzaki, S. (1992). Polyamines as a chemotaxonomic marker in bacterial systematics. Crit Rev Microbiol *18*, 261-283.

Hamana, K., Niitsu, M., Samejima, K., and Itoh, T. (2001). Polyamines of the thermophilic eubacteria belonging to the genera Thermosipho, Thermaerobacter and Caldicellulosiruptor. Microbios *104*, 177-185.

Hammer, B.K., and Bassler, B.L. (2003). Quorum sensing controls biofilm formation in Vibrio cholerae. Mol Microbiol *50*, 101-104.

Heby, O. (1995). DNA methylation and polyamines in embryonic development and cancer. Int J Dev Biol *39*, 737-757.

Hiatt, A.C., McIndoo, J., and Malmberg, R.L. (1986). Regulation of polyamine biosynthesis in tobacco. Effects of inhibitors and exogenous polyamines on arginine decarboxylase, ornithine decarboxylase, and S-adenosylmethionine decarboxylase. The Journal of biological chemistry *261*, 1293-1298.

Hurt, D.E., Widom, J., and Clardy, J. (2006). Structure of Plasmodium falciparum dihydroorotate dehydrogenase with a bound inhibitor. Acta crystallographica *62*, 312-323.

Igarashi, K., and Kashiwagi, K. (2006). Polyamine Modulon in Escherichia coli: genes involved in the stimulation of cell growth by polyamines. Journal of biochemistry *139*, 11-16.

Ikai, H., and Yamamoto, S. (1997). Identification and analysis of a gene encoding L-2,4-diaminobutyrate:2-ketoglutarate 4-aminotransferase involved in the 1,3-diaminopropane production pathway in Acinetobacter baumannii. J Bacteriol *179*, 5118-5125.

Islam, M.S., Drasar, B.S., and Sack, R.B. (1993). The aquatic environment as a reservoir of Vibrio cholerae: a review. Journal of diarrhoeal diseases research *11*, 197-206.

Iwanaga, M., Yamamoto, K., Higa, N., Ichinose, Y., Nakasone, N., and Tanabe, M. (1986). Culture conditions for stimulating cholera toxin production by Vibrio cholerae O1 El Tor. Microbiol Immunol *30*, 1075-1083.

Jackson, L.K., Baldwin, J., Akella, R., Goldsmith, E.J., and Phillips, M.A. (2004). Multiple active site conformations revealed by distant site mutation in ornithine decarboxylase. Biochemistry *43*, 12990-12999.

Jackson, L.K., Goldsmith, E.J., and Phillips, M.A. (2003). X-ray structure determination of Trypanosoma brucei ornithine decarboxylase bound to D-ornithine and to G418: insights into substrate binding and ODC conformational flexibility. The Journal of biological chemistry *278*, 22037-22043.

Jobling, M.G., and Holmes, R.K. (1997). Characterization of hapR, a positive regulator of the Vibrio cholerae HA/protease gene hap, and its identification as a functional homologue of the Vibrio harveyi luxR gene. Mol Microbiol *26*, 1023-1034.

Kallio, A., and McCann, P.P. (1981). Difluoromethylornithine irreversibly inactivates ornithine decarboxylase of Pseudomonas aeruginosa, but does not inhibit the enzymes of Escherichia coli. Biochem J *200*, 69-75.

Kaper, J.B., Morris, J.G., Jr., and Levine, M.M. (1995). Cholera. Clin Microbiol Rev *8*, 48-86.

Karatan, E., Duncan, T.R., and Watnick, P.I. (2005). NspS, a predicted polyamine sensor, mediates activation of Vibrio cholerae biofilm formation by norspermidine. J Bacteriol *187*, 7434-7443.

Kern, A.D., Oliveira, M.A., Coffino, P., and Hackert, M.L. (1999). Structure of mammalian ornithine decarboxylase at 1.6 A resolution: stereochemical implications of PLP-dependent amino acid decarboxylases. Structure *7*, 567-581.

Kidron, H., Repo, S., Johnson, M., and Salminen, T. (2006). Functional Classification of Amino Acid Decarboxylases from the Alanine Racemase Structural Family by Phylogenetic Studies. Mol Biol Evol.

Kidron, H., Repo, S., Johnson, M.S., and Salminen, T.A. (2007). Functional classification of amino acid decarboxylases from the alanine racemase structural family by phylogenetic studies. Mol Biol Evol *24*, 79-89.

Kitz, R., and Wilson, I.B. (1962). Esters of methanesulfonic acid as irreversible inhibitors of acetylcholinesterase. The Journal of biological chemistry *237*, 3245-3249.

Kossiakoff, A. (1987). Catalytic properties of trypsin. In Biological Macromolecules and Assemblies F.A. Jurnak, McPherson, A., ed. (John Wiley & Sons, Inc.), pp. 369-412.

Laskowski RA, M.M., Moss DS, Thorton JM (1993). Procheck - A program to check the stereochemical quality of protein strucutres. J Appl Crystallogr *26*, 283-291

Lee, J., Michael, A.J., Martynowski, D., Goldsmith, E.J., and Phillips, M.A. (2007). Phylogenetic diversity and the structural basis of substrate specificity in the beta/alpha-barrel fold basic amino acid decarboxylases. The Journal of biological chemistry *282*, 27115-27125.

Lenz, D.H., Mok, K.C., Lilley, B.N., Kulkarni, R.V., Wingreen, N.S., and Bassler, B.L. (2004). The small RNA chaperone Hfq and multiple small RNAs control quorum sensing in Vibrio harveyi and Vibrio cholerae. Cell *118*, 69-82.

Masse, E., Majdalani, N., and Gottesman, S. (2003). Regulatory roles for small RNAs in bacteria. Curr Opin Microbiol *6*, 120-124.

Menard, R., Sansonetti, P.J., and Parsot, C. (1993). Nonpolar mutagenesis of the ipa genes defines IpaB, IpaC, and IpaD as effectors of Shigella flexneri entry into epithelial cells. J Bacteriol *175*, 5899-5906.

Miethke, M., and Marahiel, M.A. (2007). Siderophore-based iron acquisition and pathogen control. Microbiol Mol Biol Rev *71*, 413-451.

Miller, V.L., and Mekalanos, J.J. (1988). A novel suicide vector and its use in construction of insertion mutations: osmoregulation of outer membrane proteins and virulence determinants in Vibrio cholerae requires toxR. Journal of bacteriology *170*, 2575-2583.

Minor, W., Cymborowski, M., Otwinowski, Z., and Chruszcz, M. (2006). HKL-3000: the integration of data reduction and structure solution--from diffraction images to an initial model in minutes. Acta Crystallogr D Biol Crystallogr *62*, 859-866.

Momany, C., Levdikov, V., Blagova, L., and Crews, K. (2002). Crystallization of diaminopimelate decarboxylase from Escherichia coli, a stereospecific D-amino-acid decarboxylase. Acta Crystallogr D Biol Crystallogr *58*, 549-552.

Morgan, D.M. (1999). Polyamines. An overview. Mol Biotechnol *11*, 229-250.

Morris, R.J., Perrakis, A., and Lamzin, V.S. (2003). ARP/wARP and automatic interpretation of protein electron density maps. Methods Enzymol *374*, 229-244.

Murshudov, G.N., Vagin, A.A., and Dodson, E.J. (1997). Refinement of macromolecular structures by the maximum-likelihood method. Acta crystallographica *53*, 240-255.

Nakao, H., Ishii, M., Shinoda, S., and Yamamoto, S. (1989). Purification and some properties of a novel L-2,4-diaminobutyric acid decarboxylase from Vibrio alginolyticus. Journal of general microbiology *135*, 345-351.

Nakao, H., Shinoda, S., and Yamamoto, S. (1991). Purification and some properties of carboxynorspermidine synthase participating in a novel biosynthetic pathway for norspermidine in Vibrio alginolyticus. Journal of general microbiology *137*, 1737-1742.

Nakao, H., Shinoda, S. and Yamamoto, S. (1990). Purification and properties of carboxynorspermidine decarboxylase, a novel enzyme involved in norspermidine biosynthesis, from Vibrio alginolyticus. Journal of general microbiology *136*, 1699-1704.

Nichloas, K.B., Nicholas, H.B., Jr., and Deerfield II, D.W. (1997). EMBnetnews *4*, 1-4.

O'Toole, G.A., Pratt, L.A., Watnick, P.I., Newman, D.K., Weaver, V.B., and Kolter, R. (1999). Genetic approaches to study of biofilms. Methods Enzymol *310*, 91-109.

Oredsson, S.M. (2003). Polyamine dependence of normal cell-cycle progression. Biochem Soc Trans *31*, 366-370.

Osterman, A., Grishin, N.V., Kinch, L.N., and Phillips, M.A. (1994). Formation of functional cross-species heterodimers of ornithine decarboxylase. Biochemistry *33*, 13662-13667.

Osterman, A.L., Kinch, L.N., Grishin, N.V., and Phillips, M.A. (1995). Acidic residues important for substrate binding and cofactor reactivity in eukaryotic ornithine decarboxylase identified by alanine scanning mutagenesis. The Journal of biological chemistry *270*, 11797-11802.

Page, R.D. (1996). TreeView: an application to display phylogenetic trees on personal computers. Comput Appl Biosci *12*, 357-358.

Patel, C.N., Wortham, B.W., Lines, J.L., Fetherston, J.D., Perry, R.D., and Oliveira, M.A. (2006). Polyamines are essential for the formation of plague biofilm. J Bacteriol *188*, 2355-2363.

Pegg, A.E. (2006). Regulation of ornithine decarboxylase. The Journal of biological chemistry *281*, 14529-14532.

Pegg, A.E., and McCann, P.P. (1992). S-adenosylmethionine decarboxylase as an enzyme target for therapy. Pharmacol Ther *56*, 359-377.

Pegg, A.E., and McGill, S. (1979). Decarboxylation of ornithine and lysine in rat tissues. Biochim Biophys Acta *568*, 416-427.

Pfaffl, M.W. (2001). A new mathematical model for relative quantification in real-time RT-PCR. Nucleic Acids Res *29*, e45.

Phillips, M.A., Coffino, P., and Wang, C.C. (1988). Trypanosoma brucei ornithine decarboxylase: enzyme purification, characterization, and expression in Escherichia coli. The Journal of biological chemistry *263*, 17933-17941.

Purevdorj, B.a.S., P. (2004). Hydrodynamic considerations of biofilm structure and behavior. In Microbial Biofilms, M.A.a.O.T. Ghannoum, G., ed. (ASM Press), pp. 160-173.

Qu, N., Ignatenko, N.A., Yamauchi, P., Stringer, D.E., Levenson, C., Shannon, P., Perrin, S., and Gerner, E.W. (2003). Inhibition of human ornithine decarboxylase activity by enantiomers of difluoromethylornithine. Biochem J *375*, 465-470.

R. Simon, U.P.a.A.P. (1983). A Broad Host Range Mobilization System for In Vivo Genetic Engineering: Transposon Mutagenesis in Gram Negative Bacteria. Biotechnology *1*, 784-791.

Ray, S.S., Bonanno, J.B., Rajashankar, K.R., Pinho, M.G., He, G., De Lencastre, H., Tomasz, A., and Burley, S.K. (2002). Cocrystal structures of diaminopimelate decarboxylase: mechanism, evolution, and inhibition of an antibiotic resistance accessory factor. Structure *10*, 1499-1508.

Roberts, A., G. D. Pearson, and J. J. Mekalanos (1992). Cholera vaccine strains derived from a 1991 Peruvian isolate of Vibrio cholerae and other El Tor strains. Paper presented at: 28th Joint Conference, US-Japan Cooperative Medical Science Program on Cholera and Related Diarrheal Diseases (National Institutes of Health, Bethesda, Md).

Sandmeier, E., Hale, T.I., and Christen, P. (1994). Multiple evolutionary origin of pyridoxal-5'-phosphate-dependent amino acid decarboxylases. Eur J Biochem *221*, 997-1002.

Schneider, G., Kack, H., and Lindqvist, Y. (2000). The manifold of vitamin B6 dependent enzymes. Structure *8*, R1-6.

Schwarzenbacher, R., Godzik, A., Grzechnik, S.K., and Jaroszewski, L. (2004). The importance of alignment accuracy for molecular replacement. Acta Crystallogr D Biol Crystallogr *60*, 1229-1236.

Seiler, N., Atanassov, C.L., and Raul, F. (1998). Polyamine metabolism as target for cancer chemoprevention (review). Int J Oncol *13*, 993-1006.

Shah, R., Akella, R., Goldsmith, E.J., and Phillips, M.A. (2007). X-ray structure of Paramecium bursaria Chlorella virus arginine decarboxylase: insight into the structural basis for substrate specificity. Biochemistry *46*, 2831-2841.

Shah, R., Coleman, C.S., Mir, K., Baldwin, J., Van Etten, J.L., Grishin, N.V., Pegg, A.E., Stanley, B.A., and Phillips, M.A. (2004). Paramecium bursaria chlorella virus-1 encodes

an unusual arginine decarboxylase that is a close homolog of eukaryotic ornithine decarboxylases. J Biol Chem *279*, 35760-35767.

Slocum, R.D., Kaur-Sawhney, R., and Galston, A.W. (1984). The physiology and biochemistry of polyamines in plants. Archives of biochemistry and biophysics *235*, 283-303.

Srivenugopal, K.S., and Adiga, P.R. (1980). Coexistence of two pathways of spermidine biosynthesis in Lathyrus sativus seedlings. FEBS Lett *112*, 260-264.

Stanley, N.R., and Lazazzera, B.A. (2004). Environmental signals and regulatory pathways that influence biofilm formation. Mol Microbiol *52*, 917-924.

Sturgill, G., and Rather, P.N. (2004). Evidence that putrescine acts as an extracellular signal required for swarming in Proteus mirabilis. Mol Microbiol *51*, 437-446.

Swofford, D.L. (2000). PAUP*: Phylogenetic Analysis Using Parsimony (and Other Methods) (Sunderland, MA: Sinauer Associates).

Tabor, C.W., and Tabor, H. (1984). Polyamines. Annu Rev Biochem *53*, 749-790.

Tabor, C.W., and Tabor, H. (1985). Polyamines in microorganisms. Microbiological reviews *49*, 81-99.

Tait, G.H. (1976). A new pathway for the biosynthesis of spermidine. Biochem Soc Trans *4*, 610-612.

Takatsuka, Y., and Kamio, Y. (2004). Molecular dissection of the Selenomonas ruminantium cell envelope and lysine decarboxylase involved in the biosynthesis of a polyamine covalently linked to the cell wall peptidoglycan layer. Biosci Biotechnol Biochem *68*, 1-19.

Takatsuka, Y., Yamaguchi, Y., Ono, M., and Kamio, Y. (2000). Gene cloning and molecular characterization of lysine decarboxylase from Selenomonas ruminantium delineate its evolutionary relationship to ornithine decarboxylases from eukaryotes. J Bacteriol *182*, 6732-6741.

Thompson, J.D., Gibson, T.J., Plewniak, F., Jeanmougin, F., and Higgins, D.G. (1997). The CLUSTAL_X windows interface: flexible strategies for multiple sequence alignment aided by quality analysis tools. Nucleic Acids Res *25*, 4876-4882.

Tischler, A.D., and Camilli, A. (2004). Cyclic diguanylate (c-di-GMP) regulates Vibrio cholerae biofilm formation. Mol Microbiol *53*, 857-869.

Tischler, A.D., and Camilli, A. (2005). Cyclic diguanylate regulates Vibrio cholerae virulence gene expression. Infect Immun *73*, 5873-5882.

Vagin A, T.A. (1997). MOLREP: an automated program for molecular replacement J Appl Crystallogr *30*, 1022-1025.

Wai, S.N., Mizunoe, Y., Takade, A., Kawabata, S.I., and Yoshida, S.I. (1998). Vibrio cholerae O1 strain TSI-4 produces the exopolysaccharide materials that determine colony morphology, stress resistance, and biofilm formation. Appl Environ Microbiol *64*, 3648-3655.

Waters, C.M., and Bassler, B.L. (2005). Quorum sensing: cell-to-cell communication in bacteria. Annu Rev Cell Dev Biol *21*, 319-346.

Waters, C.M., Lu, W., Rabinowitz, J.D., and Bassler, B.L. (2008). Quorum sensing controls biofilm formation in Vibrio cholerae through modulation of cyclic di-GMP levels and repression of vpsT. J Bacteriol *190*, 2527-2536.

Watnick, P.I., and Kolter, R. (1999). Steps in the development of a Vibrio cholerae El Tor biofilm. Mol Microbiol *34*, 586-595.

Watnick, P.I., Lauriano, C.M., Klose, K.E., Croal, L., and Kolter, R. (2001). The absence of a flagellum leads to altered colony morphology, biofilm development and virulence in Vibrio cholerae O139. Mol Microbiol *39*, 223-235.

Wilson, K. (1997). Preparation of Genomic DNA from Bacteria. In Current Protocols in Molecular Biology F. Ausubel, R. Brent, R.E. Kingston, D.D. Moore, J.G. Seidman, J.A. Smith, and K. Struhl, eds. (John Wiley & Sons, Inc.), pp. 2.1.1-2.4.5.

Wu, W.H., and Morris, D.R. (1973). Biosynthetic arginine decarboxylase from Escherichia coli. Purification and properties. The Journal of biological chemistry *248*, 1687-1695.

Yamamoto, S., Chowdhury, M.A., Kuroda, M., Nakano, T., Koumoto, Y., and Shinoda, S. (1991). Further study on polyamine compositions in Vibrionaceae. Canadian journal of microbiology *37*, 148-153.

Yamamoto, S., Hamanaka, K., Suemoto, Y., Ono, B., and Shinoda, S. (1986a). Evidence for the presence of a novel biosynthetic pathway for norspermidine in Vibrio. Canadian journal of microbiology *32*, 99-103.

Yamamoto, S., Sugahara, T., Tougou, K., and Shinoda, S. (1994). Cloning and nucleotide sequence of the carboxynorspermidine decarboxylase gene from Vibrio alginolyticus. Microbiology *140 (Pt 11)*, 3117-3124.

Yamamoto, S., Tsuzaki, Y., Tougou, K., and Shinoda, S. (1992). Purification and characterization of L-2,4-diaminobutyrate decarboxylase from Acinetobacter calcoaceticus. Journal of general microbiology *138*, 1461-1465.

Yamamoto, S., Yoshida, M., Nakao, H., Koyama, M., Hashimoto, Y., and Shinoda, S. (1986b). Variations in cellular polyamine compositions and contents of Vibrio species during growth in media with various NaCl concentrations. Chemical & pharmaceutical bulletin *34*, 3038-3042.

Yildiz, F.H., Dolganov, N.A., and Schoolnik, G.K. (2001). VpsR, a Member of the Response Regulators of the Two-Component Regulatory Systems, Is Required for Expression of vps Biosynthesis Genes and EPS(ETr)-Associated Phenotypes in Vibrio cholerae O1 El Tor. J Bacteriol *183*, 1716-1726.

Yildiz, F.H., and Schoolnik, G.K. (1999). Vibrio cholerae O1 El Tor: identification of a gene cluster required for the rugose colony type, exopolysaccharide production, chlorine resistance, and biofilm formation. Proceedings of the National Academy of Sciences of the United States of America *96*, 4028-4033.